EFFECTS OF INDIAN CLASSICAL MUSIC ON BRAIN AND CARDIOVASCULAR DYNAMICS

A thesis submitted toward partial fulfillment
of the requirements for the degree of

Master of Engineering
In
Biomedical Engineering

Submitted by

NILOTPAL DAS

EXAM ROLL NO: **M4BMD18005**
CLASS ROLL NO: **001630201006**
REGISTRATION NUMBER: **137406** of **2016-2017**

Under the supervision of
Dr. Monisha Chakraborty
Associate Professor
School of Bioscience and Engineering
Jadavpur University

Course affiliated to
Faculty of Engineering and Technology
Jadavpur University
Kolkata-700032
India
2018

M.E. (Biomedical Engineering) course affiliated to
Faculty of Engineering and Technology
Jadavpur University
Kolkata-700032

CERTIFICATE OF RECOMMENDATION

This is to certify that the thesis entitled **"Effects of Indian Classical Music on Brain and Cardiovascular Dynamics"** is a bonafide work carried out by **NILOTPAL DAS** under my supervision and guidance for partial fulfillment of the requirement for Post Graduate Degree of Master of Engineering in Biomedical Engineering during the academic session 2016-2018.

_____

THESIS ADVISOR
Dr. Monisha Chakraborty
Associate Professor
School of Bioscience and Engineering
Jadavpur University
Kolkata-700032

_____

DIRECTOR
School of Bioscience and Engineering
Jadavpur University
Kolkata-700032

_____

Dean
Faculty Council of Interdisciplinary Studies, Law and Management
Jadavpur University
Kolkata – 700032

M.E. (Biomedical Engineering) course affiliated to
Faculty of Engineering and Technology
Jadavpur University
Kolkata-700032

Certificate of Approval**

The foregoing thesis is hereby approved as a creditable study of an Engineering subject carried out and presented in a manner satisfactory to warrant its acceptance as a prerequisite to the degree for which it has been submitted. It is understood that by this approval the undersigned do not necessarily endorse or approve any statement made opinion expressed or conclusion drawn therein but approve the thesis only for the purpose for which it has been submitted.

_____ _____

Dr. Monisha Chakraborty
(Thesis Advisor)
Associate Professor
School of Bioscience and Engineering
Jadavpur University
Kolkata-700032

Signature of Examiner

** Only in case the thesis is approved.

DECLARATION OF ORIGINALITY AND COMPLIANCE OF ACADEMIC ETHICS

I hereby declare that this thesis contains literature survey and original research work by the undersigned candidate, as part of his Master of Engineering in Biomedical Engineering studies during academic session 2016-2018.

All information in this document has been obtained and presented in accordance with academic rules and ethical conduct.

I also declare that, as required by this rules and conduct, I have fully cited and referred all material and results that are not original to this work.

NAME: **NILOTPAL DAS**

CLASS ROLL NO.: **001630201006**

EXAMINATION ROLL NO**.: M4BMD18005**

REGISTRATION NO.:**137406 of 2016-17**

THESIS TITLE: **Effects of Indian Classical Music on Brain and Cardiovascular Dynamics**

SIGNATURE: **DATE:**

Acknowledgement

I would like to take this opportunity to express my deepest gratitude to my Guru, Sri Sri Dadaji Maharaj, under whose divine influence I was motivated to work on this topic, whose deep and immense musical knowledge has always inspired and motivated to explore the relation of music and human body systems. Words fall short to describe my gratitude towards Him.

I would like to thank my thesis advisor Dr. Monisha Chakraborty, Associate Professor, School of Bioscience and Engineering, for giving me an opportunity to work under her guidance. She has always been a constant support and the confidence she has shown in my abilities has always motivated to work harder. This thesis would not have been possible without her constant supervision and help. I would also like to thank Dr. Piyali Basak, Director of School of Bioscience and Engineering, Jadavpur University, for the immense support she has shown towards my work.

I would also like to thank my family for being a constant source of support and confidence, who are the constant source of my energy, inspiration and determination for going ahead with my higher academic pursuit.

My sincere thanks goes to Mr. Debanjan Parbat, PhD scholar, School of Bioscience and Engineering, who has helped me in every step of the whole thesis work. This work would not have been possible without his tireless support. I would also like to thank my friends Ms. Purbanka Pahari and Mr. Pratik Das, for being there whenever I needed any help. They have always went out of their way to support me, I am privileged to have such friends.

Date: ***Nilotpal Das***

Dedicated to my Guru

Sri Sri Dadaji Maharaj

Preface

Human body system is a complex physiological system based on simple physical and chemical laws. As a system it takes inputs from the environment and surroundings and correspondingly provides a response. It is a complex neural network that is always learning from the environment. The intricate details of how human mind and body works has always intrigued the minds of researchers of all ages. Through the following study we try to contribute to this field of research. We have used Indian Classical Music as a stimulus to understand the response of brain to music and cognitive tasks. A methodology was developed to study how human body responds to music and how human body responds to learning and recognition of Indian Classical Music. The thesis has been divided into chapters each covering an important stage of the whole study.

In the first chapter, a brief introduction of basic physiology of human heart and brain, and the corresponding bio-signals ECG and EEG have been given. The objective and motivation behind this study has also been described.

In the second chapter, a thorough literature review has been performed for all aspects of this study, starting from signal acquisition, denoising, science behind Indian Classical Music, preceding studies based on Indian Classical Music, how human mind interprets music and working of memory, and the effects of music on heart and brain.

In the third chapter, the methodology and experimental procedure has been developed. All steps followed during the study has been described thoroughly. Signal acquisition systems used in the experimental procedure have been discussed. Special attention has been given to signal denoising, as it is an essential step in any signal processing system. The tools and techniques necessary for this study and their working principles have also been discussed in detail.

The fourth chapter contains the experimental results, including results from the study on denoising techniques necessary for this experiment, and the effects of music on various parameters of brain and cardiovascular systems.

In the final chapters, the results have been discussed with physiological point of view and certain conclusions have been achieved.

Contents

List of Figures

List of Tables

1. Introduction

> *We are just an advanced breed of monkeys on a minor planet of a very average star. But we can understand the Universe. That makes us something very special.*
>
> ***- Stephen Hawking***

Human body, or in a broader sense, any living organism is a complex biological system based on simple physical laws and chemical interactions. Every biological phenomenon, however complex its nature might be, has some underlying simple physical and chemical workings. And these simple physical and chemical processes are the building blocks of a highly complex yet exceptionally coordinated living system – the human body. Through millions of years of evolutionary process, the intricacy with which nature has developed the human body, how through simple atoms and molecules we have developed into a system that can think, visualise, communicate, is a question that has always intrigued the minds of researchers from every field of study. Researchers of every age with whatever tools they had at their disposal, have always tried to find out how our body works, how our mind works, and how we interact with nature. There might never be a definitive answer to that question but with every step we are truly moving towards the answer. This thesis work is an ant's footing in that direction, an attempt to unravel some of the mysteries of the human brain and body.

Human body as a system is in continuous interaction with the environment. Everything happening around us is like a stimulus that gives rise to chain of processes inside us and our body generates a response to that stimulus. These responses may be voluntary or involuntary, emotional or physical, but however conspicuous or inconspicuous the response maybe, there are numerous functions going inside our body in response to the stimulus. Music is one such stimulus that gives rise to a huge range of responses in us. Music has the power to generate varied emotions, affect our mood, reduce stress, recollect memories, alter our mental state and physical state. It is interesting to note how an auditory impulse consisting of certain rhythmic patterns of frequencies can give rise to such varied effects in us. In this study we will thus see how Indian Classical Music, a rich form of music backed by centuries of practice and scientific literature, affects human mind and body.

1.1 INTERACTION OF HUMAN BODY WITH NATURE

If we look into the structural hierarchy of the human body, then at the lowest level we will find 'cells' which are the basic building blocks of the human body. These cells develop and differentiate to perform specific functions. Every organ system of the body is made of these cells. These cells are separated from their surroundings by thin selectively permeable membranes. Cell membranes play an important role in maintaining difference in concentrations of ions inside and outside the cells. The uneven concentration of cells inside and outside the cell gives rise to an electric field. Under resting conditions, the concentration of ions is distributed such that the inside of the cell is much negative (60-90mV) relative to the extracellular space. This voltage difference depends upon –

- relative difference in concentration of ions (chemical gradient).
- any external sources resulting in transport of ions across the membrane (electrical gradient).

Thus, when the resting condition of the cell is disturbed by some stimulus of a magnitude greater than a certain level (threshold), this chemical and electrical balance across the cell membrane gets disrupted and causes the cell to go through a cycle of electric changes, which is known as action potential. It is through these action potentials that impulses are transmitted from one cell to one another, giving rise to almost all the functions of the human body. Thus, every cell is a minute voltage generator, and are the basic source of bioelectric potentials. When large groups of cells work in coordinated manner to bring about some specific function of any organ system, they give rise to significant ionic voltages, called bio-potentials. these potential differences can be picked up by placing electrodes on certain points on our body and provide us information regarding the working of the corresponding organ system. Some common bio-potentials are –

Table 1.1-1 Common Bio-signals and their source of origin

BIO-ELECTRIC SIGNAL	FREQUENCY RANGE (HZ)	SIGNAL ORIGIN
ELECTROCARDIOGRAM (ECG)	0.05 – 120	Heart Muscles
ELECTROENCEPHALOGRAM (EEG)	0.1 – 100	Neural Activity of Brain
ELECTROMYOGRAM (EMG)	5 – 2000	Muscular Activity
ELECTROOCULOGRAM (EOG)	0-100	Corneal Retinal Potentials

1.2 HUMAN BODY AS A SIGNAL GENERATOR

A signal can be broadly defined as the transfer for information. This transfer of information can be through any media, at any scale, starting from communication between cells (cell signalling) to satellite communication. But here our range of interest is limited to digital signal processing of bio signals under the stimulus of Indian Classical Music. Now what is digital signal processing? In our field of interest, we can define signal as a description of how one parameter is related to another parameter. If both the parameters assume a continuous range of values, then it is called a continuous signal. For e.g., as discussed earlier, cells are minute voltage generators, that is, a voltage difference is maintained across the cell at all instants. When large groups of cells work in coordinated fashion, they produce a significant voltage signal called bio-potential or bio signal, which is directly related to the internal working of those cells. This bio signal is picked up by placing electrodes at various locations of the body, and amplified, and can be plotted on a graph as a continuous variation of voltage with time. Scope of this continuous signal is limited, and for further processing and analysis we need to feed this continuous signal into a computer system. Computers are digital systems, so this continuous signal needs to be converted by an analog-to-digital converter. The continuous signal is sampled at a specific sampling frequency, that is information is extracted from the continuous signal at specific intervals in such a manner that no significant loss of information occurs. The amplitude of the voltage signal is then quantized into possible binary levels according to the specifications of the converter. For instance, the continuous voltage signal is converted with a 12-bit A/D converter at 1000 Hz sampling rate. This means, at every $1/1000^{th}$ second, the voltage of the bio signal is taken and curtailed to 4096 (2^{12}) possible binary levels. The signal generated from the process is called a digital signal. Thus, starting from the working of cells in our body, we end up with a digital signal at our disposal.

Human Body is thus a signal generator, where almost every process of the body results in a corresponding electrical activity. Some of the electrical activity are easily captured using electrodes placed at various points on the body. In this study our scope is limited to signals generated from human heart and brain, that is, electrocardiogram and electroencephalogram, respectively.

1.3 MOTIVATION AND OBJECTIVE – MUSIC AND HUMAN BODY

Human body is a complex physiological system that not only is a signal generator but also a signal processing system. All environmental impulses are like input signals that enter the human body system. Human body accordingly processes these signals and provides an output signal. For example, when we touch a hot surface, change in temperature at the surface of the skin is the input signal. This signal is picked but sensory neurons and sent to the central nervous system where the signal is processes and analysed. The resulting output signal is sent to muscles of the arm touching the hot surface and then we remove our hands from the hot surface. An output signal is also sent to the cardiovascular system to increase the activity of the heart, and correspondingly more blood is pumped to the brain for increased alertness. Thus, any impulse or input signal produces a range of outputs. In order to understand the working of the human body, it is necessary to understand how our body reacts to various stimuli and how various stimuli affect us.

The impulse or input signal of interest here is music. Music has the unique ability to give rise to a huge range of responses in us. The most intriguing fact is that music which can be simply regarded as a rhythmic combination and pattern of audible frequencies can give rise to any emotion, it can completely change the state of our mind, reduce stress or increase vitality. A set of musical notes when played in a certain order may give rise to happiness while same set of notes when played in a different style can give rise to grief. Music and our response to it is highly subjective, thus it is quite interesting to see how our body responds to music. In this study we have thus used Indian Classical Music, which is based on various Ragas, and is backed by thousands of years of research and literature. Each raga has a distinct nature. With subtle changes in musical patterns, each raga develops its own distinct characteristics which can be realised even by a listener without any prior musical knowledge.

Music has a close relation with memory. It is a common experience that by listening to a very short segment of a song we can recognise the song. This approach has been practiced in this study, but to make the test more abstract and to understand the relationship of musical patterns and how our brain learns and recognises them, we have used instrumental music (sitar). We played short sequences of three recordings of three different ragas from archived recordings of Pandit Ravi Shankar. Three ragas were Ahir Bhairav, Bhimpalashree, and Yaman. The three

ragas have very distinct characteristics, and each of the recordings were played three times, and the subject was asked to identify musical patterns so that they can recognise the raga later. After the three ragas were played three times each, the learning phase was complete and after a short break, a one of the three ragas were played, and the subject was asked to recognise the raga. During the whole process ECG and EEG recordings are taken so that we can analyse the effect of music on our body and what happens inside our brain when we are trying to learn something as abstract as instrumental music. It is interesting to note here, for a subject without prior musical training it is not possible to consciously understand the musical patterns being played, yet in an unconscious fashion they are able to understand and learn certain features from the music and with that learning they are able to recognise the raga later. This unique relation between music and memory and human body as a whole motivated us to perform this study with the objective of unravelling the secret behind this coherent behaviour.

Before we proceed further into processing and analysis of ECG and EEG, we need to understand the origin of these signals, so that later we can correlate our findings with physiological implications.

1.4 Working of Human Heart and the ECG Signal

Heart is a vital organ of the human body responsible for pumping blood through blood vessels to all parts of the body. It is divided into four chambers – left and right atrium on the top that receive blood from other organs and left and right ventricle at the bottom which pump blood to other organs. Human heart is myogenic, meaning the pumping action of heart is controlled by special muscle cells which give rise to electric currents that flow along the heart wall and causes heart muscles to contract. The recording of this electrical activity associated with the functioning of the heart is called electrocardiography. Thus, heart can be considered as an electric generator contained inside the torso. Heart has its own specialised cells that generate and conduct electric potentials across the heart. The Sino-atrial (SA) node located in the top right atrium initiate the electrical activity of the heart and is called the primary pacemaker of heart. It generates impulses at around 72 beats per minute at normal resting condition. The impulse then flows across the left and right atrium, causing them to contract,

and reaches the Atrioventricular Node (AV node), located in the lower part of the wall between the two atria. The AV node delays the impulse slightly so that atria and ventricles do not contract at the same time. The impulse then passes through a special conductive tissue called Bundle of His to the base of the ventricles. The fibres in this bundle are called Purkinje fibres, and they split into two branches and cause each ventricle to contract.

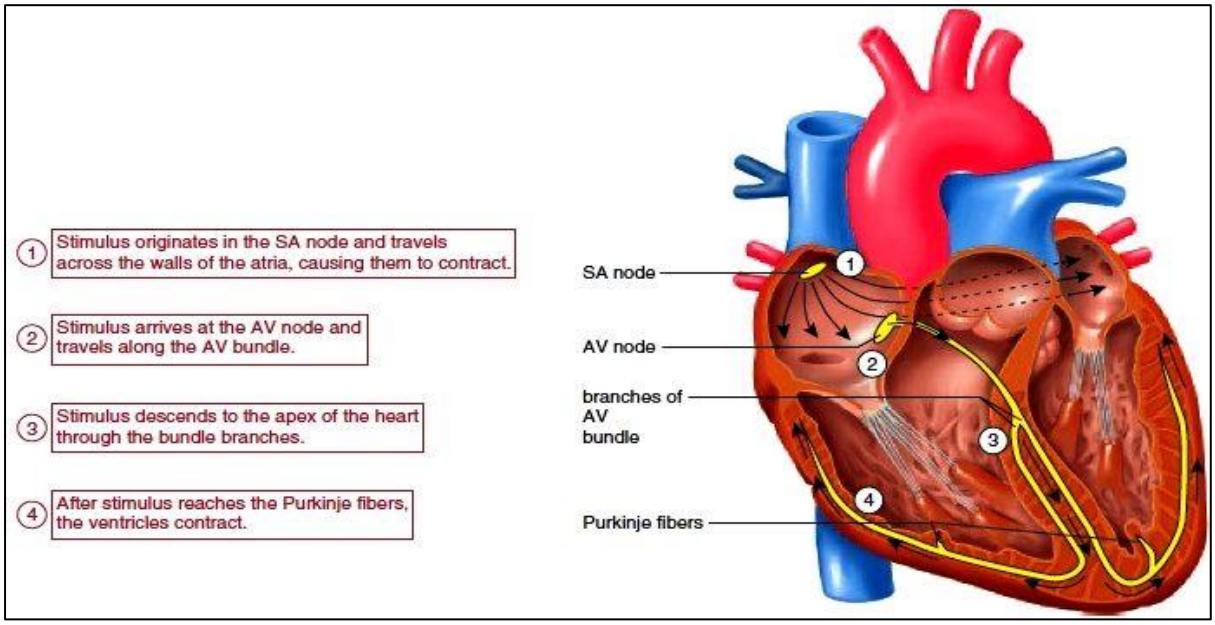

Figure 1.4-1 Pathway of electric potential through Heart (Source: encyclopedia.lubopitko-bg.com)

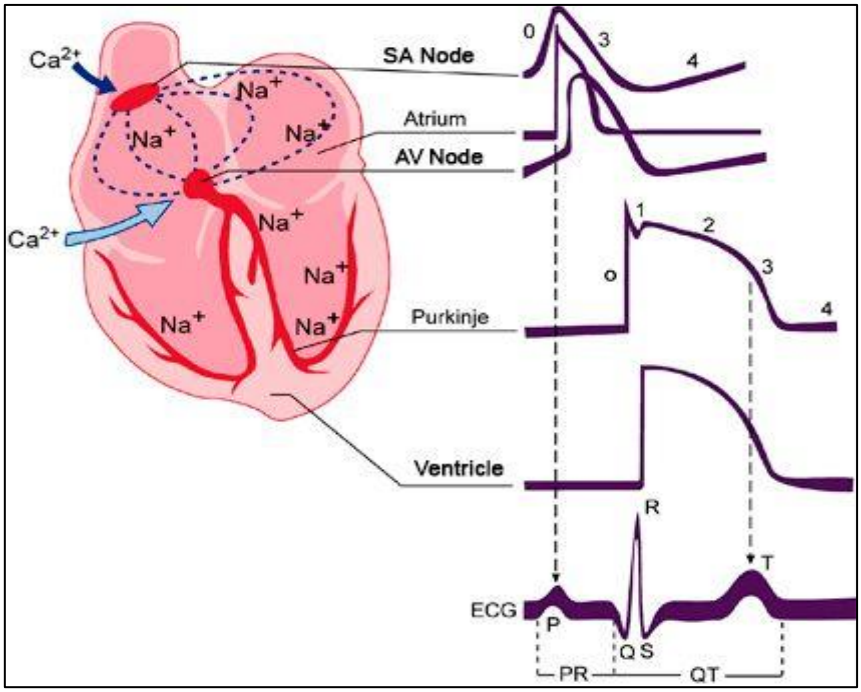

Figure 1.4-2 Action Potential generated in heart and corresponding ECG signal (source: itaca.edu.es)

The resulting Electrocardiogram generated is shown below –

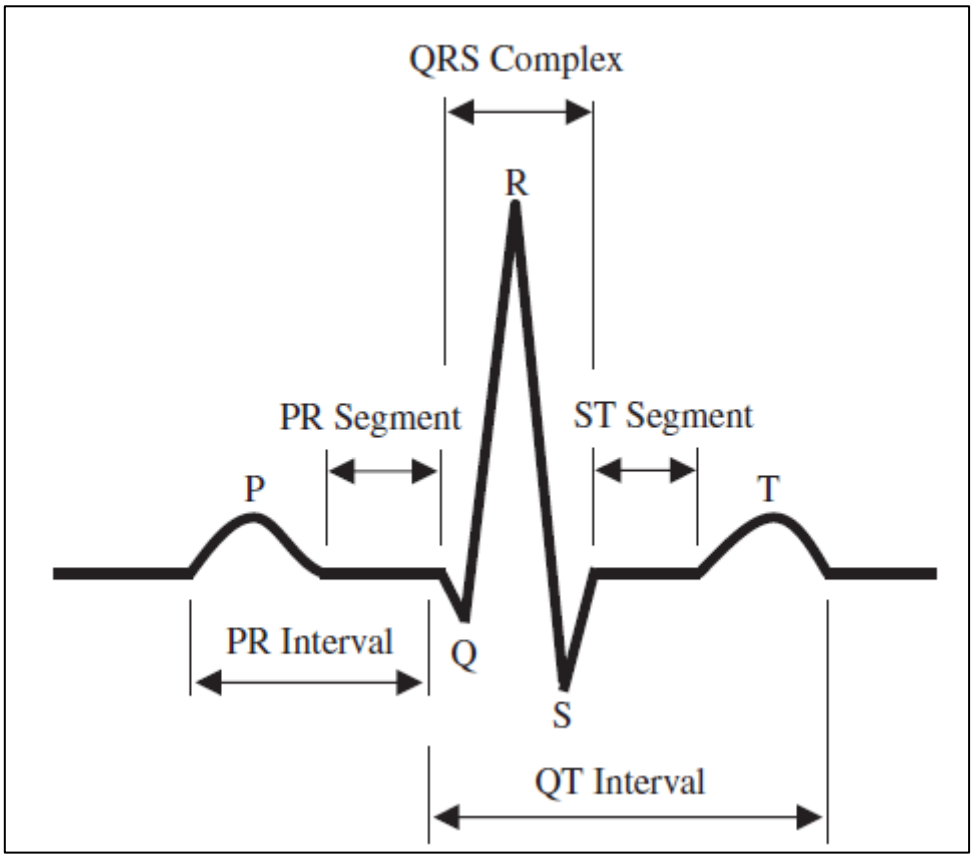

Figure 1.4-3 ECG signal

1.5 WORKING OF HUMAN BRAIN AND THE EEG SIGNAL

Brain consists billions of nerve cells or neurons arranged in various patterns that control coordinate thought, emotion, behaviour, movement, sensation, all-in-all each and every working of the human body. Every thought, every action be it voluntary or involuntary is affected by a corresponding electrical activity inside the brain. Innumerable neurons are functioning inside the brain, controlling all voluntary and involuntary activities of the body, and as a result generating voltage fluctuations. Electric potentials generated by a single neuron is of very low magnitude and cannot be individually captured, but the overall summation of the synchronous electrical activity of these innumerable neurons of the brain can be recorded by placing electrodes on the surface of the scalp. The recording of the electrical activity of the brain is called Electroencephalography, and the recorded signal is called the electroencephalogram. [1]

Brain consists of three parts –

i. Cerebrum
ii. Cerebellum
iii. Brain Stem

Cerebrum is the largest part of human brain and is divided into two well demarcated hemispheres by a longitudinal fissure, under which lies a large bands of connective nerve tracts, largest of which is known as corpus callosum. Corpus callosum connects the hemispheres of the brain, which are commonly called left-brain and right-brain, each possessing distinct characteristics and control different qualities. Each hemisphere of the brain can be further divided into four lobes – [2]

- **Frontal lobe -** The frontal lobes are the centres of intellectual function, intelligence, reasoning, motor skills, cognition and short-term memory tasks. At the back of the frontal lobe lies the motor cortex, which receives information from various parts of the brain and accordingly carries out body movements.
- **Parietal lobe** – Parietal lobe is behind the frontal lobe and is associated with sensation of touch, pain and pressure, and also language processing. Somatosensory cortex located in this lobe is responsible for processing of the body's senses.
- **Temporal lobe** – Temporal lobe is located on either side of the head, and is associated with long-term memory, hearing, emotion, language processing. Acoustic pathways terminate here, making it a hearing centre. In this region we also find neurons that respond differently to different frequencies of sound, neurons responding to high frequency sounds are located near the front of the ear and the ones responding to low frequencies are located near the back of the ear.
- **Occipital lobe** – The Occipital lobe is located at the back of the head. Visual pathways terminate here in the visual cortex, and is responsible for storing visual memories, which helps us interpret what we see.

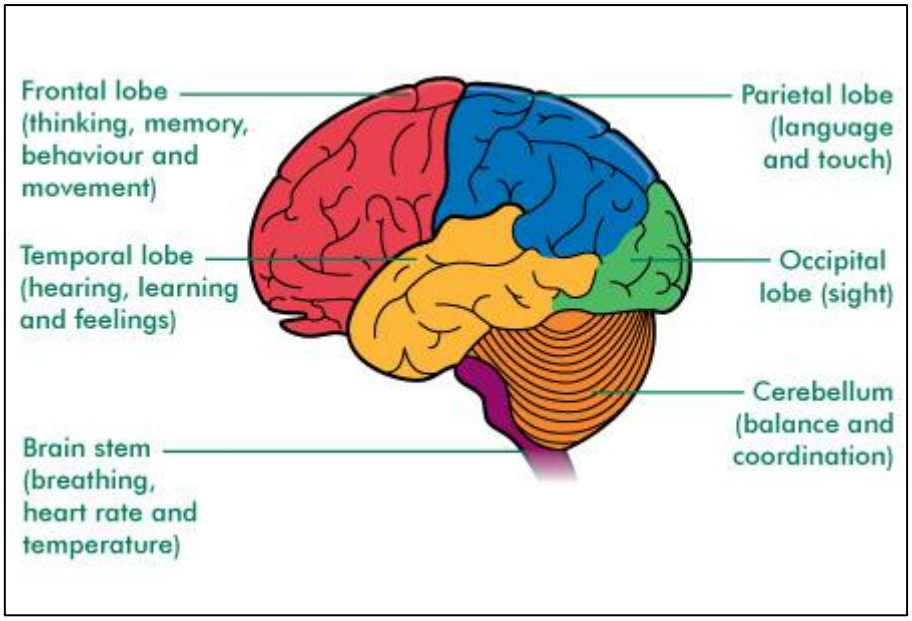

Figure 1.5-1 Lobes of the brain and corresponding functions(Source: macmillan.org.uk)

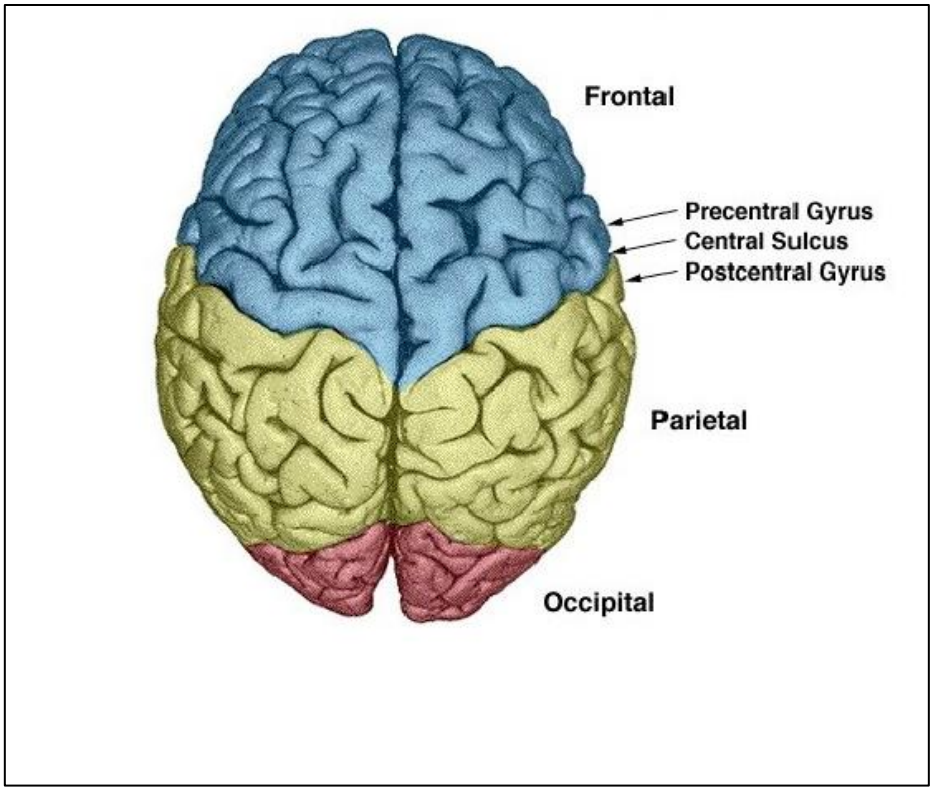

Figure 1.5-2 Top view of brain depicting locations of lobes of the brain

It is important to note here that brain areas and their corresponding functions are not exclusive. The notion that a particular point in the brain controls a certain function is outdated, rather it is seen that a particular function is a product of systems, and neurons from different areas of the brain contribute as they are a part of that system. Each area of the brain is thus linked to various functions.

ORIGIN OF EEG SIGNAL

Nerve cells or neurons are the basic building block of the brain and nervous system. Neurons are electrically polarized at rest. The interior of the neuron has a potential of -70mV relative to the exterior of the cell. Neurons are connected with one another through synaptic junctions. These synaptic junctions carry impulses in only one direction. When the neuron is exposed to a stimulus above a certain threshold, the resting condition of the neuron gets disturbed resulting in depolarization at that point. This depolarization causes nearby points in the neuron to depolarize and subsequently a wave of depolarization flows across the neuron. The neuron remains depolarized only for a fraction of a second, after which it repolarizes again. This wave of depolarization or neural impulse flows through synaptic junctions to other neurons. [2,3]

Cortical potentials are generated due to inhibitory and excitatory post-synaptic potentials developed by cell bodies and dendrites of pyramidal neurons. All processes of the brain – physiological processes, thought processes, external stimuli, all involve transmission of information through the flow of electric currents across neurons in corresponding parts of the brain. The brain thus generates rhythmic potentials originating in individual neurons of the brain. These potentials get summated as millions of cells discharge synchronously, and the resulting potentials can be recorded from the scalp surface using surface electrodes. [3] The scalp EEG is thus an average of the activity of many small zones of the cortical surface beneath the electrode. [4]

THE EEG SIGNAL

Electroencephalogram or EEG represents the electrical activity of the brain. [4] EEG signals are picked up using electrodes placed on the scalp or directly from the cerebral cortex (invasive method). The frequency spectrum of the EEG signal varies according to the activity fo the brain. The EEG frequency range varies from 0.5 to 50 Hz. [3]

The EEG frequency spectrum is divided into the following frequency band or waves –

1. Delta (δ): 0.5 to 4 Hz
2. Theta (θ): 4 to 8 Hz
3. Alpha (α): 8 to 13 Hz

4. Beta (β): > 13 Hz

Some literature further divides the high frequency spectrum of EEG, that is, above 13 Hz into two separate bands –

1. Beta (β): 13 to 22 Hz
2. Gamma (γ): ≥ 30 Hz

Alpha Rhythm – Alpha Rhythm is the principal resting rhythm of the brain and is of great significance as it reflects the state of alertness of the brain. With an increase in mental activity, alpha wave reduces markedly.

Beta Waves - Beta waves are characteristics of a strongly engaged mind and appear in tense and anxious subjects. Tasks requiring cognitive reasoning, calculation, reading, thinking leads to higher levels of beta waves. Theories suggest that increase in activity will resultingly lead to decrease in alpha activity.

Gamma Waves – Gamma waves have recently been discovered in the field of neuroscience and is supposed to be involved in processing more complex tasks.

Theta waves – theta waves appear at the beginning stages of sleep and exhibit a relaxed and open mind state. Theories suggest theta waves reflect the activity of the subconscious mind.

Delta Wave – Delta Waves appear during deep sleep stages. These brainwaves are of the greatest amplitude and slowest frequency, but they never go down to zero as that would mean brain dead. But, during deep dreamless sleep delta frequency is lowest.

In order to understand the effect of the individual brain waves let us consider an example. Suppose a person is solving a puzzle or reading a book with high concentration. At that state beta waves will be high. After reading the book, the person sits in a relaxed condition in an aesthetic environment like a garden. During this state, beta activity will reduce and there will be a marked increase in alpha activity. Next the person in a fully relaxed condition begins to day dream. During this condition theta activity will be high. After some time when the person falls asleep delta activity will be high.

In summary, there are four brainwave states ranging from the high amplitude, low frequency delta to the low amplitude, high frequency beta, reflecting activity of the brain from deep dreamless sleep to high arousal. Research has shown that although one brainwave state may predominate at any given time, depending on the activity level of the individual, the remaining three brain states are present in the mix of brainwaves at all times. In other words, while somebody is an aroused state and exhibiting a beta brainwave pattern, there also exists in that person's brain a component of alpha, theta and delta, even though these may be present only at the trace level.

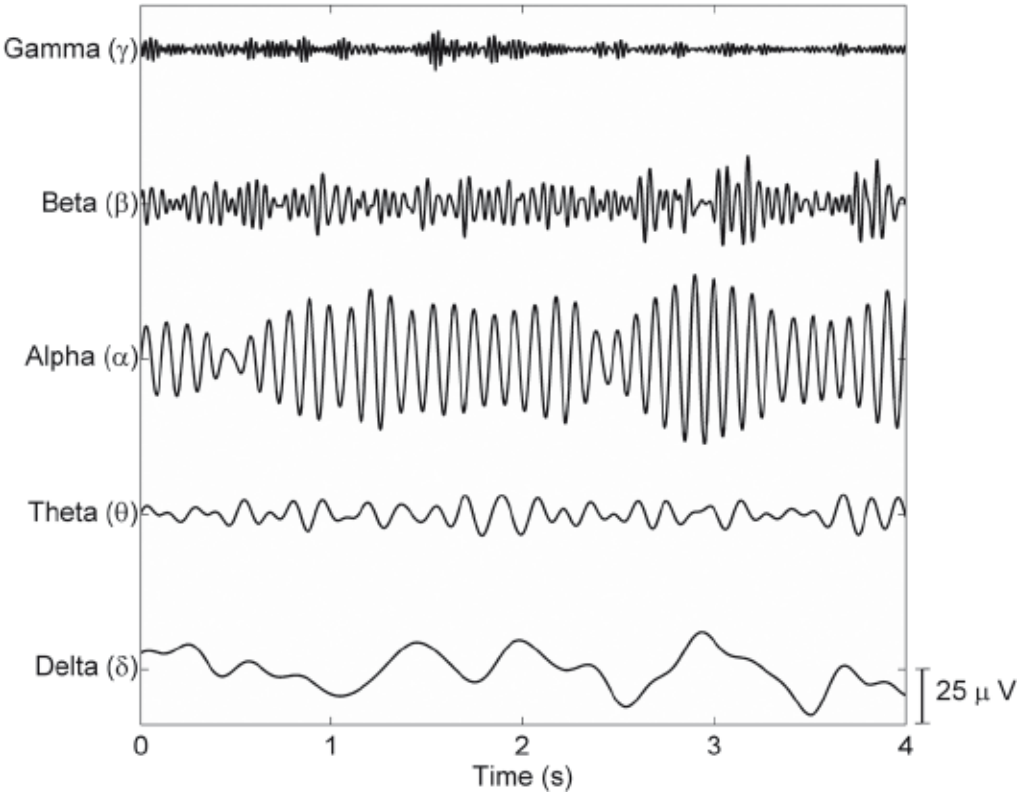

Figure 1.5-3 Different rhythms of the brain

2. Literature Review

> *Truth can be stated in a thousand different ways, yet each one can be true.*
>
> ***- Swami Vivekananda***

The relationship between music and bio-signals is not new, in-fact the first quantitative means to objectify bio-signals was based on musical notes. Francois Nicolas Marquet (1687–1759), a flute teacher, objectively described pulse pressure with music rhythm. [5] Prior to this analyses of pulses was highly subjective, and depended upon the skill of the physician, but Marquet stated that "this method will clearly show all the differences between natural and unnatural pulses", and thus aiding disease diagnosis. [6]

Centuries later, with the advent of technology, advanced techniques of bio-signal detection and acquisition has been developed. Initial breakthrough in Electrocardiography came when Willen Einthoven developed the first practical ECG machine based on string galvanometer. [7] Einthoven postulated that the electrical activity of the heart can be modelled as a current dipole, the resulting electrical flux of which can be acquired by placing electrodes on limbs. [2]

Human EEG was first recorded by Hans Berger (1873-1941) in 1924. [8] Placement of electrodes for EEG is specified by the International 10-20 System. [9] In this system electrode spacing is based on intervals of 10% and 20% of the distance between specified points on the scalp.

2.1 Signal Denoising

After the signal has been acquired, it needs to be processed and made free from noise. Bio-signals are low amplitude non-stationary signals which are easily corrupted by various forms of noise. According to [4] Butterworth, Elliptic, Bessel, Chebyshev filters are commonly used for ECG denoising. Baseline wander (BW) is a common low-frequency artifact that found

in ECG signals and is generally caused by respiration of patients or the motion of instruments. Removing baseline wander from ECG is a primary step in ECG signal analysis, for further processing and analysis. Finite impulse response (FIR) and infinite impulse response (IIR) filters are generally used to correct BW but fixed cut-off frequencies of these linear filters may lose useful information of waveform or cannot correct BW completely. [10] In [11] Mean-Median (MEM) filter and discrete wavelet transform (DWT) was used to remove baseline wander and appreciable results were obtained. In [12] quadratic variation reduction technique was used to remove baseline wander and the results were compared with high-pass filtering, adaptive filtering, median filtering and wavelet adaptive filtering, and it was seen that the proposed method outperforms the other conventional methods. Recent works [13-16] have explored the application of Empirical Mode Decomposition for baseline wander in ECG signals and found the technique to be effective in removing BW.

In [17] it was seen that FIR filters shows good performance in removing baseline wandering and powerline interference from ECG, while it was seen in [18] that IIR filters require less computation power than FIR filters and are also easier to implement. Also, IIR filters operate at a lesser order than FIR filters and are thus a better choice for removing baseline wander from ECG signals.

[19] studied the performance of adaptive digital notch filters, FIR and IIR, on noisy EEG signal and found their performance to be better than fixed notch filters. In [20] reference noisy signal was used to remove powerline interference from EEG signal and found the method to be more effective than notch filters or adaptive filtering in removing the primary noisy frequency along with its harmonic frequencies.

Savitzky and Golay proposed a method of data smoothing based on local least-squares polynomial approximation. [21] They showed that by fitting a polynomial to a set of input samples and then evaluating the resulting polynomial at a single point within the approximation interval is equivalent to discrete convolution with a fixed impulse response. The lowpass filters obtained by this method are known as Savitzky Golay filter. [22] In [23] ECG denoising was performed using Savitzky-Golay filtering technique, and it was seen Savitzky Golay filter performs better than bandpass filter implemented in Pan Tompkins algorithm. Various studies have used different parameters while using Savitzky-Golay Filtering. When the parameters of Savitzky-Golay Filters, polynomial degree is decreased, and frame size is increased, better

denoising results are obtained. [24] Savitzky Golay filters have also found application in EEG signal processing. [25,26]

Wavelet based techniques are also commonly used for ECG denoising. Wavelet based denoising methods are based on the fact that a signal can be represented by various wavelet coefficients and reducing certain wavelet coefficients to zero, the noise can be removed by preserving the characteristics of the signal. [27] Wavelet based denoising depends of the amount of noise present in the signal, i.e., when the amount of noise is low, IIR filters are better than wavelet based denoising techniques. [28] In the study [29] experimental results show that Daubechies mother wavelet of order 8 is the most appropriate wavelet basis function for ECG denoising. [30] Effectiveness of wavelet denoising on EEG signal processing was studied in [31], and db8 wavelet was found to be effective for denoising EEG signals of healthy patients. Comparative analysis of 4^{th} order Butterworth filter and Stationary Wavelet Transform for EEG signal denoising was performed in [32], and it was seen Stationary Wavelet Transform is more effective in denoising EEG signal. Other methods like Independent Component Analysis (ICA) and application of Neural Networks is also used for denoising EEG signals. [33,34]

2.2 MUSIC AND HUMAN BODY

What is music without a mind to appreciate it? Natural sounds existed before the existence of men, and music we know as of today has been influenced by these natural sounds.

Scientific research in the domain of music is not new and has been initiated since ancient times. [35] India has a rich historical background of Music. Through a series of articles published from 2001 to 2011, Sitar Maestro Prabal Chowdhury, through his immense research work in the field of music and spirituality, described the origin of Indian Classical Music, and how music is closely related to our human body system. [36] The omnipresent fundamental sound of nature ‘Om’ is the basis of creation of all sounds and music. [37] In this universe, starting from galaxies, stars, planets to electrons and protons, all objects are in motion. Their resulting vibration is the source of sound. Human ear can hear only a small range of this sound spectrum, from 20 Hz to 20,000 Hz. Every object has a natural frequency, and when the natural frequency matches with a sound source, resonance occurs. Thus, specific frequencies of sound cause resonance is specific parts of our body. This relation of Music and Human Body has been known to Indian sages since ancient times. Sitar Maestro Prabal Chowdhury described in his

articles how the seven notes of music, namely Sa Re Ga Ma Pa Dha Ni relate to the seven chakras (nervous plexuses) of Human Body, and thus explained the relationship of music and spirituality. [37] Out of the four Vedas, Samaveda is completely based on music. The origin of Indian Classical Music as we know today can be attributed to the time of the Vedas, even though music was practised since even more ancient times. This period saw the development of simple musical instruments and saw the development of dance forms with music. The seven notes of music we used in different permutations and combinations to give rise to melodic structures which later took the form of Ragas and Raginis. [37]

Indian Classical Music is closely linked with nature. [38] Nature affects our mind and body in a highly conspicuous manner. Similar effect on mind and body is created through different ragas. Thus, ragas can be classified based on time of the year, and even more specifically on the time of the day. [38] For example, if an experienced musician analyses the various forms of Raga Sarang, he will definitely understand and realize how the influence of Summer and the tune of Raga Sarang on our mind is very similar. The reflection of the mood of the rainy season is similarly projected by listening to Raga Malhar. When this Raga is played, its nuances spontaneously create this mood in one's mind even when their eyes are closed. When we hear these Ragas we instantly understand how deftly their mood has balanced the natural environment outside. The word Raga, in Sanskrit, originates from the phrase 'Ranjayate Iti Raga', meaning – that which can elicit in the mind of the connoisseur a particular sentiment or emotion, a state of mind (Ras). The nine ras or emotions are 'Shanta Ras' (tranquility and calmness), 'Bhayanak Ras' (fear), 'Karuna Ras' (sorrow), 'Hasya Ras' (laughter), 'Shringar Ras' (love), 'Vivatsya Ras' (horror), 'Bhakti Ras' (devotion). Although the interplay of these 'Ras' are more marked in the spiritual world its presence and influence in the world of music is also quite remarkable. [38]

Listening to Music involves much of the brain and coordinates a wide range of processing mechanisms. How music cognition relates to other complex cognitive abilities has always been a field of interest for research work. Very little serious research has been done into analysing the mechanism behind music's ability to physically influence the brain and even now the knowledge about the neurological effects of music is scarce. [35]

In ancient ages, lack of technological advancement hindered research into the effects of music on our mind and body. Sir C V Raman is noted for his pioneering work on Indian

Classical Music. [39] From 1909 to 1935 his research was primarily on studying the acoustics of musical instruments. On the basis of superposition velocities, he formulated the theory of transverse vibrations of bowed strings. He was the first to investigate the harmonics of Indian percussion instruments like tabla and mridangam. [35,40] Rigorous research was performed in the area of music by ITC Sangeet Research Academy from 1983 to 2010. Currently Sir C V Raman Centre of Physics and Music, Jadavpur University, is engrossed in pioneering research work in this field. [35]

Human brain is the most complex organic systems, involving billions of interrelated physiological and chemical processes. Music is an input to the brain system influencing human mind and body with time. Thus, the analysis of EEG while listening to music will reflect the level of consciousness and the areas of the brain affected by music. It is anticipated that this approach will provide a new perspective on cognitive musicology. Effects of music has also been studied with the Heart Rate variability (HRV), which aim to explain the effect of music on cognition and stress relaxation. [35] It is commonly believed that each music has a distinct frequency and it may or may not resonate with the body's rhythm (heart rate). [41]

Music of different genres and musical pattern lead to the production of distinct type of messengers in the body. This has been reported in a number of earlier studies. While the music of Johann Strauss induced enhancement in atrial filling fraction and atrial natriuretic peptide and decrement in cortisol and tissue-type plasminogen activator (t-PA), Ravi Shankar's music resulted in lowered concentrations of cortisol, noradrenaline, and t-PA [42-44]. Research on music therapy has shown that it can decrease pain and anxiety in critical care patients. Music has demonstrated effectiveness in reducing pain, decreasing anxiety, and increasing relaxation. In addition, music has been used as a process to distract persons from unpleasant sensations and empower them with the ability to heal from within [45,46]. Music is an effective adjunct to a pharmacologic antiemetic regimen for lessening nausea and vomiting, and this study merits further investigation through a larger multi-institutional effort [47]. Listening to music under general anaesthesia did not reduce preoperative stress hormone release or opioid consumption in patients undergoing gynaecological surgery [48].

It is very well-known and understood that Music affects emotions and mood. It is intensely connected to memories. By hearing to a few lines of a song or a tune, one can identify the respective song. The emotional content of music is very subjective. A piece of music may

be undeniably emotionally powerful, and at the same time be experienced in very different ways by each person who hears it. [35]

2.3 How Music affects Human Brain

The perception of music takes place in three stages: the first is an elementary perception of the auditory musical stimulus; the second corresponds to the structural analysis of music, at both an elementary (pitch, intensity, rhythm, duration, timbre) and an advanced level (phrasing, timing, themes); the third stage is identification of the work being played. Different cortical centers come into play for each of these functions. [49]

There are two distinct aspects of memory processes - the first refers to processes of the working memory system WMS, the second to long-term memory system LTMS. Any cognitive process depends on the resources of both systems. As an example, let us consider an everyday cognitive process such as recognizing a familiar object. The basic idea here is that after a sensory code is established, semantic information in long-term memory LTM is accessed which is used to identify the perceived object. If the matching process yields a positive result, the object is recognized which in turn leads to the creation of a short-term memory STM code. Complex cognitive processes such as speaking, and thinking may also be described in terms of a close interaction between the WMS and LTMS. The difference with the previous example is that in this case sensory code is lacking and a code is generated in STM which in the case of speaking represents a ‘plan’ of what to say. The codes generated in STM trigger search processes in LTM to retrieve the relevant knowledge about the appropriate semantic, syntactic and articulatory information. Cognitive performance is closely related and linked to the performance of the WMS and LTMS. With respect to the functional anatomy of memory, there is good evidence that brain structures that lie in the medial temporal lobe comprising the hippocampal formation and prefrontal cortex support various functions of the WMS. [50]

Passive listening to musical sounds induces activity in the temporal region, with greater prevalence on the right side, and this activity is more profound along with activity in the frontal lobe when the listener tries to discriminate pitch and timbre. Studies based on haemodynamics have revealed that specialized neural systems in right superior temporal cortex are involved in perceptual analysis of melodies, pitch comparisons involve right prefrontal cortex, but remembering the pitch involves activity of right temporal and frontal cortices. [49]

An experiment involving two groups of non-musicians who were musically trained for 2 weeks, with one group learning how to play a musical sequence on piano, while the other group listened and made judgements about the music, revealed that both sensorimotor training (learning to play the instrument), and auditory training (listening to music) causes plastic reorganizational changes in the auditory cortex, with the sensorimotor group showing greater changes. [49,51]

Another study on neural correlation of music and memory was performed using f-MRI revealed that musical memory involves right area of the hippocampus, temporal regions, interior left frontal gyrus, and left praecuneus. Activity of right hippocampal area is related to rate of success in recalling musical passage, thus this area is essential in musical memory. [49,52]

Independent studies have revealed that pleasant music decreases alpha power in the left frontal lobe and unpleasant music decreases alpha power in right frontal lobe. [53-55] Also, activity in the alpha frequency band has been found to be negatively related to the activity of the cortex, such that larger alpha frequency values are related to lower activity in the cortical areas of the brain, while lower alpha frequencies are associated with higher activity in the cortical areas [56,57].

Frontal midline (F_m) theta has been mostly related to heightened mental effort and sustained attention during various functions. The F_m theta power was positively correlated not only with scores of internalized attentions but also with subjective scores of the pleasantness of the emotional experience. Furthermore, two studies on the relationship between F_m theta and anxiety reported negative correlations between F_m theta during mental tasks and anxiety measures [57,58]. It has also been shown that pleasant music would elicit an increase of F_m theta power [59].

Recent researches have demonstrated that the modulation of gamma band activity (GBA) in time windows between 200 and 400 ms following the onset of a stimulus is associated with perception of coherent visual objects [60] and may be a signature of active memory. GBA has also been found sensitive to emotional vs. non-emotional stimuli and more specifically it was related to the arousal effect: GBA was enhanced in response to aversive or highly arousing stimuli compared to neutral picture [61]. While listening to music, degrees of the gamma band

synchrony over distributed cortical areas were found to be significantly higher in musicians than non-musicians [62,63].

A study of non-linear analysis of brain dynamics based on Indian Classical Music was done in [41]. The objective was to study how long the memory of music remains after the music has stopped. Detrended Fluctuation Analysis was used to obtain Fractal Dimension of segments of EEG with and without music. The study revealed complexity of alpha frequency rhythm was high during music in left and right frontal lobes during music, and when the music was turned off the variation of degree of complexity revealed retention of the previous state, suggesting a hysteresis like phenomenon.

Changes in alpha power in frontal and right parieto-temporal regions are involved in emotions. [64] Alpha pattern appears in wakefulness during relaxed alertness which is evoked while listening to Indian Classical Music. Greater left frontal EEG activity was seen in happy music, while sad music saw greater activity in right frontal EEG. [65] EEG alpha power is inversely related to activity; thus, lower alpha power means greater activity. [66] Also, Fractal Dimension values without music are generally lower than with music. [65]

2.4 How music affects the Cardiovascular System

Effects of music on the cardiovascular studies have not shown consistent results in various studies – some studies showed Heart Rate (HR) and Blood Pressure (BP) decreases with sedative or self-selected music, whereas, other studies showed no changes in HR and BP with music. It is hypothesised that inconsistencies across studies is due to individual response specificity in autonomic nervous system. Since HR is usually used as an index of stress, thus changes in HR with respect to music needs to be studied to understand the stress relaxing properties of music. [67]

Spectral analysis of Heart Rate Variability reveals three distinct peaks – a peak in the frequency range less than 0.05 Hz is called Very Low Frequency (VLF) and is considered to be related to body temperature, frequency band around 0.05 Hz to 0.15 Hz is called Low Frequency (LF) component. This band reflects the combined effect of both sympathetic and parasympathetic nervous systems. The frequency band ranging from 0.15 Hz to 0.5 Hz is called

the High Frequency (HF) component and reflects the activity of the parasympathetic nervous system. [67]

Slow paced classical music should usually have a relaxing effect, thus would activate the parasympathetic nervous (PNS) and reduce the effects of the sympathetic nervous system (SNS). A study by Iwanaga et al in 1997 based on six music segments revealed that sedative music caused an increase in the HF component of HRV. [68] Similar results were obtained in other studies too. [67] The coherent results indicate that sedative or relaxing music induces PNS activity, thereby showing a greater HF component in HRV. The LF component represents the combined activity of both PNS and SNS. This is due to the fact that in some conditions, associated with sympathetic excitation, a decrease in the absolute power of the LF component is observed. [69] In [70] it is concluded that LF/HF ratio serves as an index of SNS activity.

A study of HRV with repeated exposure to music was performed in [67]. It was seen Heart Rate gradually decreased with repeated exposure to music. LF component and LF/HF Ratio increased with exposure to both sedative and excitatory music but reduced when no music stimulus was present. It can be concluded from this that presence of music stimuli help activate the SNS. On the contrary, HF component was higher with sedative music than with excitatory music. Thus, HF component of HRV reflects the activity of PNS which decreases with excitatory music. Presence of music stimuli activates both the SNS and PNS, though PNS activity was profound in the case of sedative music. [67]

3. Methodology

> *The true laboratory is the mind, where behind illusions we uncover the laws of truth.*
> *- Acharya Jagadish Chandra Bose*

The basic steps followed from recording of a bio signal to analysis of the signal can be represented with the help of a flowchart:

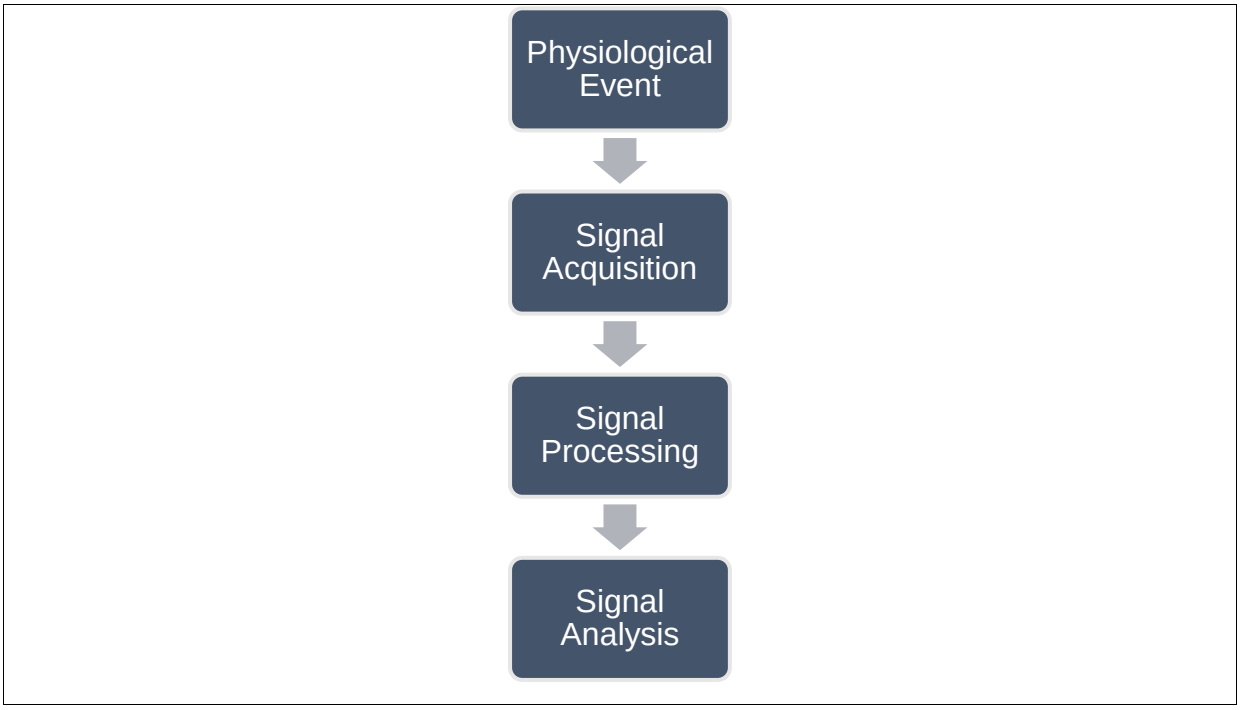

Figure 2.4-1 Overview of steps from physiological event to analysis

In order to study the effect of music on human mind and body we designed a methodology that would help us understand the effects of music as well as how we perceive and try to memorise musical patterns. It is a common experience that we can remember a song just by listening to the first lines. In order to understand how our brain works in response to music we designed the following methodology.

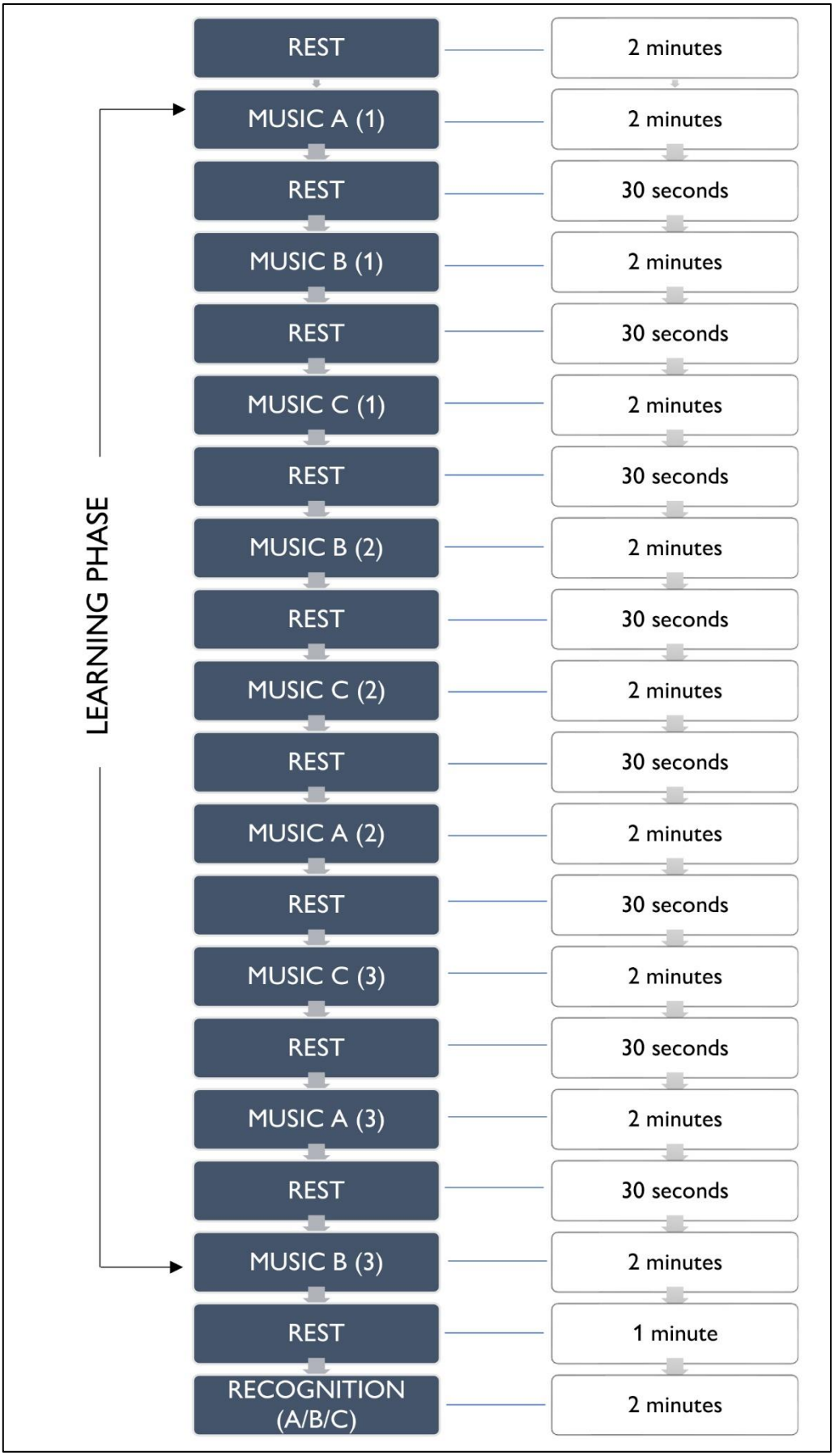

Figure 2.4-2 Protocol followed to record effect of music on Human Body

In the experimental protocol we have used 3 different Indian Classical Ragas, namely Ahir Bhairav, Bhimpalashree, and Yaman, recorded by late Pandit Ravi Shankar, an exceptional exponent of the stringed classical instrument – Sitar. The overall emotion linked with the three ragas is sadness, but the three different ragas have completely different characteristics, making them very distinct from each other. Even though three ragas are linked with pathos and sadness, they elicit in the mind of the listener emotions quite distinct from each other. The musical segments used is called 'alaap', in which the musician in a very slow manner demonstrates the character of the raga. The 'alaap' portion of a musical performance does not follow any tempo or rhythm. These conditions were maintained so that to a new listener the musical segment will be highly abstract, yet the subject will be able to differentiate between the three different ragas.

The whole experimental procedure is divided into two phases – learning phase and recognition phase. During the learning phase the subjects mind was trained to repeated exposure to short segments of music. The three ragas were played three times each. Each music segment was 2 minutes long and each music segment was slightly different from each other. Also, the order in which the three ragas were played were completely randomised. In between each musical segment, a gap of 30 seconds was maintained. At the beginning of each segment of music the name of the corresponding raga was mentioned. After completion of the learning phase, the subject was given a resting time of 1 minute after which one of the three ragas were played and the subject was asked to recognise the unknown musical segment.

The subjects participating in the study were all students and interns of School of Bioscience and Engineering, Jadavpur University, who gave their wilful consent to participate in the study. The total duration of the experiment is 27 minutes, during which EEG and ECG signals were recorded.

3.1 SIGNAL ACQUISITION

EEG was recorded using RMS EEG systems with 21 electrodes (Ag/AgCl sintered ring electrodes) placed according to the International 10/20 system.

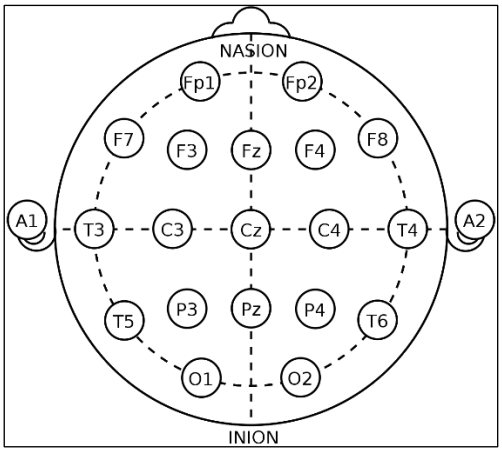

Figure 3.1-1 Placement of electrodes according to International 10.20 system

Impedance were checked below 20 kOhms. The ear electrodes A1 and A2 linked together have been used as the reference electrodes. The same reference electrode is used for all the channels. EEG has been recorded in the common average referential montage. The forehead electrode, FPz has been used as the reference electrode. The EEG recording system (Recorders and Medicare Systems) was operated at 256 samples/s recording on customized software of RMS. Each subject was seated comfortably in a relaxed condition in a chair in a shielded measurement cabin and were also asked to close their eyes. Professional monitoring headphones with flat frequency response (Audio Technica ATH-M20x) was used to play the musical segments. ECG was measured using ECG electrodes inbuilt into the RMS EEG recording system. Lead I of ECG recording was used which provided clean ECG signal adequate for HRV analysis. Sampling frequency was 256 samples/s. ECG electrodes were placed near shoulders of right and left arm. The ground electrode was placed on the right wrist.

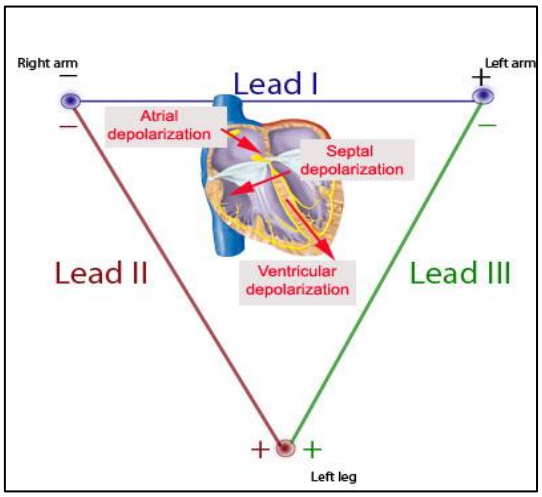

Figure 3.1-2 Placement of ECG electrodes

3.2 SIGNAL PROCESSING

The signals from the acquisition system was recorded into a PC with Intel i5 processor, 8GB RAM, and loaded into MATLAB® software for further processing and analysis. An important step of signal processing is signal denoising.

Since bio signals are very low amplitude signals, and are nonstationary in nature, they are easily corrupted by various forms of noise. Care must be taken while denoising ECG signal as noise and information spectra overlap. Hence the aim of any filtering technique must be to ensure minimum information loss and maximum noise elimination. In order to understand the optimal noise removal technique a study preceding this experiment was performed. Performance analysis of FIR IIR filters, wavelet denoising methods and Savitzky Golay filters were performed.

3.2.1 PERFORMANCE ANALYSIS OF FIR AND IIR FILTERS

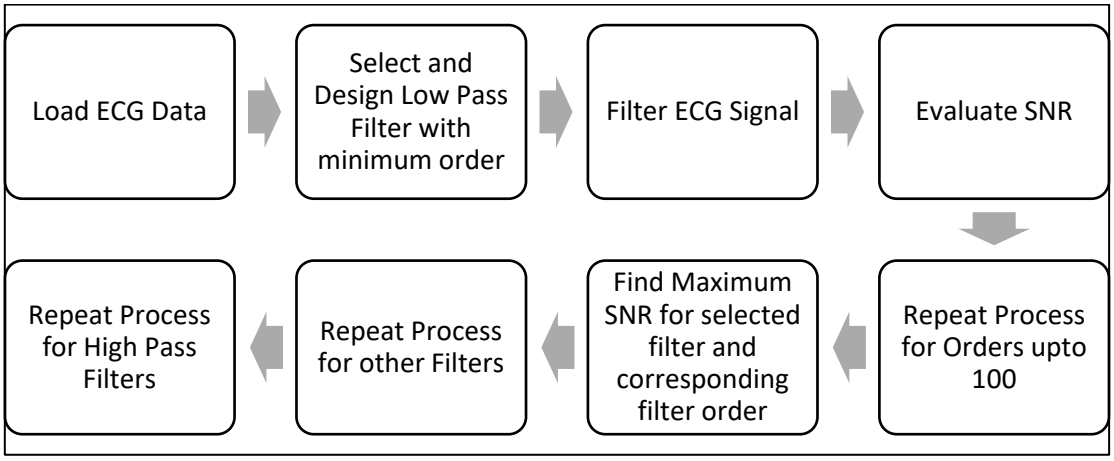

Figure 3.2-1 Methodology followed for analysis of FIR and IIR filters

- **Load ECG Data -** In this study, the SNR of various filter designs are obtained at different orders of the filter. For this purpose, we have used MIT-BIH ECG-ID Database, which contains both raw and filtered ECG Data, sampled at a frequency of 500 Hz [71][72]. 8 sets of raw and filtered data have been taken from the database for this study.

- **Select and Design Low Pass Filter with minimum order** - In this study, we will be using various FIR and IIR filter designs. FIR and IIR filters are two basic classes of Linear Time Invariant (LTI) filters.

  The FIR filters used in this study are:

  - Equiripple
  - Least Square
  - Constrained Least Square
  - Window Method
    i. Rectangular Window
    ii. Bartlett Window
    iii. Hanning Window
    iv. Hamming Window
    v. Blackman Window
    vi. Kaiser Window
  - Maximally Flat

  The IIR filters used in this study are:

  - Butterworth
  - Chebyshev type I
  - Chebyshev type II
  - Elliptic

The filters were designed in MATLAB software using the designfilt function. The filters were first designed with minimum order, and then after every iteration the order is incremented by 1 up till order 100.

- **Filter ECG Signal** – Frequency range of diagnostically useful ECG signa is 0.05 Hz to 150Hz, with maximum energy present in 0.5-45 Hz region. But for monitoring purposes and HRV analysis, a smaller range of the frequency spectrum can be used. ECG filtering can be done for diagnostic or for monitoring purposes. The diagnostically useful frequency range is accepted as 0.05 to 150 Hz [2]. In monitoring mode, frequency range of 0.5 to 40 Hz is used [78]. 8 sets of raw unfiltered ECG data with sample frequency of 500 Hz and sample length of 10,000 are taken and filtered with the designed filters.

In this study, SNR response of filter designs in both the diagnostic and monitoring ECG frequency ranges have been examined. Filter parameters have been set constant in order to effectively compare filter designs. The filter parameters are:

- Monitoring Frequency Range:
  i. Passband corner frequency = 40 Hz
  ii. Stopband corner frequency = 60 Hz
- Diagnostic Frequency Range:
  i. Passband corner frequency = 150 Hz
  ii. Stopband corner frequency = 160 Hz

- **Evaluate SNR** - SNR is ratio of the signal power (meaningful information) to the noise power (unwanted signal) and is expressed in dB.

$$\text{SNR} = \frac{P_{signal}}{P_{noise}} = \left(\frac{A_{signal}}{A_{noise}} \right)^2$$

$$\text{SNR}_{\text{dB}} = 10\log_{10}(\text{SNR})$$

Various filters are effectively compared for each set of data. Noise signal is extracted by taking the difference of raw signal and filtered signal obtained from MIT-BIH ECG-ID database.

Noise = Given Raw ECG Signal – Given Filtered Signal.

Since the denominator, that is, the noise data is constant in SNR across all filter designs, it is now possible to compare SNR of various filter designs.

- **Repeat process upto 100th order filter** - After SNR has been evaluated for the minimum possible order of the selected filter, the process is repeated in the form of a loop for all filter orders up till 100th order filter. Thus, relationship of SNR with filter order is obtained.

- **Find Maximum SNR for Selected Filter and find corresponding Filter Order** - SNR values for all order values of filter up to 100 are stored in an array, with corresponding filter orders. The array values are then analysed to find out the rate of change of SNR with filter order. The filter order above which there is no significant change in SNR, that is change in SNR is less than 10-2 units, is chosen as the filter order at which maximum SNR performance is obtained.

- **Repeat process for remaining filters -** The above stated steps are repeated for all of the selected filters and corresponding SNR and filter order relationship, and maximum value of SNR are obtained in both diagnostic and monitoring mode.

3.2.2 OPTIMIZATION OF DENOISING TECHNIQUES WITH ADDED GAUSSIAN NOISE

The methodology followed while analysis of various denoising techniques after addition of white Gaussian noise is given below –

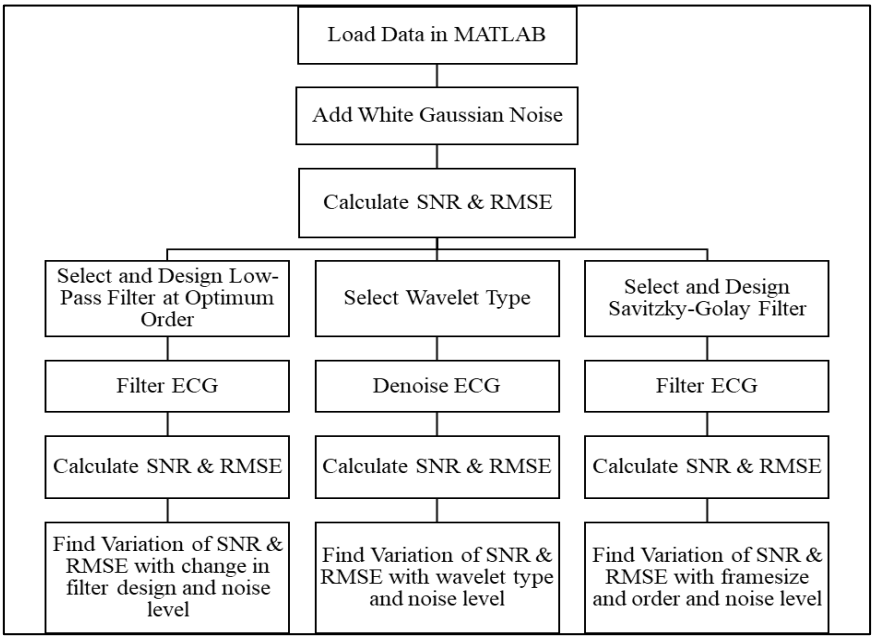

Figure 3.2-2 Methodology for analysis of denoising techniques after addition of white Gaussian noise

- **Add White Gaussian Noise** - White Gaussian noise of varying amplitude to the clean ECG signal, in order to study the variation of filter performance with amount of noise present in the signal. [73] We have added random white Gaussian noise of 10db, 15dB, 20dB, 25dB and 30dB successively to the signal, using the MATLAB function ‘wgn’.

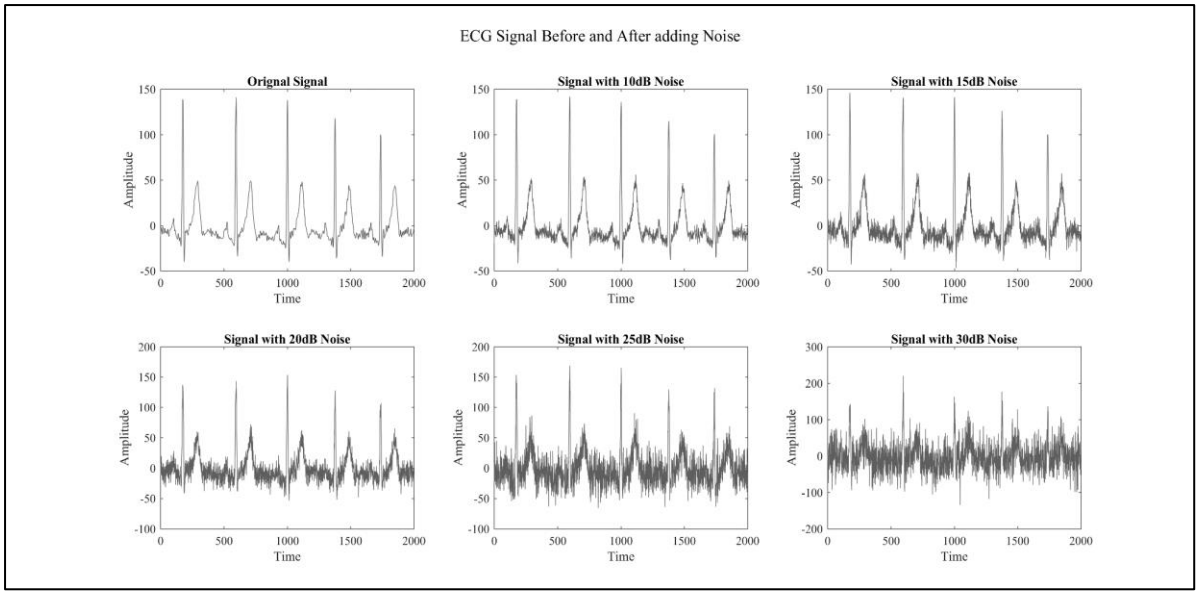

Figure 3.2-3 ECG signal before and after addition of noise.

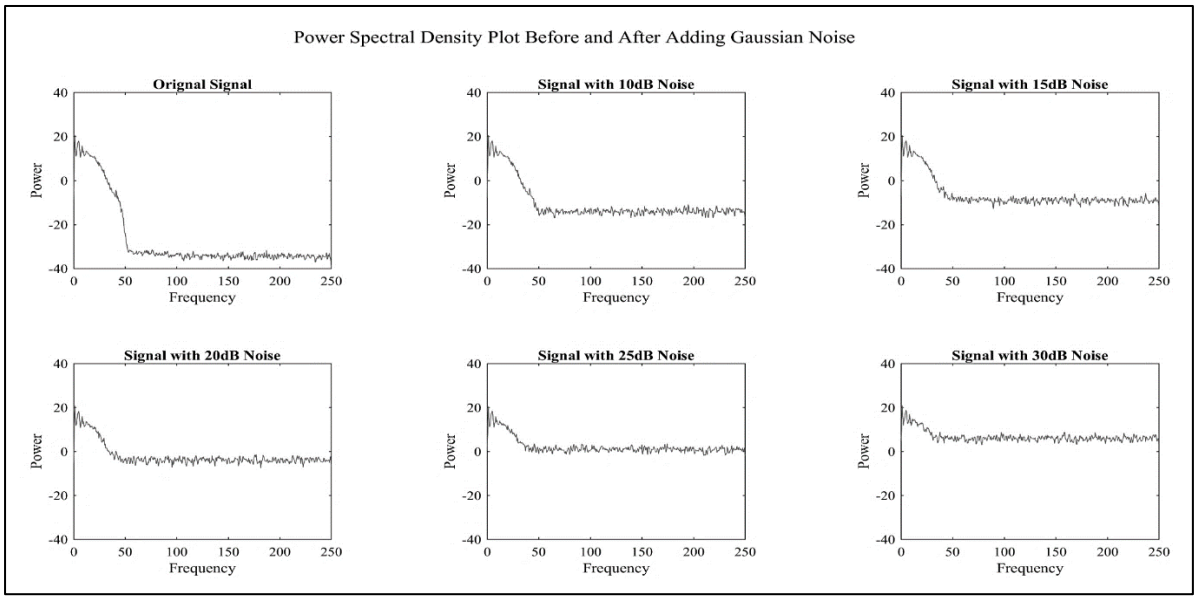

Figure 3.2-4 Frequency Spectrum of ECG Signal before and after adding noise.

- **Compute RMSE** - RMSE or Root Mean Square Error (also called Root Mean Square Deviation) is a parameter that quantifies the difference between two sets of values, generally one being observed values and the other being a modelled estimator. Thus, RMSE quantifies how closely the estimate matches to the actual values. RMSE is a measure of accuracy, quantifying the error between two sets of values. Thus, if RMSE value is low, the estimate closely represents the actual value. Mathematically RMSE or RMSD is represented as –

$$RMSE = \sqrt{\frac{\sum_{i=1}^{n}(x' - x)^2}{n}}$$

In our study we have considered three different filtering techniques – FIR & IIR filters, wavelet based denoising method and Savitzky Golay filters.

- **Select and Design Low Pass Filter with Optimum Order -** In our previous study we have already calculated the filter order at which we get maximum SNR performance for each filter. Next, we design the corresponding filter at its optimum filter order and then find the relation between SNR and amount of noise in the signal for each filter. For this we corrupt the ECG signal with 10dB, 15dB, 20dB, 25dB and 30dB noise respectively and then filter the corrupted ECG signals with the designed filter, and subsequently evaluate SNR in each case. The process is repeated for all filters.

3.2.3 WAVELET TRANSFORM AND WAVELET BASED DENOISING TECHNIQUES –

Fourier transform is very commonly used to understand the frequency content of a signal. While Fourier transform (FT) gives us the frequency amplitude representation of a signal, it is unable to tell us at what time a specific frequency occurs. This information is not required if the signal is stationary in nature, that is, its frequency components do not change with time. But most signals around us, including bio-signals, are non-stationary in nature. Thus, if we want to know at what specific time a certain frequency occurred in a bio-signal, Fourier transform will not be able provide that information.

In order to overcome this drawback of Fourier Transform, Short Term Fourier Transform (STFT) was developed. In STFT the signal is broken down into segments, and these small segments of signals are considered to be stationary and Fourier Transform is computed for each of these segments. For this purpose, a window function is employed which allows us to look into a small segment of the signal at a time, and by translating the window along the length of the signal, the frequency representation of the entire signal is obtained, while retaining time information also, which is obtained from the position of the window along the length of the signal. Thus, STFT gives us time-frequency representation of a signal. But STFT faces a serious drawback. In STFT, the signal is broken down into small segments using a window function inside which the signal is considered to be stationary. If the length of the window function is infinitely long, STFT is same as FT, that it has no time resolution but very high

resolution in frequency domain. As the window length is reduced, time resolution increases, that is we obtain some information about the time of occurrence of the frequencies, but we lose resolution in the frequency domain. Thus, narrower the window, the better the time resolution, and better assumption of stationarity, but poorer frequency resolution. [74]

Fourier Transform is represented by the equation -

$$X(f) = \int_{-\infty}^{\infty} x(t)\, e^{-2\pi jft} dt$$

where, *t* is time, *f* stands for frequency, and *x* denotes the signal whose transform is to be computed.

STFT is represented by the equation –

$$\text{STFT}\{x(t)\}(\tau, f) \equiv X(\tau, f) = \int_{-\infty}^{\infty} x(t) w(t-\tau) e^{-2\pi jft} dt$$

where, *w(t)* is the window function. Thus, STFT of signal is nothing but Fourier Transform of a signal multiplied by a window function.

Continuous wavelet transform was developed in order to overcome the problem of resolution faced in STFT. Wavelet is a short wave like oscillation of a short duration. A wavelet transform is can be defined as the representation of a function using wavelets. The wavelets are scaled and translated copies (daughter wavelets) of a finite-length or fast-decaying oscillating waveform, known as mother wavelet. Wavelet analysis is similar to STFT as in both the cases the signal is multiplied by a function, in STFT a window function, and in Wavelet Transform a mother wavelet. Wavelet transform is based on correlation analysis; therefore, the output is expected to be high when the input signal resembles the mother wavelet. [74][75] Continuous wavelet transform (CWT) is represented by the following equation –

$$CWT_x^{\varphi}(\tau, s) = \frac{1}{\sqrt{|s|}} \int_{-\infty}^{\infty} x(t) \overline{\psi}\left(\frac{t-\tau}{s}\right) dt$$

where $\overline{\psi}(t)$ is a continuous function in both the time domain and the frequency domain called the mother wavelet and the overline represents operation of complex conjugate. The main purpose of the mother wavelet is to provide a source function to generate the daughter wavelets which are simply the translated and scaled versions of the mother wavelet.

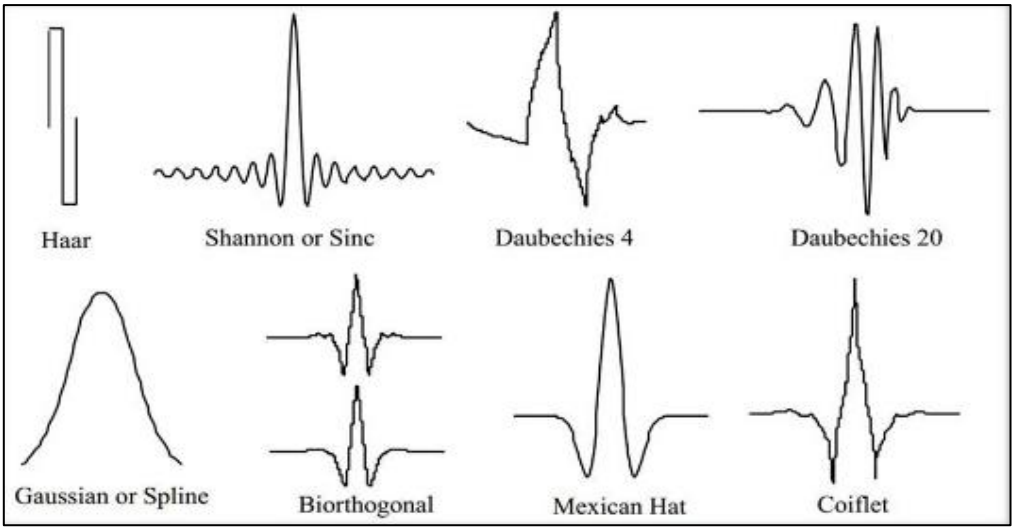

Figure 3.2-5 Some common types of wavelets

CONCEPT OF SCALE

The concept of scale in wavelet analysis can be simply understood by considering an analogy. Suppose an object on the ground is seen by a viewer standing on a ladder (scale) at a specific height from the ground. If the viewer moves higher up the scale away from the object, he will be able to see lesser details of the object and will get a global view of the object. Similarly, if the viewer moves down the scale he will be able to see finer details of the object and will get a closer view. Thus, higher scales correspond to global non-detailed view of the signal (low frequencies), whereas lower scales correspond to finer detailed view of the signal (higher frequencies).

Scaling as a mathematical function means either dilating or compressing a signal (in this case the mother wavelet). Consider the mother wavelet to be a piece of string. If the piece of string is stretched or compressed by holding its ends, the scale of the mother wavelet will change. Larger scales correspond to stretched or dilated mother wavelet, while on the other hand, smaller scales mean compressed mother wavelet.

In CWT, the mother wavelet at scale = 1 is initially placed at the start of the signal. The wavelet is then multiplied by the signal and translated along the length of the signal. At points the shape of the signal closely matches the wavelet, the wavelet coefficient will be high. The scale is then incremented slightly, and the process is repeated.

The wavelet coefficients thus carry information about the signal, with high coefficients referring to significant features of the signal, and thereby thresholding the wavelet coefficients

will remove unnecessary information from the signal, and subsequently denoise the input signal.

The wavelet types used in this study are –

i. Haar wavelet
ii. Daubechies wavelets
iii. Symlets
iv. Coiflets

Wavelet denoising is accomplished using the function 'wden' in MATLAB. The wavelet types considered in this study have been listen in the above section. ECG signal corrupted with 10dB noise is denoised with the 'wden' function using each wavelet type. SNR of the denoised signal is then calculated. The process is repeated for ECG signal corrupted by 15dB, 20dB, 25dB, 30dB noise, and the corresponding SNR is calculated.

3.2.4 SAVITZKY GOLAY FILTERS –

Savitzky and Golay proposed a method of data smoothing based on local least-squares polynomial approximation. [76] They showed that by fitting a polynomial to a set of input samples and evaluating the resulting polynomial at a single point within the approximation interval is equivalent to discrete convolution with a fixed impulse response. The lowpass filters obtained by this method are widely known as Savitzky Golay filters (S-G filters). [77]

In our work we are considering two parameters that affect the performance of Savitzky Golay Filters, namely, filter order and framesize, that is, the length of the filter. Filter order must always be less than framesize, when filter order = framesize – 1, the filter produces no smoothing. [78] But the question is what values of framesize and filter order will give the best results. For this purpose, we will compute SNR and RMSE for all possible values of Filter Order and Framesize up to 100 and find at which set of values of filter order and framesize we get the best result.

3.3 Analysis of Cardiovascular Dynamics with Music

The methodology followed for analysis of cardiovascular dynamics can be represented with the help of a flow chart –

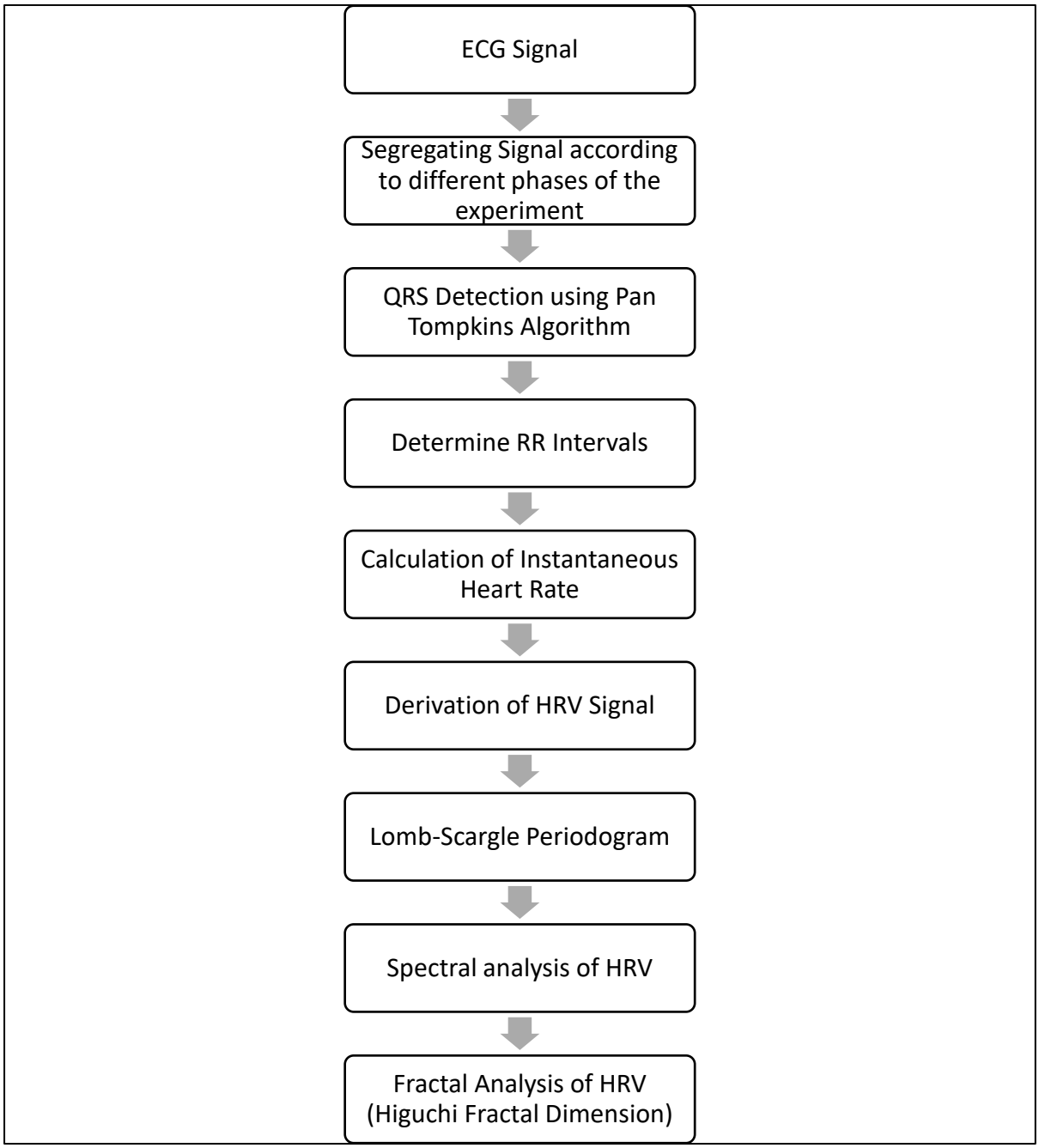

Figure 3.3-1 Methodology followed for analysis of Cardiovascular Dynamics with music

3.3.1 ECG PEAK DETECTION: PAN TOMPKINS ALGORITHM

The QRS peak detection algorithm introduced by Jiapu Pan and Willis J. Tompkins is the most widely used and often cited algorithm for the extraction of QRS complexes from electrocardiograms. [79] ECG is first passed through a series of low-pass and a high-pass filters. Then the filtered signal is passed through derivative, squaring and window integration phases. Finally, a thresholding technique is applied, and the R-peaks are detected.

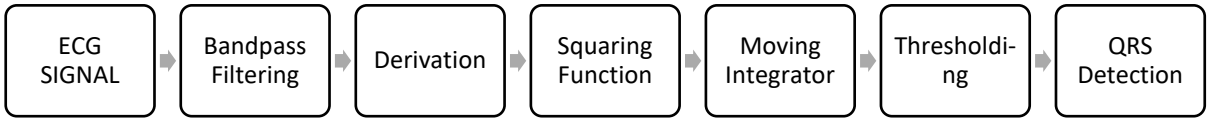

Figure 3.3-2 Flowchart of Pan Tompkins QRS detection algorithm

The purpose of the bandpass filtering is to isolate the predominant QRS energy centred at 10 Hz, and to attenuate the low frequencies characteristic of P and T waves and baseline drift, and also remove higher frequencies associated with muscle noise and power line interference. The next processing step is differentiation, which is a standard technique for finding high slopes that distinguish the QRS complexes from other ECG components. All the above processes are accomplished using linear filters. Next is a nonlinear transformation that consists of point-by-point squaring of the signal samples. This is done to make all the data positive prior to subsequent integration, and also makes the higher frequencies in the signal obtained from the differentiation process more conspicuous. These higher frequencies are normally characteristic of the QRS complex. The squared waveform passes through a moving window integrator. This integrator sums the area under the squared waveform over a 150-ms interval, then moves forward by one sample interval, and then integrates the new 150-ms window. The windows width is chosen to be long enough to include the time duration of extended abnormal QRS complexes, but short enough so that it does not overlap both a QRS complex and a T wave. Adaptive amplitude thresholds applied to the bandpass-filtered waveform and to the moving integration waveform are based on continuously updated estimates of the peak signal level and the peak noise. After preliminary detection by the adaptive thresholds, decision processes make the final determination as to whether or not a detected event was a QRS complex. A measurement algorithm calculates the QRS duration as

each QRS complex is detected. Thus, two waveform features are available for subsequent arrhythmia analysis—RR interval and QRS duration. [80]

3.3.2 HEART RATE VARIABILITY

Heart rate (HR) is not constant. It changes according to the needs of the body, with stress, sympathetic and parasympathetic stimulation. Analysis of the variations in instantaneous heart rate using the beat-to-beat RR-intervals (the RR tachogram) is known as Heart Rate Variability (HRV) analysis. The normal variability in heart rate results activity occurring in the two branches of the ANS, namely the sympathetic and parasympathetic nervous system. At rest, both sympathetic and parasympathetic nerves are active, with the effects of parasympathetic nervous system more predominant. Heart rate estimated at any instant of time represents the net effect of both the sympathetic and parasympathetic nervous system, where the sympathetic nervous system accelerates heart rate while parasympathetic nerves decelerate it. There is a direct natural relationship between HR and HRV. As HR increases there is less time between heartbeats for variability to occur, so HRV decreases, while at lower HRs there is more time between heartbeats, so variability naturally increases.

Spectral analysis of the RR tachogram is typically used to estimate the effect of the sympathetic and parasympathetic modulation of the RR-intervals. The two main frequency bands of interest are referred to as the Low-Frequency (LF) band (0.04 to 0.15 Hz) and the High-Frequency (HF) band (0.15 to 0.4 Hz). Sympathetic nervous system is believed to influence the LF component whereas both sympathetic and parasympathetic activity have an effect on the HF component. The ratio of the power contained in the LF and HF components has been used as a measure of the sympatho-vagal balance [69].

3.3.3 LOMB-SCARGLE PERIODOGRAM

RR tachogram is developed by sampling the heart (ECG signal) once per beat, which is thus uneven in time. Since the Fourier transform algorithm requires even sampling, it is necessary to re-sample the tachogram using interpolation. However, this approach has its own sets of problems: for example, linear interpolation is a poor approximation, and cubic splines create unacceptable oscillations when one RR interval is unusually longer than its predecessor. In order to avoid the drawbacks of interpolation, one method is to compute the Fourier spectrum

directly from the unevenly sampled tachogram. The Lomb periodogram is an excellent method for this operation, since it weights the data on a point-by-point basis rather than on a per-interval basis. It has been shown that the Lomb periodogram can provide a more accurate estimate of a tachogram's power spectral density (PSD) than interpolation followed by a regular Fourier transform. [81]

The Lomb-Scargle periodogram (Lomb 1976; Scargle 1982) is a well-known algorithm for detecting and characterizing periodicity in unevenly-sampled time-series. Lomb-Scargle method works directly with the nonuniform samples and thus makes it unnecessary to resample or interpolate. [82,83]

The periodogram at frequency *f* is estimated using -

$$P_{ls}(f) = \frac{1}{2\sigma^2}\left\{\frac{\left[\sum_j X_j \cos\omega(t_j-\tau)\right]^2}{\sum_j \cos^2\omega(t_j-\tau)} + \frac{\left[\sum_j X_j \sin\omega(t_j-\tau)\right]^2}{\sum_j \sin^2\omega(t_j-\tau)}\right\}$$

Where the time delay τ is defined by the formula,

$$\tan 2\omega\tau = \frac{\sum_j \sin 2\omega t_j}{\sum_j \cos 2\omega t_j}.$$

Thus, spectral estimation of HRV data, which is non-uniformly sampled in time, can be computed using Lomb-Scargle periodogram. The Lomb-Scargle periodogram is computed using the function *plomb*. From the obtained periodogram we can calculate the power of spectral bands – Low-Frequency (LF) band (0.04 to 0.15 Hz) and the High-Frequency (HF) band (0.15 to 0.4 Hz).

3.3.4 SPECTRAL ANALYSIS OF HRV

Three main spectral components of HRV signal of short durations, of 2 to 5 minutes, are - very low frequency (VLF), low frequency (LF), and high frequency (HF) components.

The distribution of the power and the central frequency of LF and HF are not fixed but changes with variations of the heart period. The physiological explanation of the VLF component is much less defined. The non-harmonic component which does not have coherent properties, and which is affected by algorithms of baseline or trend removal is commonly accepted as a major constituent of VLF. Thus, VLF assessed from short-term recordings is a dubious measure and should be avoided when interpreting the PSD of short-term ECGs.

Vagal activity (parasympathetic activity) is the major contributor to the HF component. LF components on the other hand represent activity of both the sympathetic and parasympathetic nervous system. Consequently, the LF/HF ratio is considered by some investigators to mirror sympatho/vagal balance or to reflect sympathetic modulations.

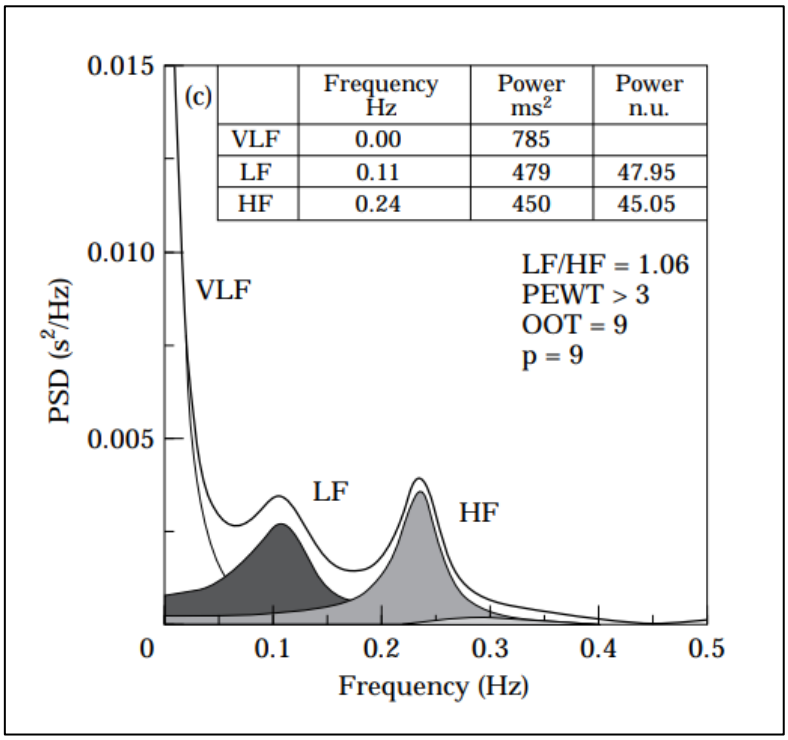

Figure 3.3-3 Spectral Components of HRV

Measurement of VLF, LF and HF power components is usually made in absolute values of power (ms^2), but LF and HF may also be measured in normalized units (n.u.) which represent the relative value of each power component in proportion to the total power minus the VLF component. The representation of LF and HF in n.u. emphasizes the controlled and balanced behaviour of the two branches of the autonomic nervous system.

3.4 ANALYSIS OF BRAIN DYNAMICS WITH MUSIC

The methodology followed for analysis of cardiovascular dynamics can be represented with the help of a flow chart –

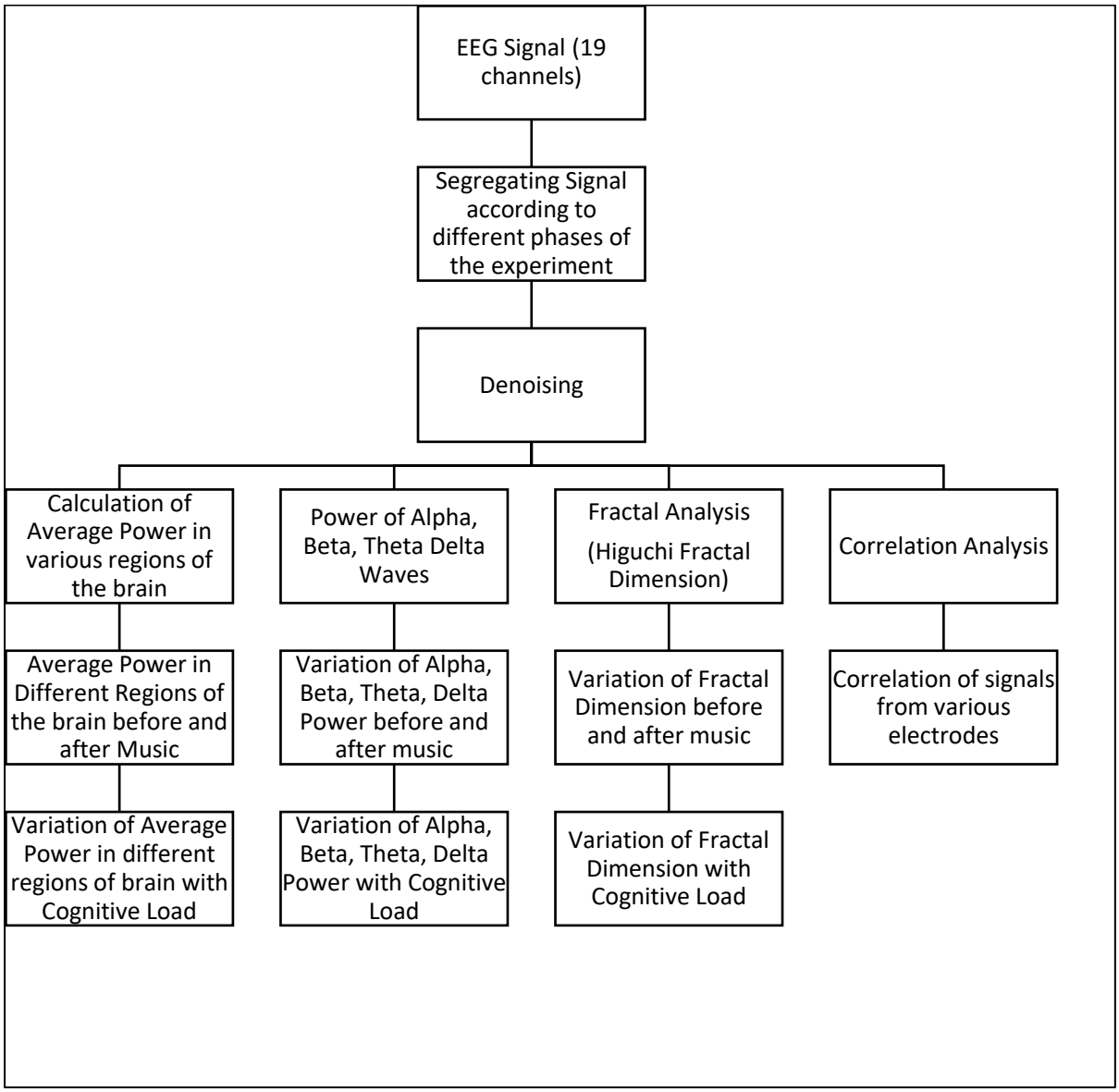

Figure 3.4-1 Methodology followed for analysis of Cardiovascular Dynamics with music

3.4.1 EEG DENOISING

EEG Denoising has been performed using Wavelet based denoising methods. 'db8' wavelet has been used, and the signal has been decomposed to level 8 using discrete wavelet transform. [31] Then thresholding of the wavelet coefficients has been done. Soft thresholding has been used. The threshold value has been set in such a way that only significant trends are

retained while high frequency noise has been removed. The threshold value has been determined manually and the same threshold has been set for all levels of decomposition. Thus, only significant features of all levels have been retained.

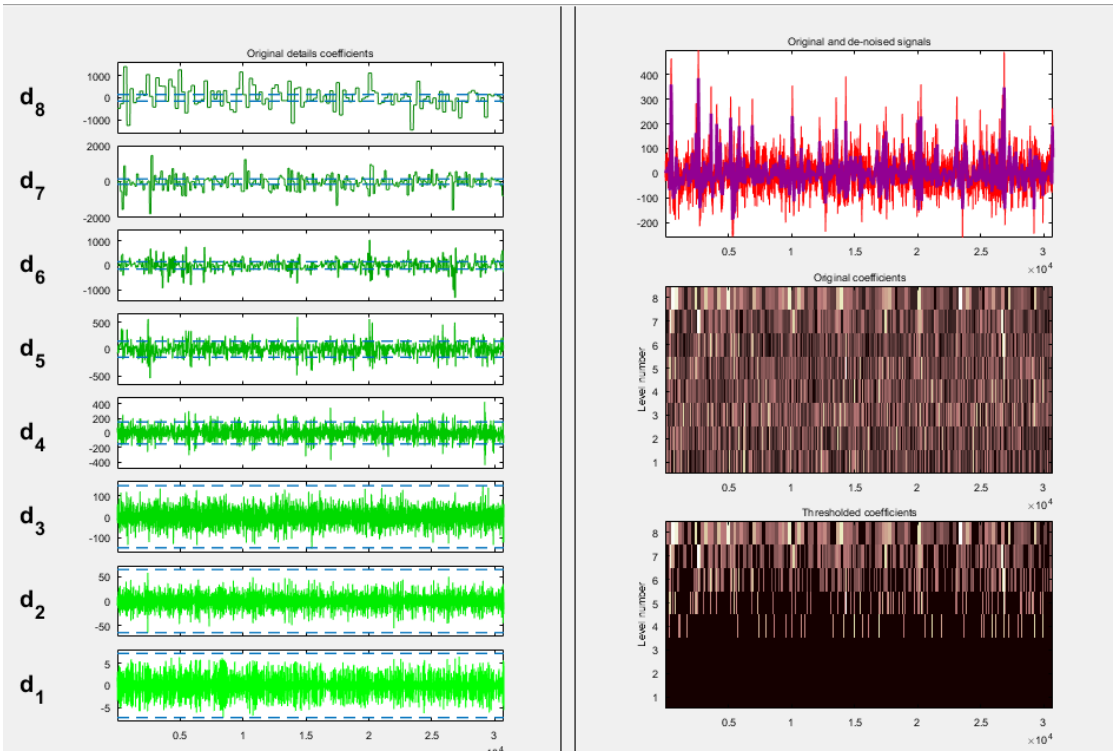

Figure 3.4-2 EEG denoising using wavelets

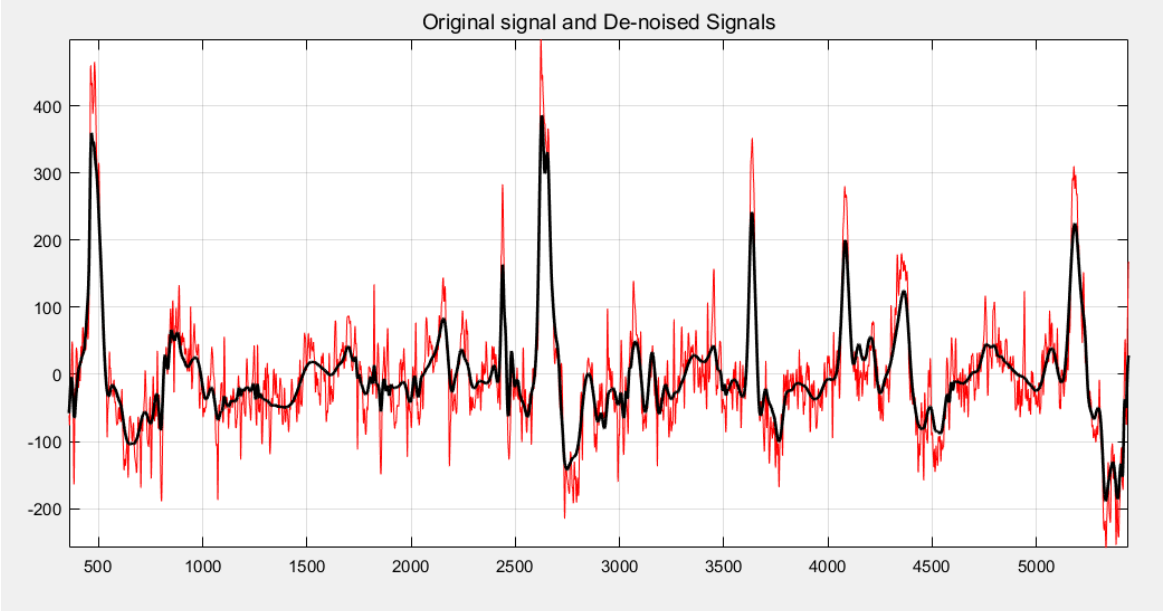

Figure 3.4-3 EEG signal before and after denoising

3.4.2 ANALYSIS OF POWER OF EEG SIGNALS

The power of a signal is the sum of the absolute squares of its time-domain samples divided by the signal length, or, equivalently, the square of its RMS level.

The average power of EEG signals in different phases of the experiment has been calculated on the basis of location of the electrodes. The electrodes have been clubbed according to its location, that is, frontal-polar, frontal, central, temporal, parietal and occipital. The average of power of electrodes in these regions have been calculated and compared.

3.4.3 ANALYSIS OF DIFFERENT BRAIN WAVES (ALPHA, BETA, THETA, DELTA).

The power of alpha, beta, theta, delta waves have been computed by Power Spectral Density (PSD) estimation of the waves. PSD estimate is calculated using Welch Power Spectral Density. The periodogram is not a consistent estimator of the true power spectral density of a wide-sense stationary process. Welch's technique to reduce the variance of the periodogram breaks the time series into segments, usually overlapping. Welch's method computes a modified periodogram for each segment and then averages these estimates to produce the estimate of the power spectral density. Because the process is wide-sense stationary and Welch's method uses PSD estimates of different segments of the time series, the modified periodograms represent approximately uncorrelated estimates of the true PSD and averaging reduces the variability. The segments are typically multiplied by a window function, such as a Hamming window, so that Welch's method amounts to averaging modified periodograms. Because the segments usually overlap, data values at the beginning and end of the segment tapered by the window in one segment, occur away from the ends of adjacent segments. This guards against the loss of information caused by windowing. [84] Power of alpha, beta, theta and delta waves have been computed from Welch Periodogram, during different phases of the experiment and then compared.

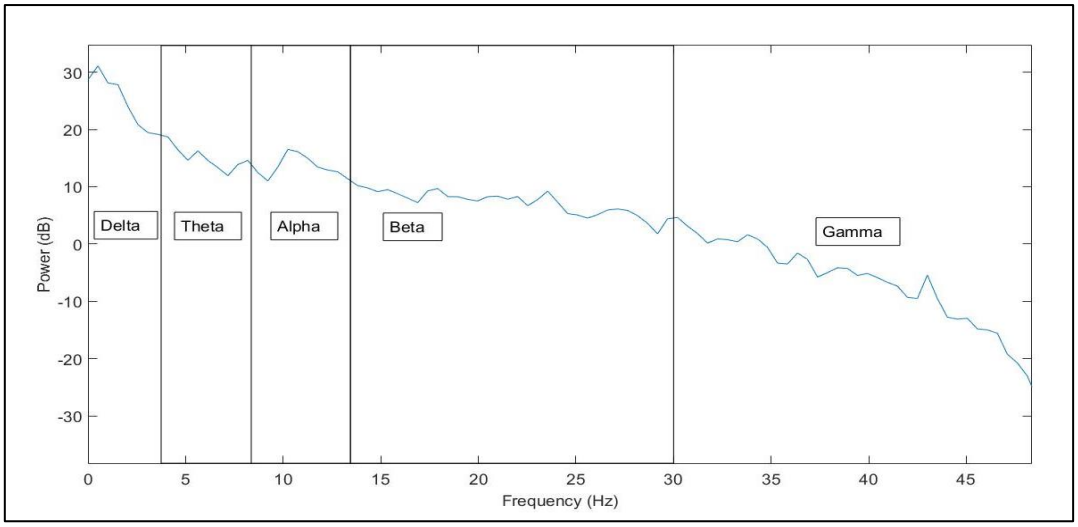

Figure 3.4-4 Welch Power Spectral Density Estimate of EEG showing different brain waves

3.4.4 CORRELATION ANALYSIS

Correlation quantifies the strength of a linear relationship between two variables. When two variables are highly correlated, increase in one variable will result in a subsequent increase in the second variable. When there is no correlation between two variables, then there is no tendency for the values of the variables to increase or decrease in tandem. Two variables that are uncorrelated are not necessarily independent, however, because they might have a nonlinear relationship. [85]

The population correlation coefficient $\rho_{X,Y}$ between two random variables X and Y with expected values μ_X and μ_Y and standard deviations σ_X and σ_Y is defined as

$$\rho_{X,Y} = \operatorname{corr}(X,Y) = \frac{\operatorname{cov}(X,Y)}{\sigma_X \sigma_Y} = \frac{E[(X-\mu_X)(Y-\mu_Y)]}{\sigma_X \sigma_Y}$$

where E is the expected value operator, *cov* means covariance, and *corr* is a widely used alternative notation for the correlation coefficient.

Methodology followed in Correlation Analysis in the protocol is given below –

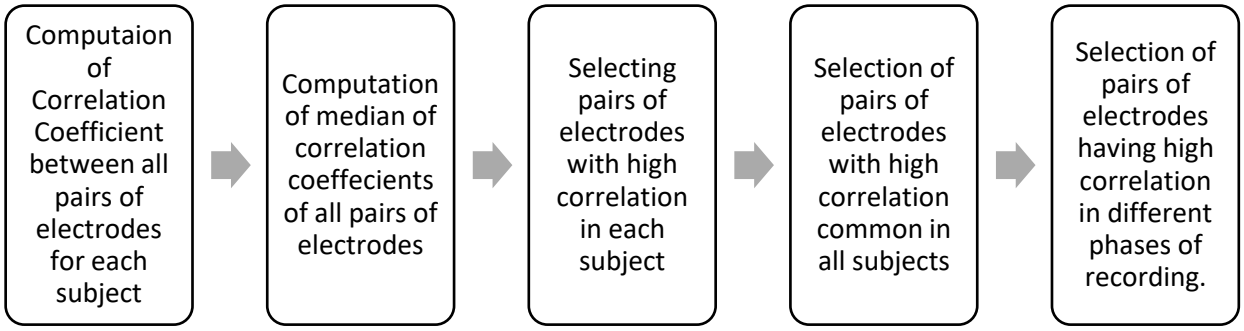

Figure 3.4-5 Methodology for correlation analysis of EEG Signals

Correlation coefficient for each pair of electrodes is calculated for all subjects. For each subject, statistical median of correlation coefficients is calculated. Pairs of electrodes with correlation coefficient greater than value of median are then marked. Pairs of electrodes with high correlation coefficient and common in all the subjects are then identified. And eventually pairs of electrodes having high correlation coefficient in each recording phase is identified.

3.5 Fractal Analysis of Brain and Cardiovascular Dynamics

The term "fractal" was first used introduced by mathematician Benoit Mandelbrot in 1975 and is derived from the Latin word *frāctus* which means "broken" or "fractured" and used it to describe objects whose complex geometry cannot be characterized by an integral dimension. [86] The main attraction of fractal geometry lies in its ability to describe the irregular or fragmented shape of natural features as well as other complex objects that traditional Euclidean geometry fails to analyse.

An important characteristic of all fractal objects is that their measured metric properties, such as length or area, are a function of the scale of measurement. [87] This can be explained by the classic example used by Mandelbrot himself in 1967 to describe the ‘‘length” of a coastline (Mandelbrot, 1967). According to Mandelbrot, the length of a coastline depends upon the length of the ruler used to measure the coastline. By using a large scale, the intricate details of the coastline cannot be captured. On the other hand, using an infinitely small scale, the length of the coastline will be infinitely large. When measured at a given spatial scale *d*, the total length of a crooked coastline *L(d)* is estimated as a set of *N* straight-line segments of length *d*. Since, the small details of the coastline not recognized at lower spatial resolutions but become apparent at higher spatial resolutions, the measured length *L(d)* increases as the scale of

measurement *d* increases. Thus, in fractal geometry, the Euclidean concept of ‘‘length” becomes a process rather than an event, and this process is controlled by a constant parameter. [88]

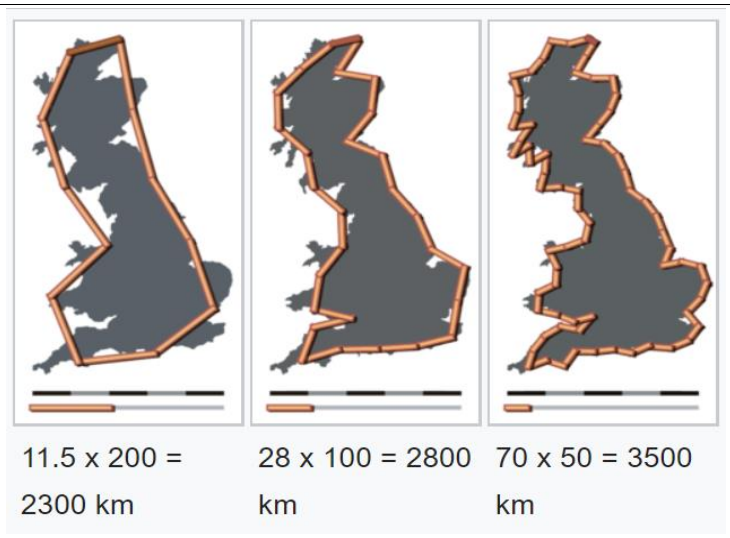

Figure 3.5-1 Classical example of coastline used by Mandelbrot to demonstrate characteristics of fractal objects.

The fractal nature of any object is quantified by Fractal Dimension. The general concept of dimension is that a line has 1 dimension, a plane has 2 dimensions, and a cube has three dimensions. There are two intuitively different ways to understand this statement, and both conclude to the same result. First, the dimension of an object is attributed to the degree of freedom of the object, that is, a line can move only in own direction – forward or backward, thus it’s dimension is 1. A plane on the other hand can be move up or down, forward or backward, thus has 2 dimensions. Similarly, a cube has dimension 3 as it can be moved in 3 directions, forward or backward, up or down, and into or away from the plane of paper. The second method is to understand the concept of scaling. Suppose the length of a straight line is divided by two, it would result into two sets of line with size half of the original line. If the length of each side of the square is divided by two, we get four sets of squares with size $1/4^{th}$ the original size of the square. Similarly dividing each side of a cube by 2 results in 8 different individual cubes, each having its size scaled down by $1/8^{th}$. This relation can be established by the formula –

$$N = S^D$$

where, N = number of self-similar objects, S = scale of magnification, D = dimension. Thus,

$$D = \frac{\log N}{\log S}$$

This dimension is called the Hausdorff-Besicovitch dimension.

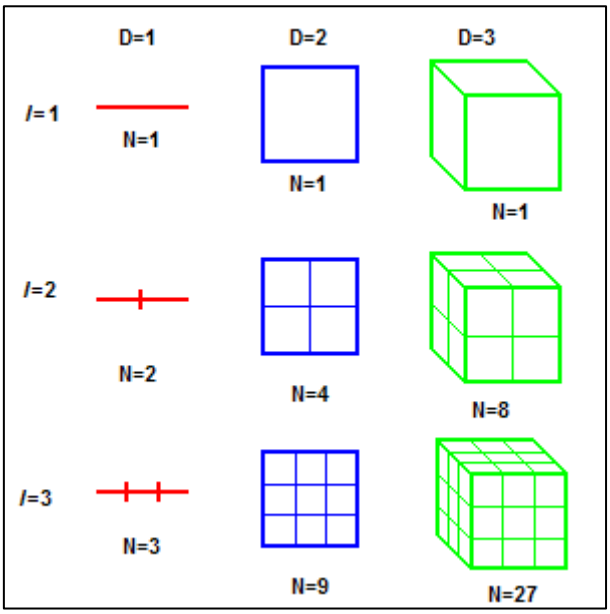

Figure 3.5-2 Definition of traditional scaling and dimension

Now, if we want to calculate the dimension of Sierpinski triangle, we will see that if the length of each side is divided by 2, or the triangle is scaled by a factor of $1/2$ it results in 3 self-similar triangles. Thus, the corresponding dimension is $\log 3 / \log 2 \approx 1.58$.

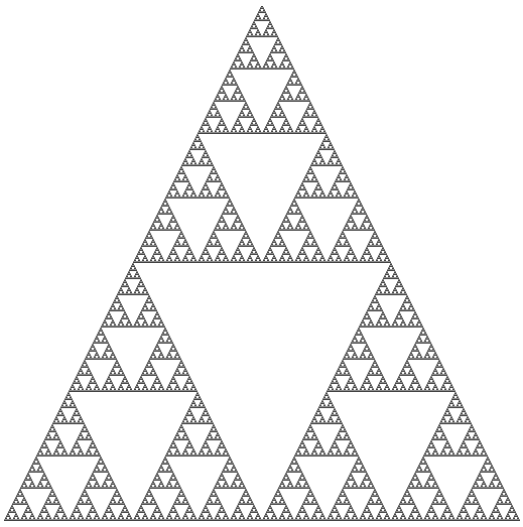

Figure 3.5-3 Sierpinski triangle

Thus, in mathematics, or to be more specific, in fractal geometry, fractal dimension provides a statistical index of complexity comparing how details in a pattern changes with the scale at which it is measured. Fractal dimension also describes the space-filling capacity of a pattern, for example, a curve with fractal dimension close to 1, behaves quite like an ordinary

line, but a curve with fractal dimension 1.9 winds in a complex pattern through space almost resembling a surface.

There are various methods of calculating the Fractal Dimension of a complex signal. In our study we have used Higuchi Fractal Dimension as it directly computes the fractal dimension of a complex system.

HIGUCHI FRACTAL DIMENSION

Higuchi's (1988) algorithm is based on the measure of the mean length of the curve *L(k)* by using a segment of *k* samples as a unit of measure. From a given time series *X(1), X(2),. . . , X(N),* the algorithm constructs *k* new time series; each of them, X^k_m, is defined as

$$X_m^k: X(m), X(m+k), X(m+2*k), \ldots\ldots, X\left(m+\left[\frac{N-m}{k}\right].k\right) \qquad m = 1,2,3..k$$

where, $\left[\frac{N-m}{k}\right]$ is Gauss' notation and m and k are integers indicating the initial time and the interval time, respectively. For time interval *k*, we get *k* sets of time series. In the case of *k = 3* and *N = 1000*, for example, three time series are produced:

$$X_1^3: X(1), X(4), X(7), \ldots\ldots, X(997)\ X(1000)$$
$$X_2^3: X(2), X(5), \ldots., X(998)$$
$$X_3^4: X(3), X(6), \ldots., X(999)$$

Then, the length of the curve X^k_m is defined as:

$$L_m(k) = \frac{\left\{\left(\sum_{i=1}^{\left[\frac{N-m}{k}\right]} | X(m+ik) - X(m+(i-1).k)|\right)\frac{N-1}{\left[\frac{N-m}{k}\right].k}\right\}}{k}$$

$\frac{N-1}{\left[\frac{N-m}{k}\right].k}$ is the normalization factor for the curve length of subset time series.

Finally, the length of the curve for the time interval k is calculated as the average value of k sets of $L_m(k)$, and is represented as $\langle L(k)\rangle$. If the given curve is a fractal then the relation will be true –

$$L_m(k)\ \alpha\ k^{-D}$$

Finally, the fractal dimension can be obtained by logarithmic plotting of $\langle L(k) \rangle$ against different value of *k* ranging to k_{max}. The data then should fall on a straight line with slope *-D,* where D is the fractal dimension obtained by Higuchi's method, and thus called Higuchi's fractal dimension. [89,90,91]. Thus, Higuchi's method gives direct estimation of fractal dimension by selecting a suitable value of $k_{max.}$

The suitable value of k_{max} is determined by initially plotting values of fractal dimension *D* for a range of values of *k*. The value of *k* after which the variation of *D* saturates, and the curve represents a plateau is chosen as the optimal value of k_{max} . [92]

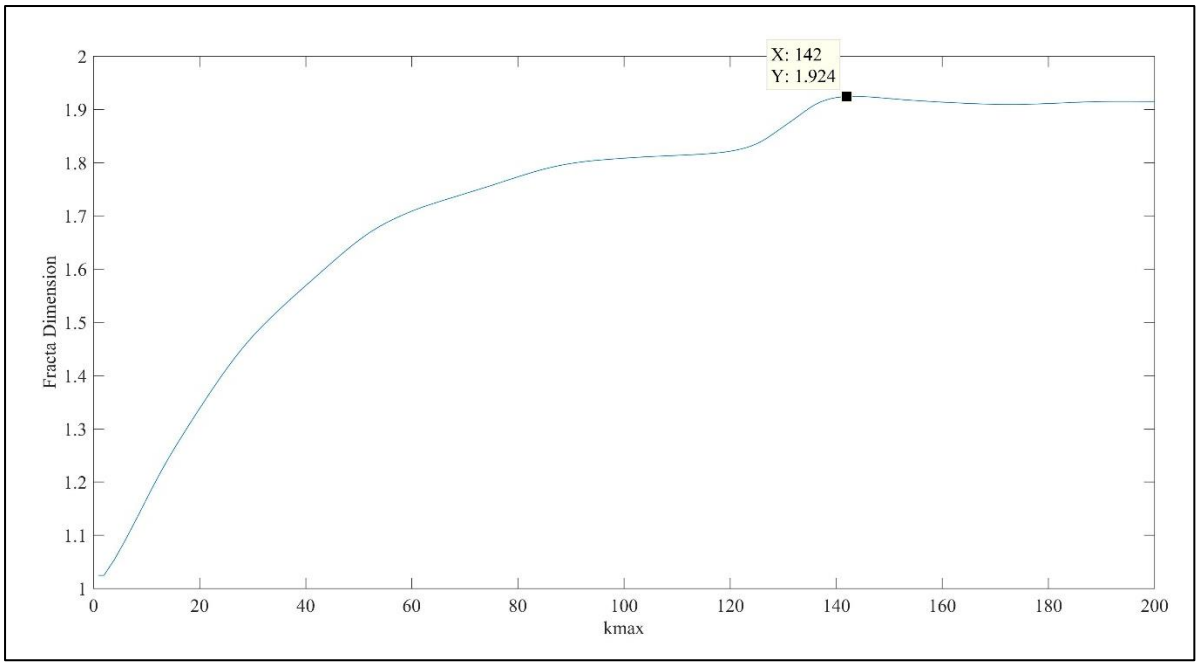

Figure 3.5-4 Selection of kmax to obtain Fractal Dimension by Higuchi's Method

4. Results

4.1 ECG DENOISING

4.1.1 LOWPASS FILTER PERFORMANCE IN MONITORING MODE

COMPARISON OF PEAK SNR VALUE ACROSS FILTERS (MONITORING MODE)

Average maximum SNR value for eight data sets, and the corresponding filter order are given in the table below:

Table 4.1-1 Comparison of Peak SNR of FIR Filters (Monitoring Mode)

Filter	Average Peak SNR (dB)	S.D.	Corresponding Filter Order
Equiripple	8.0789	1.3195	7
Least Square	6.3348	1.3203	9
Constrained Least Square	4.8133	1.3382	23
Rectangular Window	6.1650	1.3719	24
Bartlett Window	5.2214	1.0830	3
Hanning Window	5.2214	1.0830	3
Hamming Window	5.3494	1.0670	2
Blackman Window	5.2213	1.0830	3
Kaiser Window	6.0367	1.3698	24
Maximally Flat	4.5362	1.3300	16

Table 4.1-2 Comparison of Peak SNR of IIR Filters (Monitoring Mode)

Filter	Average Peak SNR (dB)	S.D.	Corresponding Filter Order
Butterworth	4.7240	1.2318	2-4
Chebyshev type I	5.0909	1.1066	1
Chebyshev type II	4.5516	1.3260	12-14
Elliptic	5.0909	1.1066	1

From Table I, it is seen that FIR Equiripple filters have the highest SNR value. Amongst the various window-based filter designs methods, Kaiser and Rectangular window have the highest SNR value, but at a higher filter order. Hamming window achieves an appreciable SNR value at a very low order. Amongst the IIR filters, Chebyshev type I and Elliptic filters have the highest SNR values at order 1. Butterworth filter achieve highest SNR values when filter

order is in the range of 2 to 4, and Chebyshev type II filters achieve maximum SNR values when filter order is in between 12 and 14. Maximally flat filters can be designed only with even number order values.

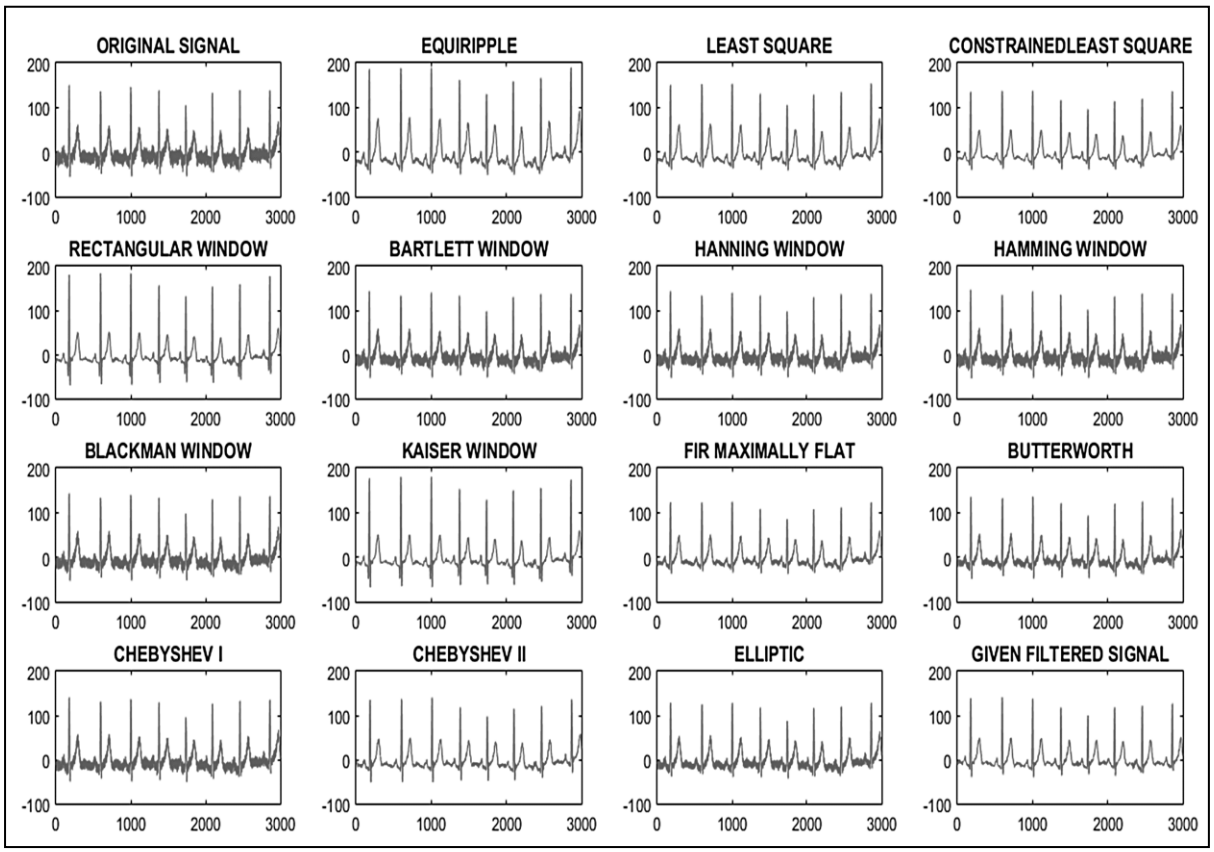

Figure 4.1-1 ECG Denoising by Various Filters in Monitoring Mode

RELATIONSHIP OF SNR AND FILTER ORDER (MONITORING MODE):

The variation of SNR with respect to filter order of various filters has been represented through graphs. For the sake of simplicity and neat representation, only one data set has been shown in the graphs. All the data sets show similar patterns for respective filters.

It is seen that in all cases, SNR values saturate or decrease as filter order increases. Maximum SNR performance is realized in a low order, after which there is not much significant change in SNR values with increase in filter order.

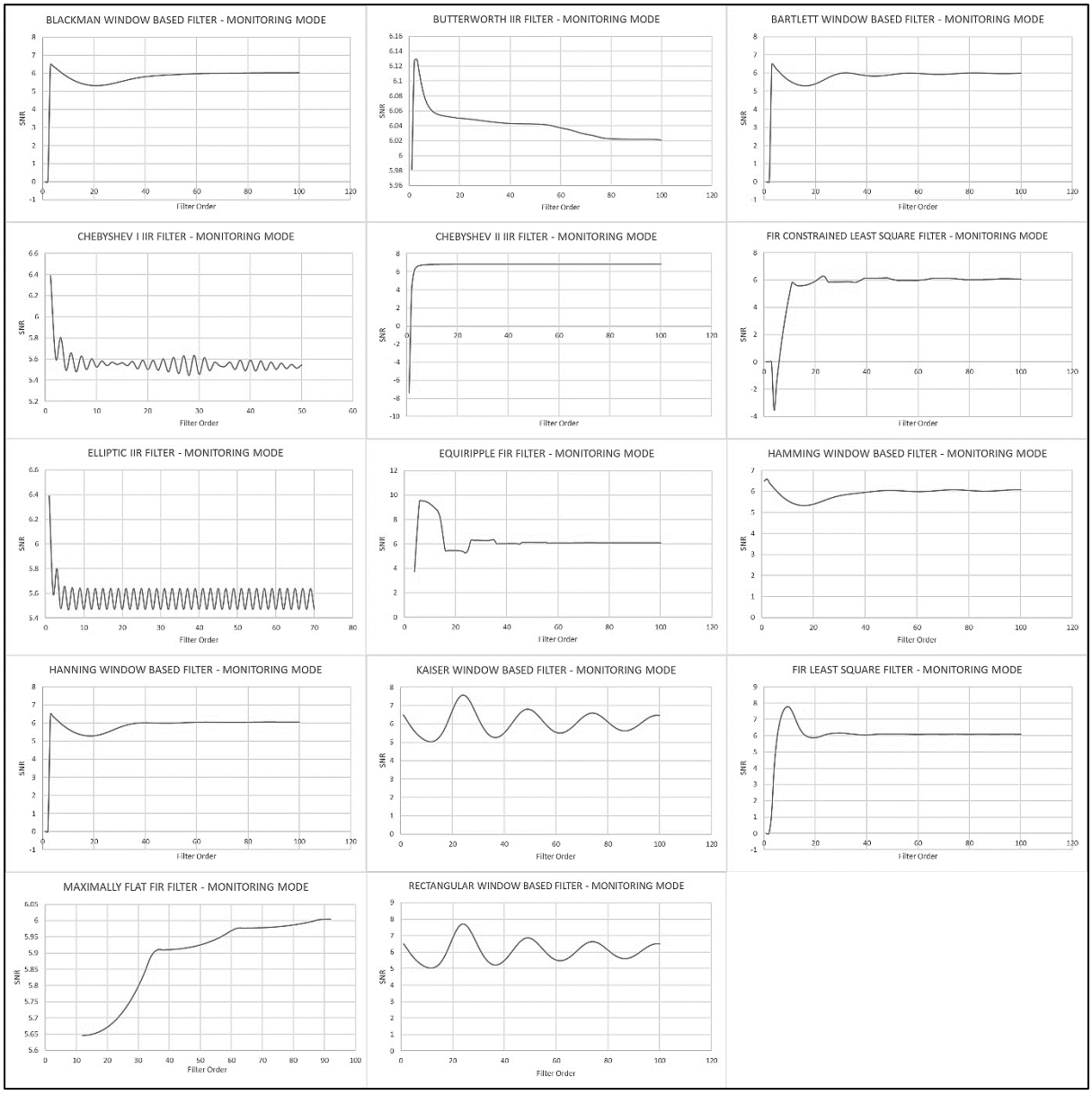

Figure 4.1-2 Variation of SNR with filter order in monitoring mode

4.1.2 LOWPASS FILTER PERFORMANCE IN DIAGNOSTIC MODE

COMPARISON OF PEAK SNR VALUE ACROSS FILTERS (DIAGNOSTIC MODE)

Average of the maximum value of SNR for each data set, and the corresponding filter order are given in the table below:

Table 4.1-3 Comparison of Peak SNR of FIR Filters (Diagnostic Mode)

Filter	Average Peak SNR	S.D.	Corresponding Filter Order
Equiripple	11.6345	1.1166	3
Least Square	7.4529	1.1037	3

Filter	Average Peak SNR	S.D.	Corresponding Filter Order
Constrained Least Square	5.8469	1.0592	4
Rectangular Window	6.3689	0.92412	6
Bartlett Window	5.5043	1.0313	8
Hanning Window	5.4749	1.0377	10
Hamming Window	5.4728	1.0415	12
Blackman Window	5.4569	1.0841	3
Kaiser Window	6.2844	0.9323	6
Maximally Flat	5.4564	1.0483	14

Table 4.1-4 Comparison of Peak SNR of IIR Filters (Diagnostic Mode)

Filter	Average Peak SNR	S.D.	Corresponding Filter Order
Butterworth	5.4566	1.0477	2-4
Chebyshev type I	5.4627	1.0521	1
Chebyshev type II	5.4325	1.0467	6-10
Elliptic	5.4180	1.0974	1

In diagnostic mode, Equiripple FIR filters show the highest SNR values. In general, Peak SNR performance is achieved at a lesser filter order than in monitoring mode.

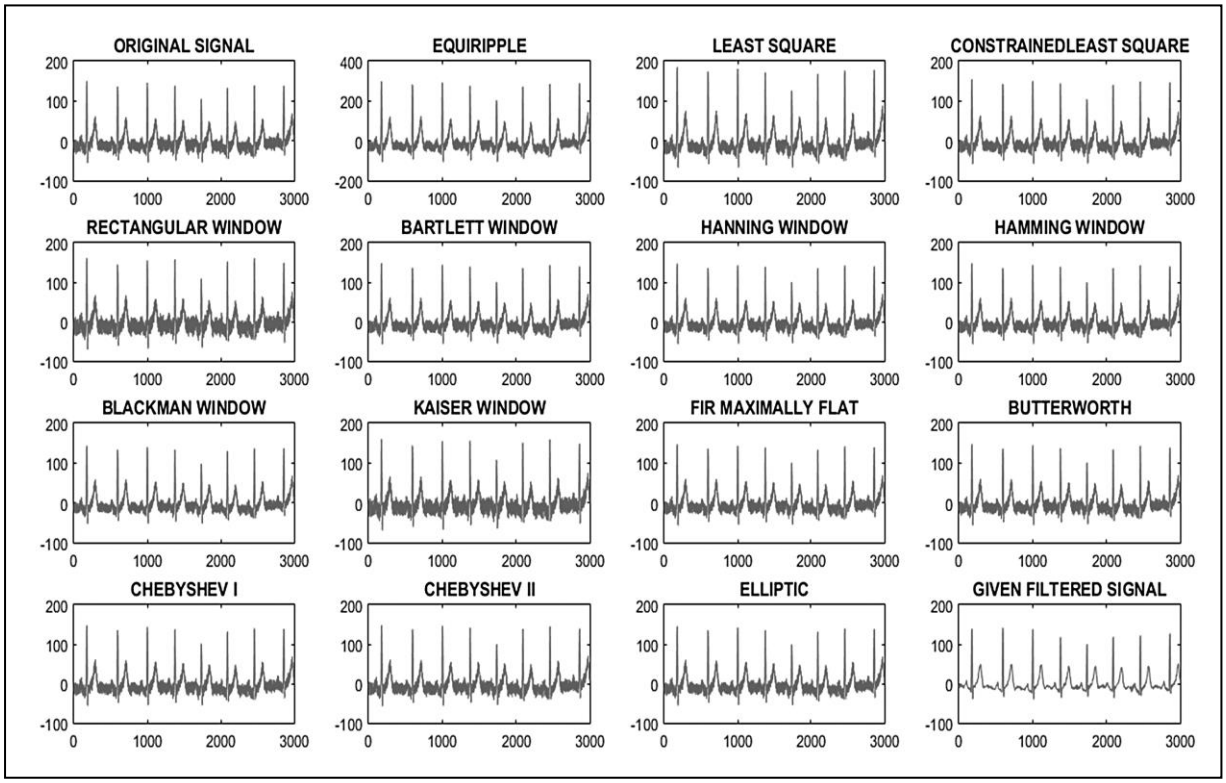

Figure 4.1-3 ECG Denoising by Various Filters in Monitoring Mode

RELATIONSHIP OF SNR AND FILTER ORDER (DIAGNOSTIC MODE):

The variation of SNR with respect to filter order of various filters in diagnostic mode has been shown below:

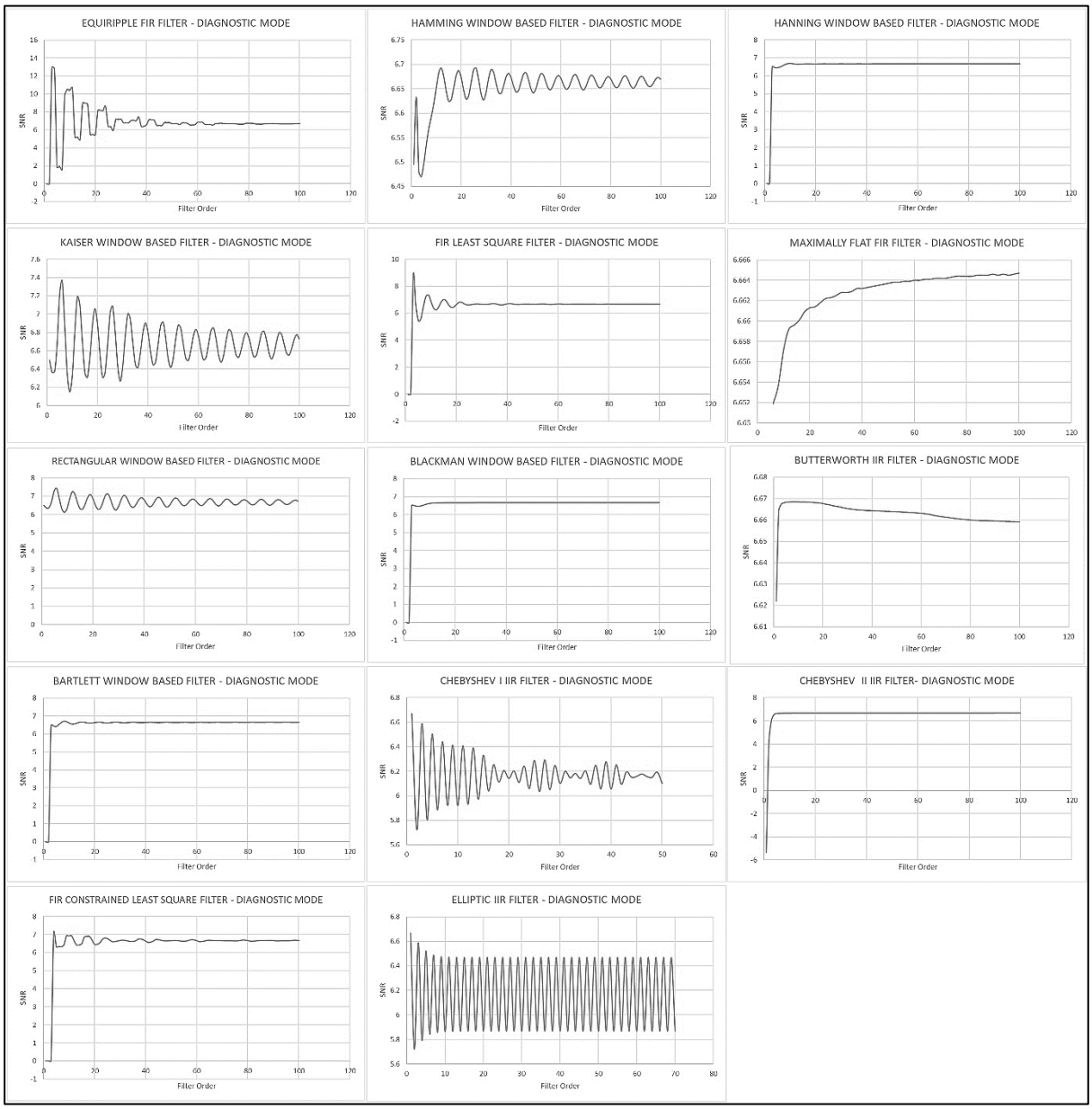

Figure 4.1-4 Variation of SNR with filter order in diagnostic mode

It is interesting to note here that in both diagnostic and monitoring mode, the SNR response of all filters either saturate or decrease with increasing filter order. Also, a particular filter, the variation of SNR with filter order may or may not be same in monitoring and diagnostic mode. In either case, the optimum filter order at which maximum SNR performance is achieved has been identified.

4.1.3 VARIATION OF SNR WITH AMOUNT OF ADDED NOISE AT OPTIMAL FILTER ORDER

The filter order at which the filters give maximum SNR performance have been obtained from the previous results. Now we will study the variation of SNR across filter order as amount of noise is incrementally increased.

Table 4.1-5 Variation of SNR and RMSE with added Noise at Optimal Filter Order

Filter	Noise Power (dB)	Average Peak SNR (dB)	SD	RMSE	SD	Optimal Filter Order
Equiripple	10	21.7023	0.6212	14.5205	1.1490	3
	15	16.7692	0.6291	15.0837	1.0738	
	20	11.8936	0.6551	16.8702	0.9694	
	25	7.4131	0.5653	21.3518	0.7378	
	30	3.5601	0.3988	31.9494	0.8336	
Least Square	10	19.5875	0.6213	8.0932	0.7092	3
	15	14.6608	0.6283	8.7806	0.6442	
	20	9.8046	0.6514	10.7556	0.5218	
	25	5.3755	0.5556	15.3503	0.3884	
	30	1.6334	0.3823	24.9228	0.4960	
Constrained Least Square	10	18.7065	0.6220	8.9516	0.8564	4
	15	13.7905	0.6275	9.5593	0.8041	
	20	8.9666	0.6462	11.3340	0.6589	
	25	4.6213	0.5409	15.6610	0.4978	
	30	1.0514	0.3588	24.8427	0.5534	
Rectangular Window	10	18.6279	0.6262	13.1276	1.3003	6
	15	13.7351	0.6286	13.6831	1.2526	
	20	8.9794	0.6378	15.3664	1.0812	
	25	4.8037	0.5143	19.7331	0.8541	
	30	1.5552	0.3199	29.6398	0.8195	
Bartlett Window	10	18.4883	0.6227	16.4615	1.6008	8
	15	13.5759	0.6278	16.7997	1.5720	
	20	8.7627	0.6448	17.8698	1.4494	
	25	4.4445	0.5365	20.8902	1.2120	
	30	0.9286	0.3517	28.4563	1.1444	
Hanning Window	10	18.4757	0.6225	19.8219	1.8896	10
	15	13.5608	0.6279	20.0951	1.8656	
	20	8.7405	0.6460	20.9684	1.7596	
	25	4.4042	0.5397	23.4962	1.5210	

Filter	Noise Power (dB)	Average Peak SNR (dB)	SD	RMSE	SD	Optimal Filter Order
	30	0.8519	0.3568	30.2113	1.4455	
Hamming Window	10	18.4803	0.6223	22.8761	2.1273	12
	15	13.5676	0.6273	23.1240	2.1042	
	20	8.7542	0.6447	23.9153	2.0098	
	25	4.4351	0.5367	26.2218	1.7609	
	30	0.9167	0.3517	32.5756	1.6834	
Blackman Window	10	18.4362	0.6213	6.7744	0.6212	3
	15	13.5191	0.6269	7.5061	0.5664	
	20	8.6917	0.6459	9.5119	0.4335	
	25	4.3374	0.5415	14.0935	0.3242	
	30	0.7501	0.3599	23.2621	0.4142	
Kaiser Window	10	18.6154	0.6259	13.0928	1.2959	6
	15	13.7205	0.6286	13.6351	1.2493	
	20	8.9586	0.6387	15.2820	1.0811	
	25	4.7681	0.5167	19.5674	0.8550	
	30	1.4928	0.3232	29.3157	0.8211	
Maximally Flat	10	18.4700	0.6214	25.4965	2.3075	14
	15	13.5649	0.6252	25.7449	2.2833	
	20	8.7739	0.6394	26.5325	2.1970	
	25	4.5115	0.5251	28.8290	1.9210	
	30	1.1011	0.3359	35.2674	1.8386	
Butterworth	10	18.4706	0.6215	4.0154	0.2669	3
	15	13.5655	0.6252	5.3605	0.2080	
	20	8.7746	0.6395	8.3384	0.1420	
	25	4.5130	0.5252	14.0688	0.1715	
	30	1.1032	0.3358	24.6050	0.3014	
Chebyshev type I	10	18.4750	0.6200	2.8254	0.0333	1
	15	13.5879	0.6216	4.8593	0.0363	
	20	8.8481	0.6276	8.5725	0.0852	
	25	4.7113	0.5006	15.2047	0.1478	
	30	1.5323	0.3024	26.9906	0.2094	
Chebyshev type II	10	18.4707	0.6215	8.3654	0.7955	8
	15	13.5660	0.6250	9.0810	0.7386	
	20	8.7761	0.6395	11.1118	0.5817	
	25	4.5183	0.5250	15.8965	0.4413	
	30	1.1124	0.3326	25.7646	0.4972	
Elliptic	10	18.4545	0.6210	2.8892	0.0933	1
	15	13.5477	0.6252	4.5481	0.0683	

Filter	Noise Power (dB)	Average Peak SNR (dB)	SD	RMSE	SD	Optimal Filter Order
	20	8.7508	0.6397	7.7645	0.0876	
	25	4.4740	0.5269	13.6122	0.1324	
	30	1.0382	0.3382	24.0932	0.2413	

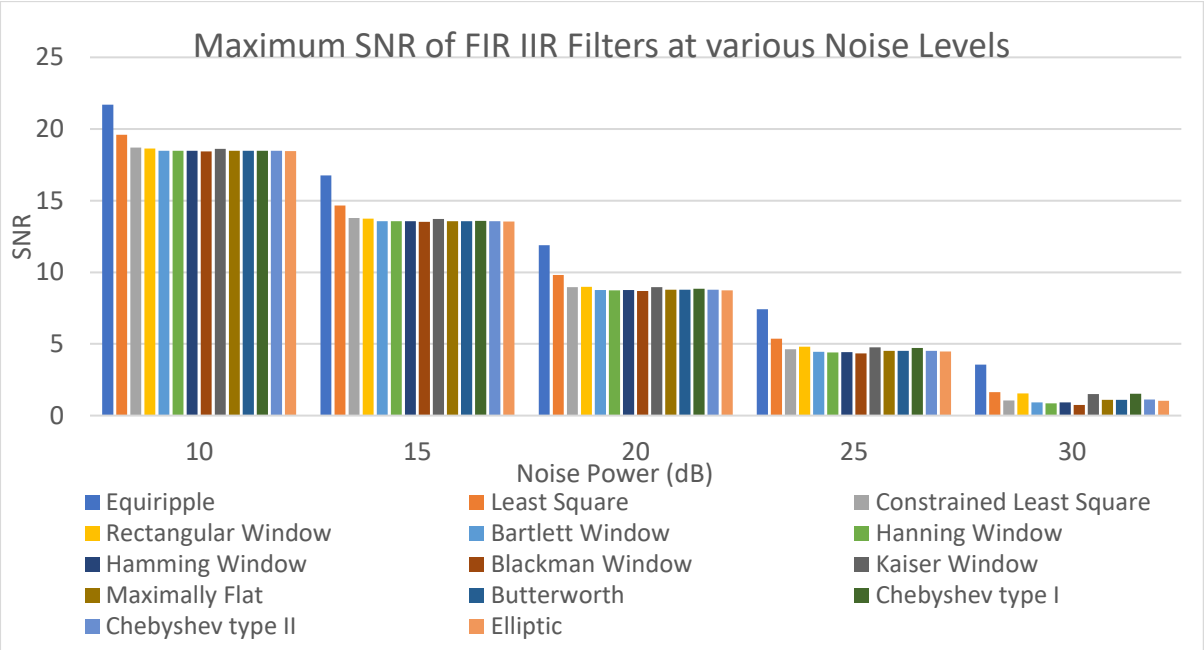

Figure 4.1-5 Maximum SNR across FIR IIR FIlters at various noise levels

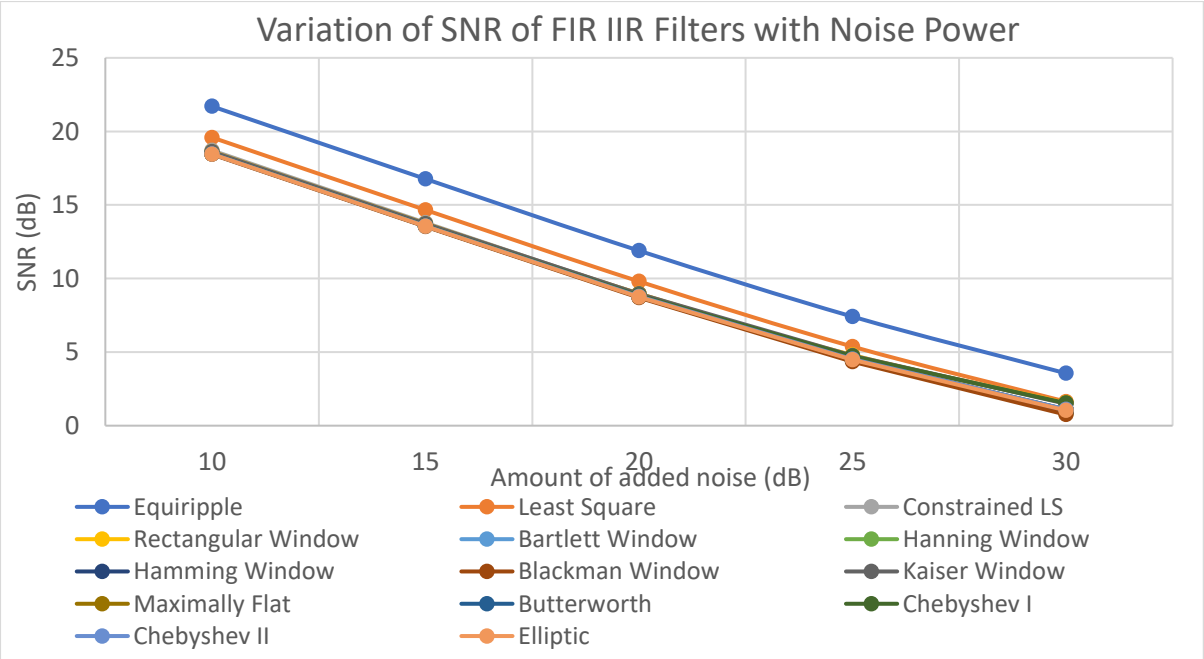

Figure 4.1-6 Variation of SNR of FIR IIR Filters with Noise Power.

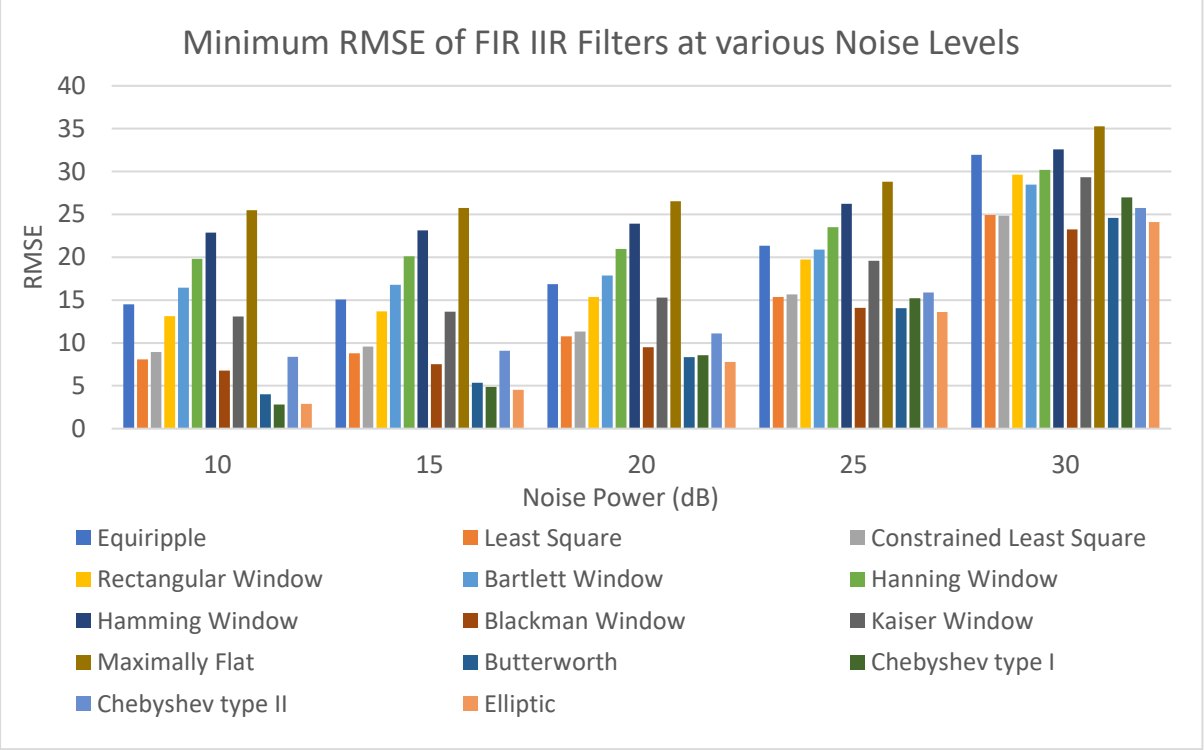

Figure 4.1-7 Minimum RMSE of FIR IIR Filters at various Noise Levels

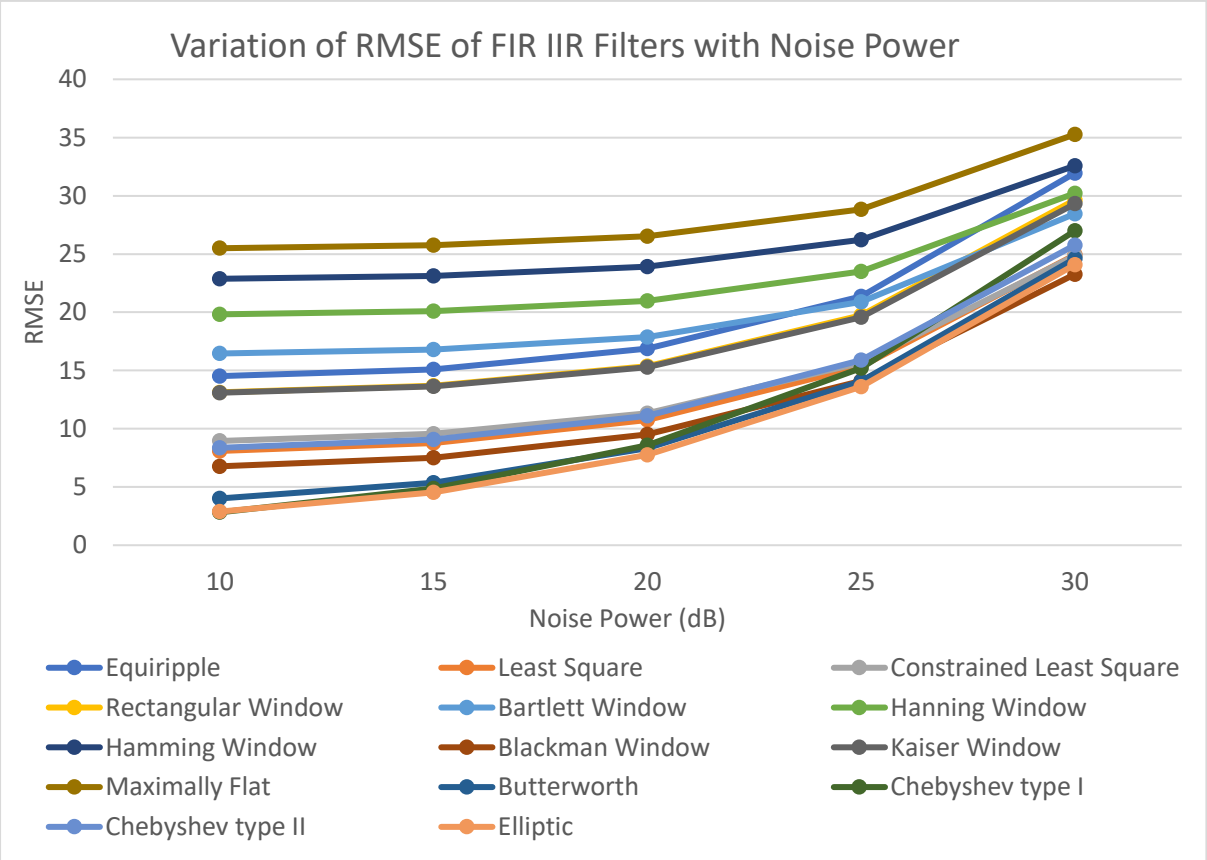

Figure 4.1-8 Variation of RMSE of FIR IIR Filters with Noise Power

Significant conclusions that can be drawn from this table are listed below –

- Equiripple filters achieve appreciably higher SNR compared to other filters.
- Except Equiripple and Least Square Filters, almost all filters achieve similar SNR performance.
- Elliptic and Chebyshev Type I filters achieve minimum RMSE.
- Maximally flat and Hamming Window filters have very high error.
- As observed from the standard deviations noted above, the results are quite consistent across the data set.
- SNR decreases almost linearly with noise.
- Variation of RMSE increases non-linearly with noise.
- Elliptic and Chebyshev I filters achieve average SNR with minimal error, while Equiripple filters achieve maximum SNR with average amount of error.

4.1.4 ANALYSIS OF WAVELET BASED DENOISING –

Table 4.1-6 Variation of SNR and RMSE across Wavelet Types

Wavelet Type	Noise Power (dB)	Average Peak SNR (dB)	SD	RMSE	SD
HAAR	10	18.4053	0.6520	2.5641	0.9883
	15	13.4033	0.6214	2.5641	0.9883
	20	8.3639	0.6535	2.5641	0.9883
	25	3.4108	0.6503	2.5641	0.9883
	30	-1.6054	0.6493	2.5641	0.9883
DB1	10	18.4053	0.6520	2.5641	0.9883
	15	13.4033	0.6214	2.5641	0.9883
	20	8.3639	0.6535	2.5641	0.9883
	25	3.4108	0.6503	2.5641	0.9883
	30	-1.6054	0.6493	2.5641	0.9883
DB2	10	18.4309	0.6568	2.1458	0.8632
	15	13.4289	0.6214	2.1458	0.8632
	20	8.3894	0.6576	2.1458	0.8632
	25	3.4364	0.6553	2.1458	0.8632
	30	-1.5798	0.6537	2.1458	0.8632
DB3	10	18.4375	0.6576	2.1990	0.9622
	15	13.4356	0.6247	2.1990	0.9622
	20	8.3961	0.6581	2.1990	0.9622
	25	3.4431	0.6560	2.1990	0.9622
	30	-1.5732	0.6543	2.1990	0.9622

Wavelet Type	Noise Power (dB)	Average Peak SNR (dB)	SD	RMSE	SD
DB4	10	18.4401	0.6579	2.0852	0.8868
	15	13.4381	0.6251	2.0852	0.8868
	20	8.3987	0.6583	2.0852	0.8868
	25	3.4457	0.6563	2.0852	0.8868
	30	-1.5706	0.6545	2.0852	0.8868
DB5	10	18.4413	0.6581	2.2609	1.1019
	15	13.4394	0.6252	2.2609	1.1019
	20	8.3999	0.6585	2.2609	1.1019
	25	3.4469	0.6565	2.2609	1.1019
	30	-1.5694	0.6547	2.2609	1.1019
DB6	10	18.4420	0.6582	2.4396	1.3148
	15	13.4400	0.6254	2.4396	1.3148
	20	8.4005	0.6586	2.4396	1.3148
	25	3.4475	0.6566	2.4396	1.3148
	30	-1.5688	0.6548	2.4396	1.3148
DB7	10	18.4423	0.6583	2.2363	1.1427
	15	13.4404	0.6254	2.2363	1.1427
	20	8.4009	0.6586	2.2363	1.1427
	25	3.4479	0.6566	2.2363	1.1427
	30	-1.5684	0.6548	2.2363	1.1427
DB8	10	18.4426	0.6583	2.4964	1.3032
	15	13.4406	0.6254	2.4964	1.3032
	20	8.4012	0.6587	2.4964	1.3032
	25	3.4481	0.6567	2.4964	1.3032
	30	-1.5681	0.6549	2.4964	1.3032
DB9	10	18.4428	0.6583	2.4283	1.3046
	15	13.4408	0.6254	2.4283	1.3046
	20	8.4014	0.6587	2.4283	1.3046
	25	3.4483	0.6567	2.4283	1.3046
	30	-1.5679	0.6549	2.4283	1.3046
DB10	10	18.4429	0.6583	2.4972	1.2984
	15	13.4409	0.6255	2.4972	1.2984
	20	8.4014	0.6587	2.4972	1.2984
	25	3.4484	0.6567	2.4972	1.2984
	30	-1.5679	0.6549	2.4972	1.2984
SYM2	10	18.4309	0.6568	2.1458	0.8632
	15	13.4289	0.6247	2.1458	0.8632
	20	8.3894	0.6576	2.1458	0.8632
	25	3.4364	0.6553	2.1458	0.8632

Wavelet Type	Noise Power (dB)	Average Peak SNR (dB)	SD	RMSE	SD
	30	-1.5798	0.6537	2.1458	0.8632
SYM3	10	18.4375	0.6576	2.1990	0.9622
	15	13.4356	0.6251	2.1990	0.9622
	20	8.3961	0.6581	2.1990	0.9622
	25	3.4431	0.6560	2.1990	0.9622
	30	-1.5732	0.6543	2.1990	0.9622
SYM4	10	18.4402	0.6579	2.3490	1.1584
	15	13.4382	0.6253	2.3490	1.1584
	20	8.3987	0.6584	2.3490	1.1584
	25	3.4457	0.6563	2.3490	1.1584
	30	-1.5706	0.6546	2.3490	1.1584
SYM5	10	18.4413	0.6581	2.2904	1.1555
	15	13.4393	0.6253	2.2904	1.1555
	20	8.3999	0.6585	2.2904	1.1555
	25	3.4468	0.6565	2.2904	1.1555
	30	-1.5694	0.6547	2.2904	1.1555
SYM6	10	18.4420	0.6582	2.4776	1.3687
	15	13.4400	0.6254	2.4776	1.3687
	20	8.4005	0.6586	2.4776	1.3687
	25	3.4475	0.6565	2.4776	1.3687
	30	-1.5688	0.6548	2.4776	1.3687
SYM7	10	18.4424	0.6582	2.4352	1.2720
	15	13.4404	0.6254	2.4352	1.2720
	20	8.4009	0.6586	2.4352	1.2720
	25	3.4479	0.6566	2.4352	1.2720
	30	-1.5684	0.6548	2.4352	1.2720
SYM8	10	18.4426	0.6583	2.4409	1.3359
	15	13.4406	0.6255	2.4409	1.3359
	20	8.4012	0.6587	2.4409	1.3359
	25	3.4481	0.6567	2.4409	1.3359
	30	-1.5681	0.6549	2.4409	1.3359
COIF1	10	18.4316	0.6571	2.2126	0.9156
	15	13.4296	0.6250	2.2126	0.9156
	20	8.3902	0.6579	2.2126	0.9156
	25	3.4372	0.6556	2.2126	0.9156
	30	-1.5791	0.6540	2.2126	0.9156
COIF2	10	18.4404	0.6580	2.1983	0.9910
	15	13.4384	0.6253	2.1983	0.9910
	20	8.3990	0.6585	2.1983	0.9910

Wavelet Type	Noise Power (dB)	Average Peak SNR (dB)	SD	RMSE	SD
	25	3.4460	0.6564	2.1983	0.9910
	30	-1.5703	0.6547	2.1983	0.9910
COIF3	10	18.4421	0.6582	2.3268	1.1431
	15	13.4401	0.6254	2.3268	1.1431
	20	8.4007	0.6586	2.3268	1.1431
	25	3.4477	0.6566	2.3268	1.1431
	30	-1.5686	0.6548	2.3268	1.1431
COIF4	10	18.4427	0.6583	2.4841	1.3008
	15	13.4407	0.6254	2.4841	1.3008
	20	8.4013	0.6587	2.4841	1.3008
	25	3.4482	0.6567	2.4841	1.3008
	30	-1.5680	0.6549	2.4841	1.3008
COIF5	10	18.4429	0.6584	2.6204	1.3734
	15	13.4410	0.6255	2.6204	1.3734
	20	8.4015	0.6587	2.6204	1.3734
	25	3.4485	0.6567	2.6204	1.3734
	30	-1.5678	0.6549	2.6204	1.3734

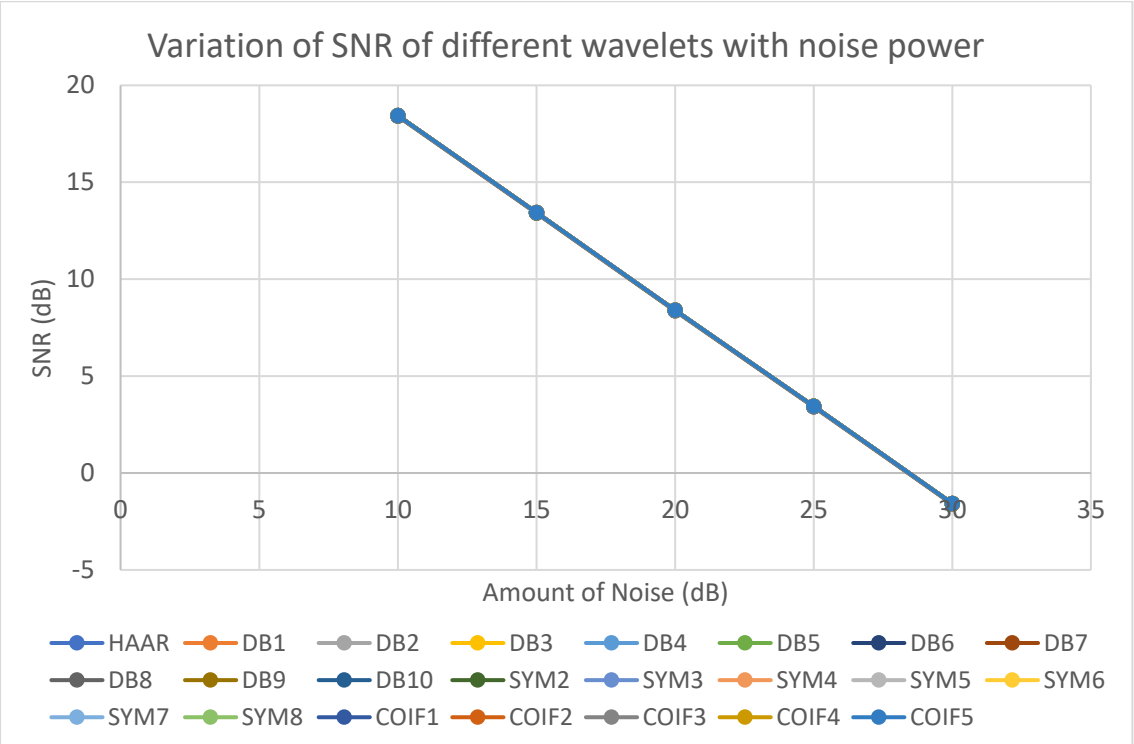

Figure 4.1-9 Variation of SNR of different wavelets with noise power

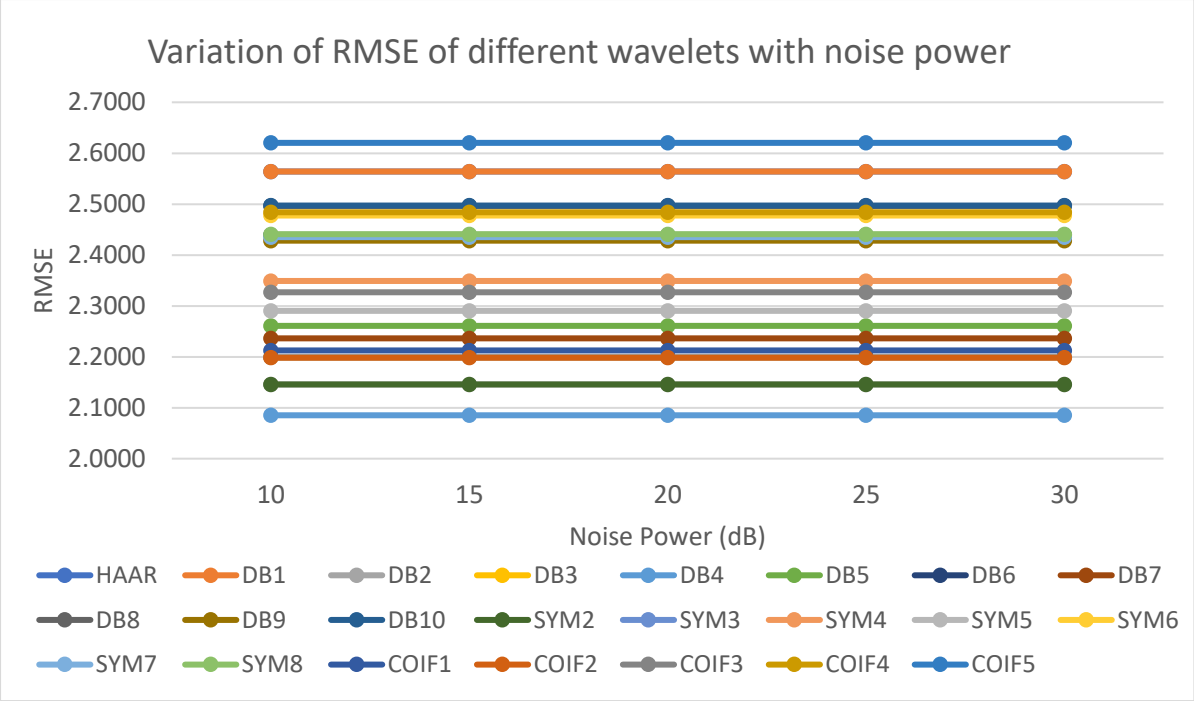

Figure 4.1-10 Variation of RMSE of different wavelets with noise power

Some interesting results that can be noted from the above tables and graphs are listed below –

- All wavelet types achieve similar SNR performance.
- RMSE does not change with noise power. Thus, it can be concluded that wavelet denoising is independent of noise power.
- Haar and DB1 wavelet have exactly similar performance, which is quite expected as Haar wavelet is same as DB1.
- DB4 wavelet produces the least error (RMSE) when compared to the clean ECG signal.
- SNR decreases linearly as noise power increases.

4.1.5 SAVITZKY-GOLAY FILTERS

Table 4.1-7 Variation of Savitzky Golay Filter Parameters and Outputs with Noise Power

Noise Power (dB)	Framesize	SD	Filter Order	SD	RMSE	SD	SNR	SD
10	81	16.40	22	5.60	1.404	0.03	17.405	0.06
15	43	6.52	10	2.35	2.405	0.10	12.362	0.02
20	30	5.67	5	1.14	3.993	0.11	7.336	0.04
25	20	1.07	2	0.53	6.628	0.27	2.274	0.06
30	12	1.05	1	0.00	10.704	0.33	-2.862	0.18

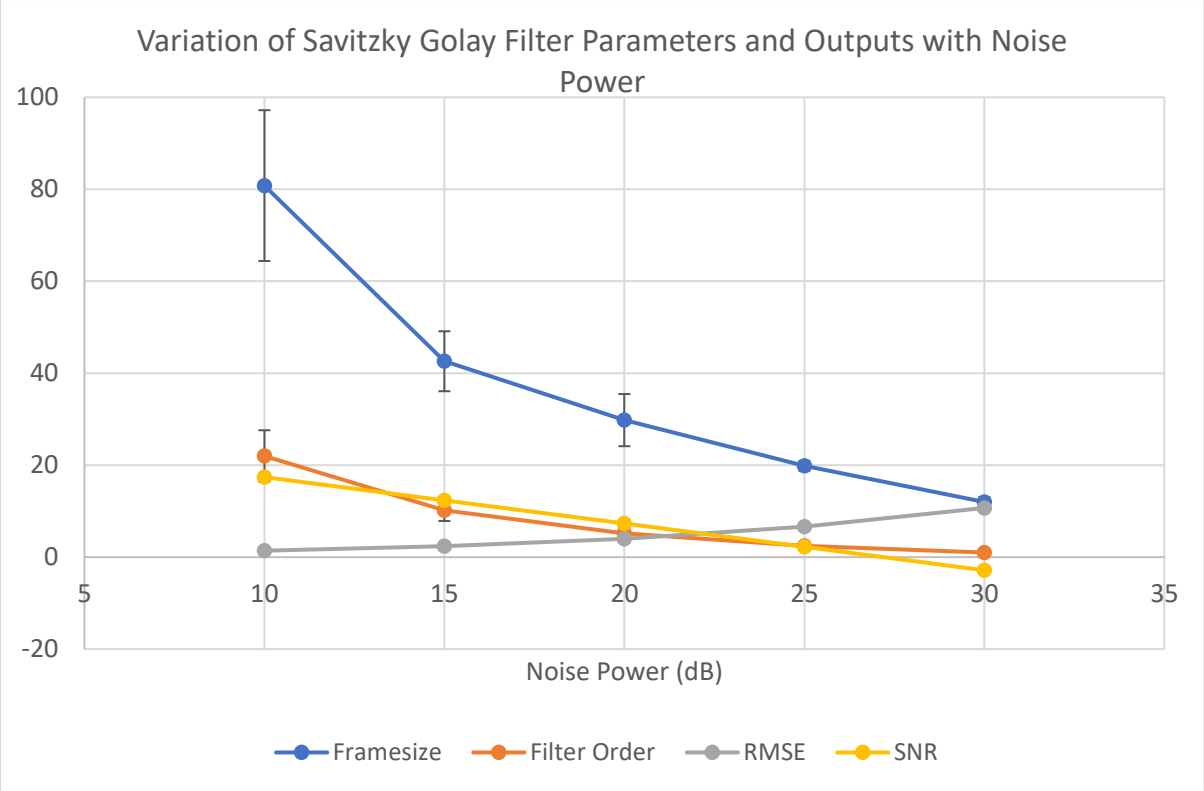

Figure 4.1-11 Variation of Savitzky Golay Filter Parameters and Outputs with Noise Power

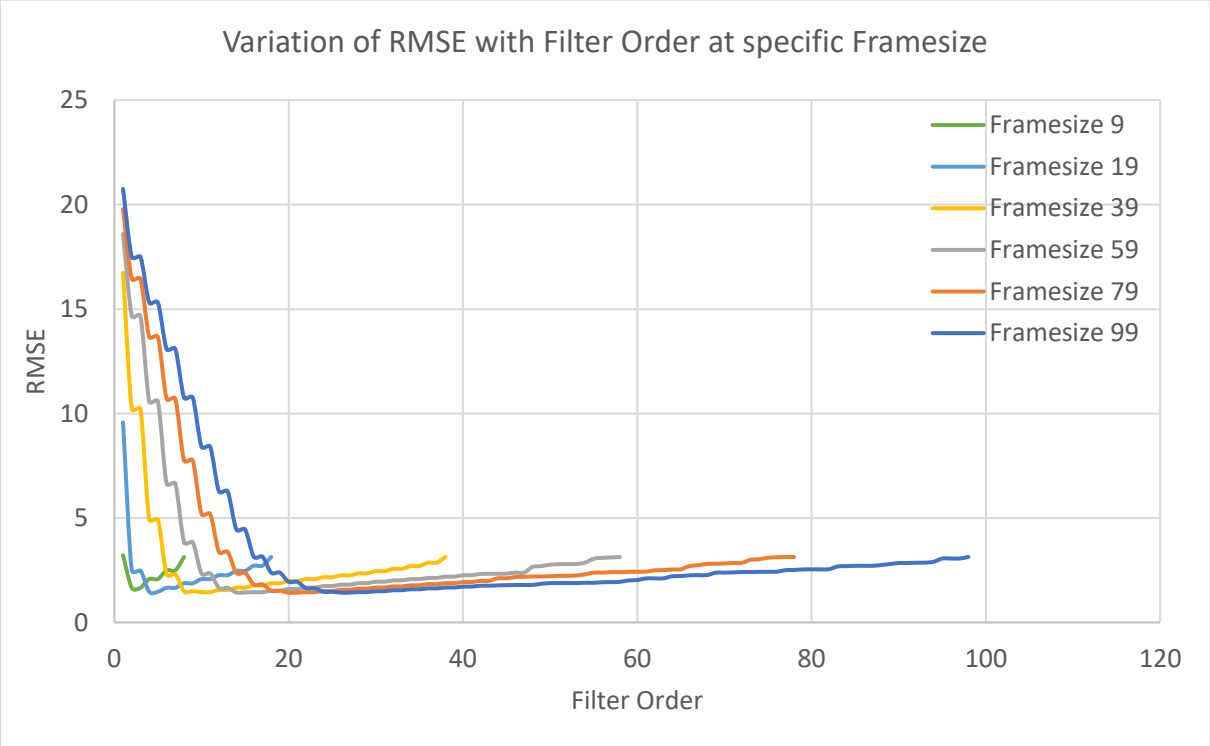

Figure 4.1-12 Variation of RMSE with Filter Order at specific Framesize

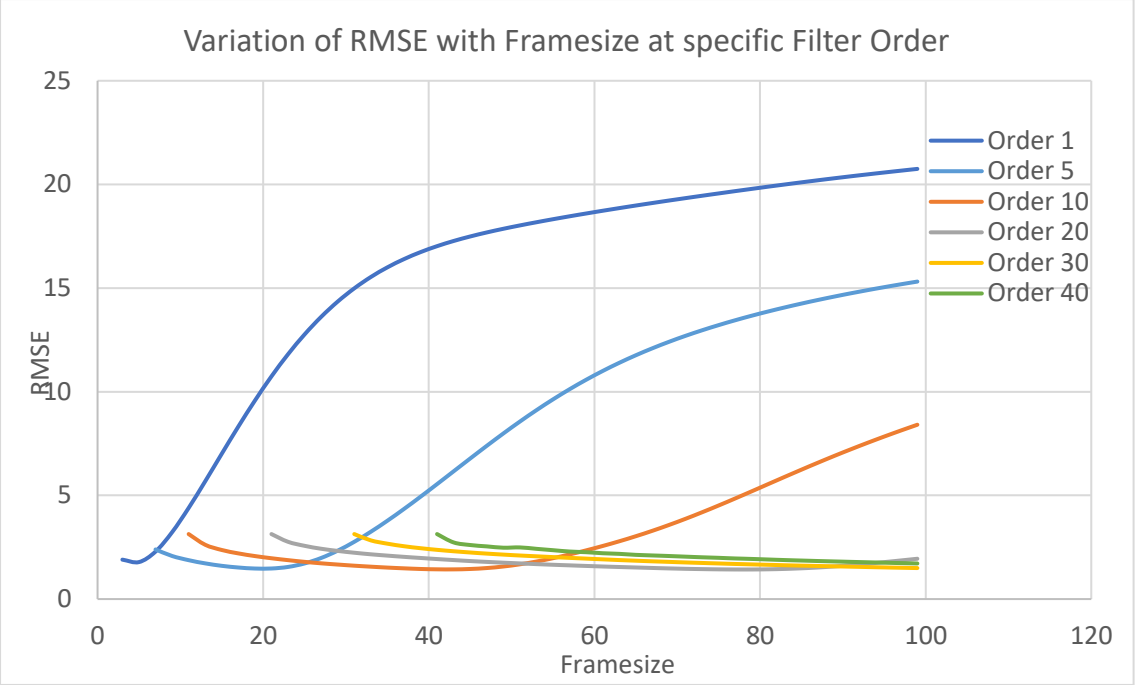

Figure 4.1-13 Variation of RMSE with Framesize at specific Filter Order

The above two charts show the variation of RMSE in two different cases –

- when framesize is fixed at and filter order is changed.
- when filter order is fixed and framesize is changed.

Significant conclusions that can be drawn from the above given charts and data are –

- Framesize and filter order at which optimum ECG filtering is obtained decreases with increase in noise power.
- Variance (or Standard Deviation) of optimum framesize and filter order decreases with increase in noise power.
- RMSE increases with increase in noise power.
- SNR decreases with increase in noise power.
- Variance (or Standard Deviation) of RMSE or Noise Power remains almost constant across the whole data.
- Even-though values of optimum Framesize and filter order for a particular noise level is showing considerable variation, quality of filtering (RMSE and SNR) is almost constant.

4.1.6 SIDE-BY-SIDE COMPARISON OF FIR IIR FILTERS, WAVELET BASED DENOISING, SAVITZKY GOLAY FILTERS

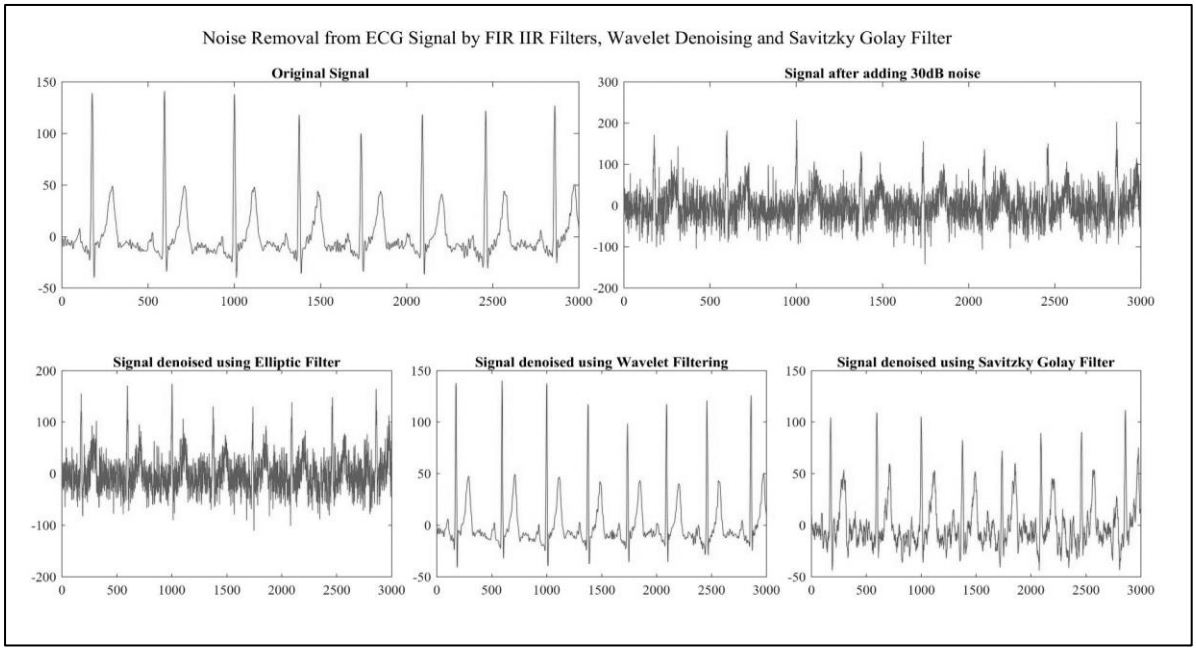

Figure 4.1-14 Comparison of Elliptic Filter, Wavelet Denoising and Savitzky Golay Filter

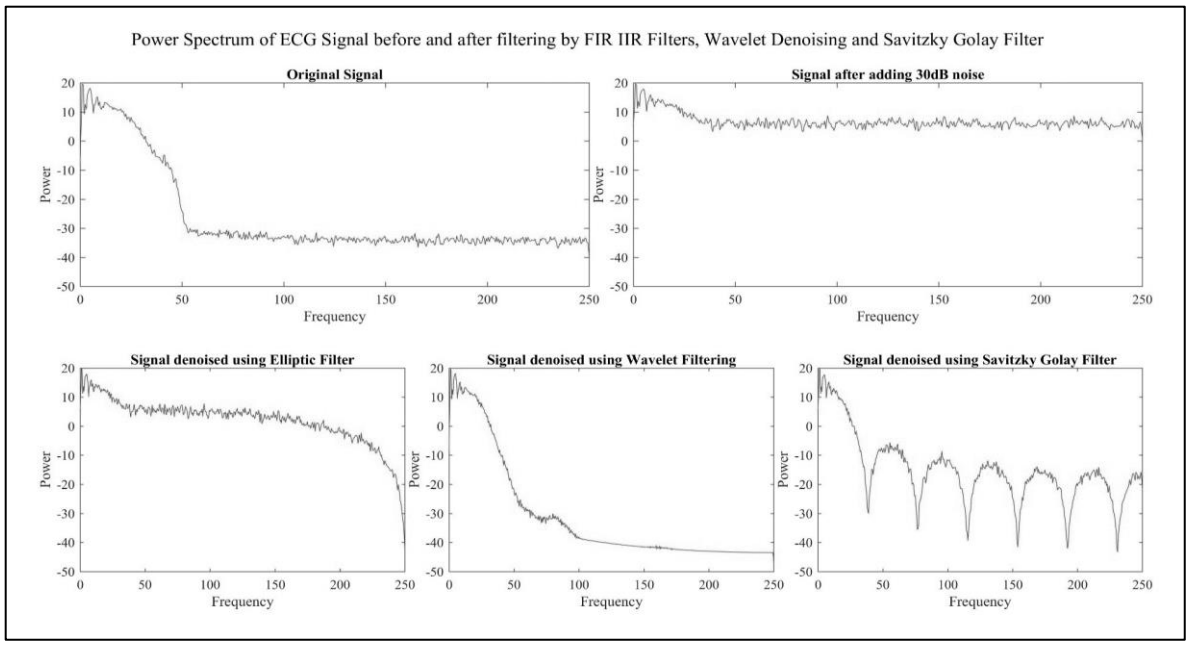

Figure 4.1-15 Comparison of Power Spectrum of Elliptic Filter, Wavelet Denoising and Savitzky Golay Filter before and after denoising

From the above two figures, it is seen that Wavelet Denoising method provides the cleanest ECG signal among all the other techniques when 30dB noise is added to the signal.

4.2 Dynamics of Cardiovascular System with Music

Variation of Heart rate before and after music stimulus

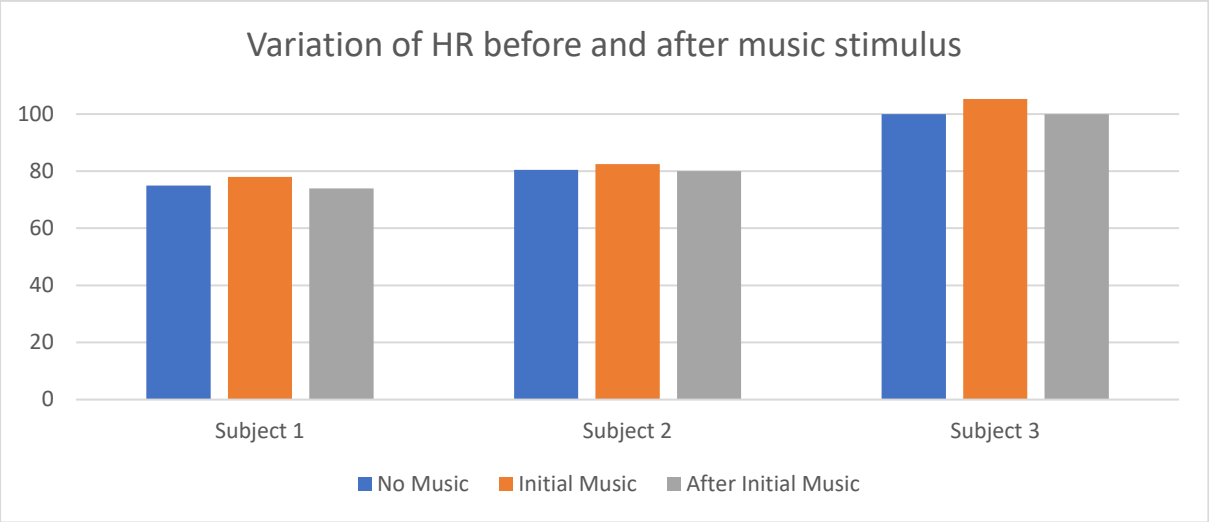

Figure 4.2-1 Variation of HR before and after music stimulus

- In all the three subjects, Heart Rate rises marginally when music stimulus is applied.
- A subsequent decrease in Heart Rate is observed when music is stopped.

Variation of Heart Rate with Cognitive Load (Music)

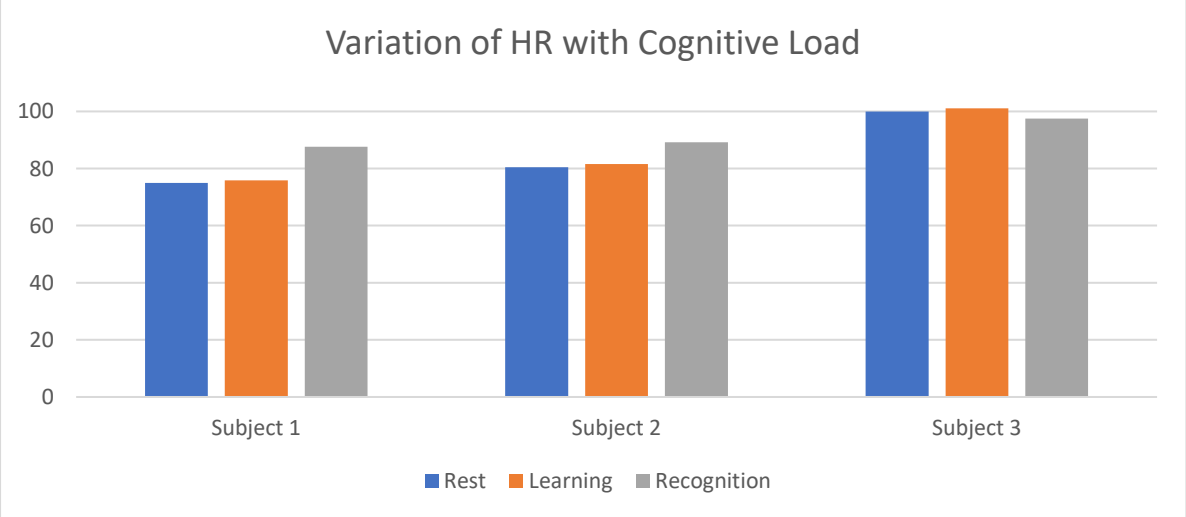

Figure 4.2-2 Variation of HR with Cognitive load

- In all three subjects, Heart Rate increases during learning phase. The response during recognition phase is subjective and depends on how well the subject has identified the music.

VARIATION OF LF/HF RATIO BEFORE AND AFTER MUSIC STIMULUS

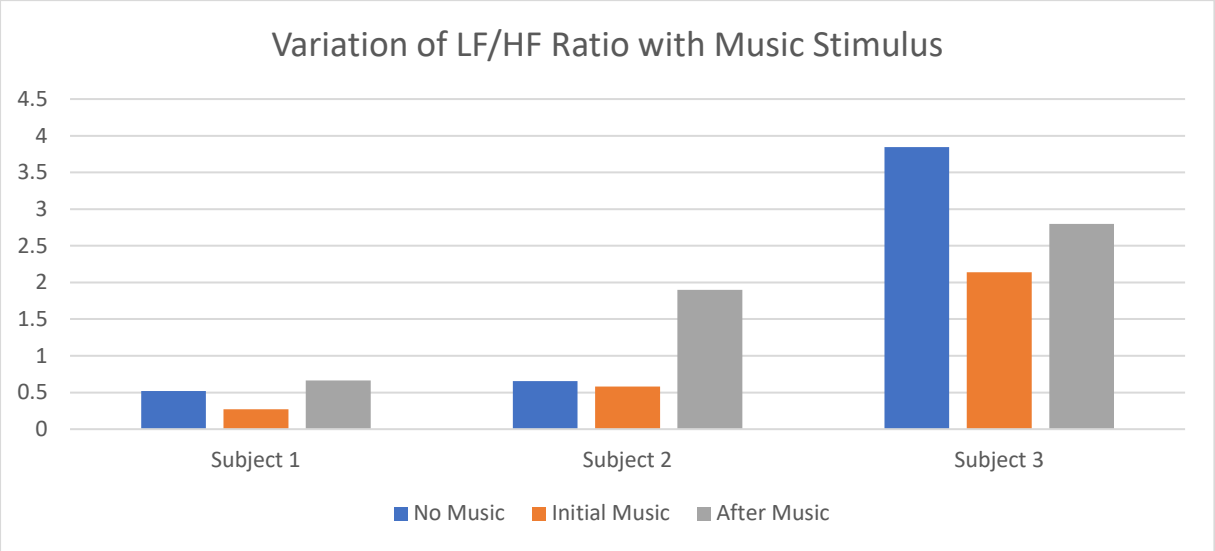

Figure 4.2-3 Variation of LF/HF Ratio before and after music stimulus

- In all the three subjects, LF/HF ratio decreases when music stimulus is applied. Thus, there is a subsequent increase in the activity of parasympathetic nervous system due to the application of music. LF/HF ratio increases again when music is stopped. This again indicates that music stimulus causes stress relaxation.

VARIATION OF LF/HF RATIO WITH COGNITIVE LOAD (MUSIC)

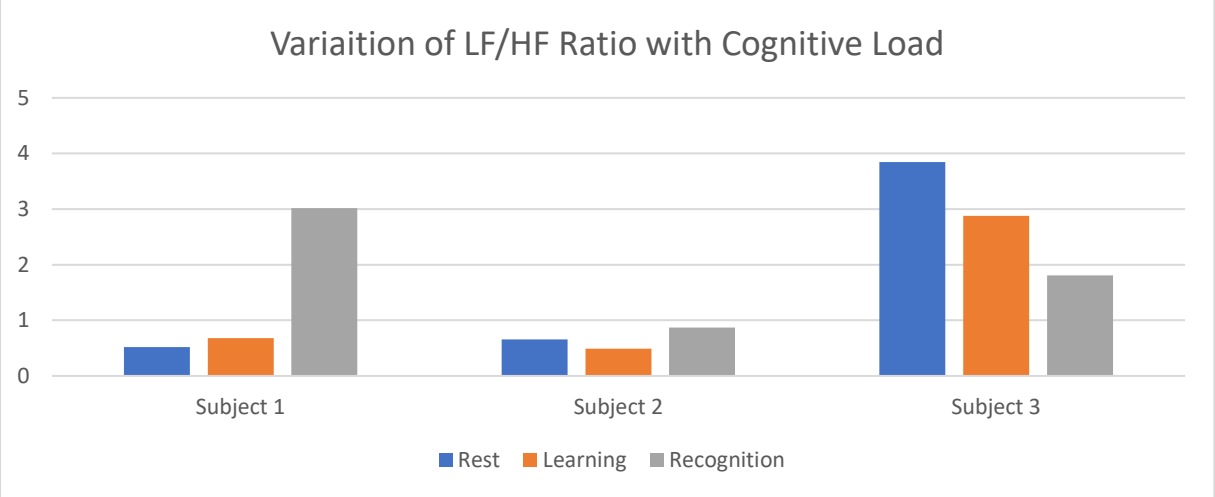

Figure 4.2-4 Variation of LF/HF Ratio with Cognitive Load

- Variation of LF/HF ratio, which is a marker of sympatho/vagal balance, is different for different subjects. This may be due to the approach taken by the subject towards the task, while some might appreciate the music, some subjects might have stressed while trying to understand the musical segments. It is interesting to note here that all the subjects have successfully recognized the music in recognition phase, but the variation of LF/HF ratio is

different for different subjects. Thus, no conclusive relationship between cognitive load and sympathetic parasympathetic activity can be established when a task of music recognition is given.

VARIATION OF HF COMPONENT BEFORE AND AFTER MUSIC STIMULUS

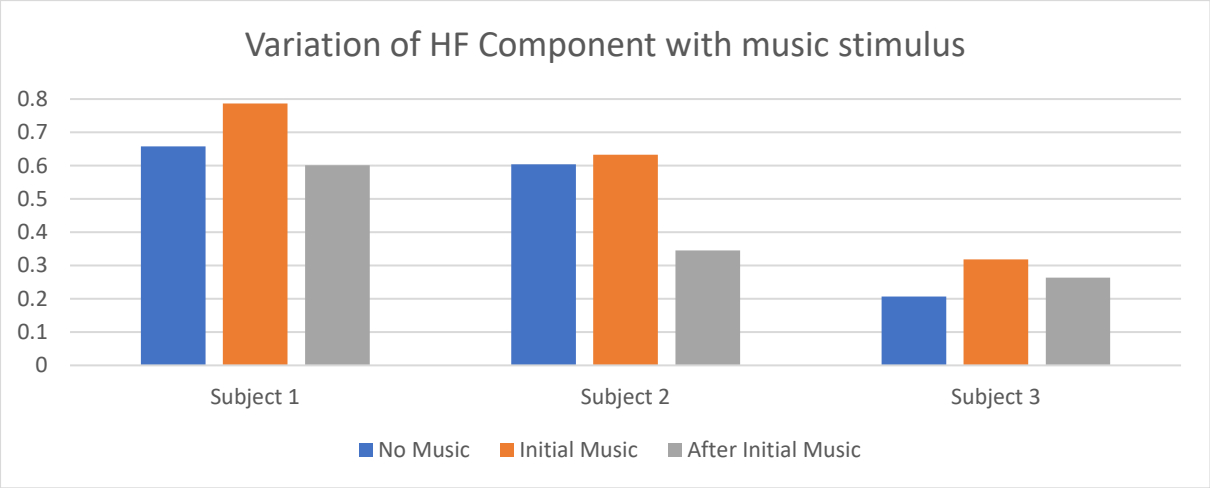

Figure 4.2-5 Variation of HF Component before and after music stimulus

- In all the three subjects, there is a rise in the HF component with music stimulus. Since, HF ratio is a marker of the activity of parasympathetic nervous system, the rise in HF component with application of music indicates the stress relaxing effect of music.

VARIATION OF HF COMPONENT WITH COGNITIVE LOAD (MUSIC)

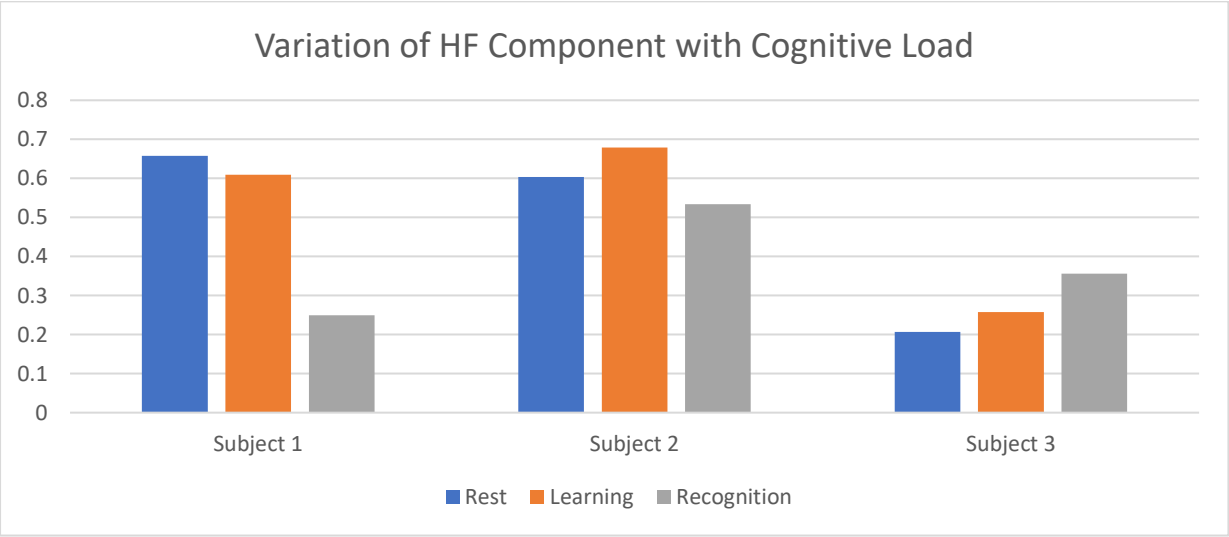

Figure 4.2-6 Variation of HF component with Cognitive Load

- In all the three subjects, as seen in the comparison of LF/HF ratio, the variation of HF component with cognitive load is highly subjective and depends how the subject responds with the task requirements.

4.3 Fractal Analysis of HRV with Music

Variation of Fractal Dimension Before and After Music –

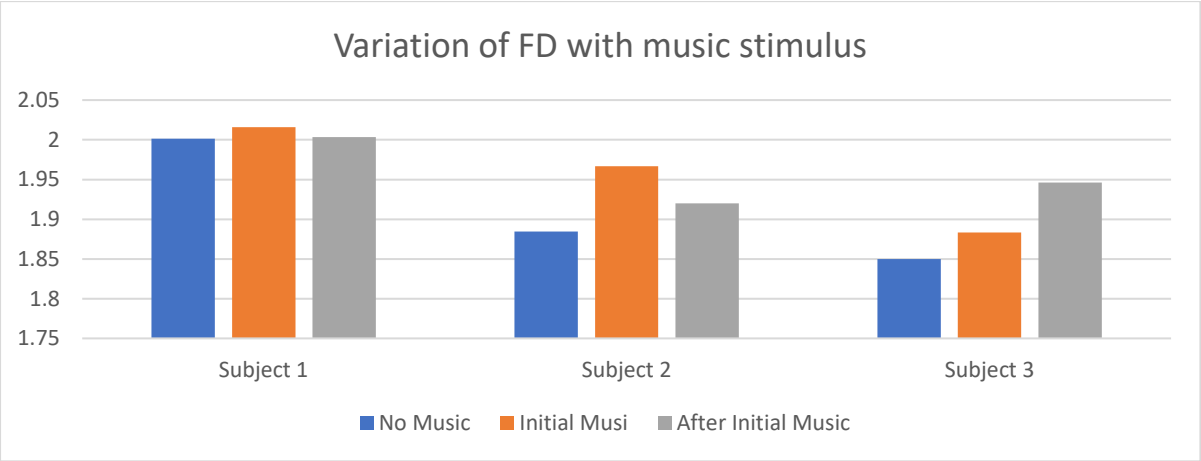

Figure 4.3-1 Variation of fractal dimension with music stimulus

- In all the three subjects, there is a rise in Fractal Dimension of HRV with music stimulus, indicating an increase in the complex nature of HRV with music. After the music stimulus has stopped, the response is much more subjective, indicating the persistence of the effects of music on HRV is different for different subjects.

Variation of Fractal Dimension with Cognitive Load –

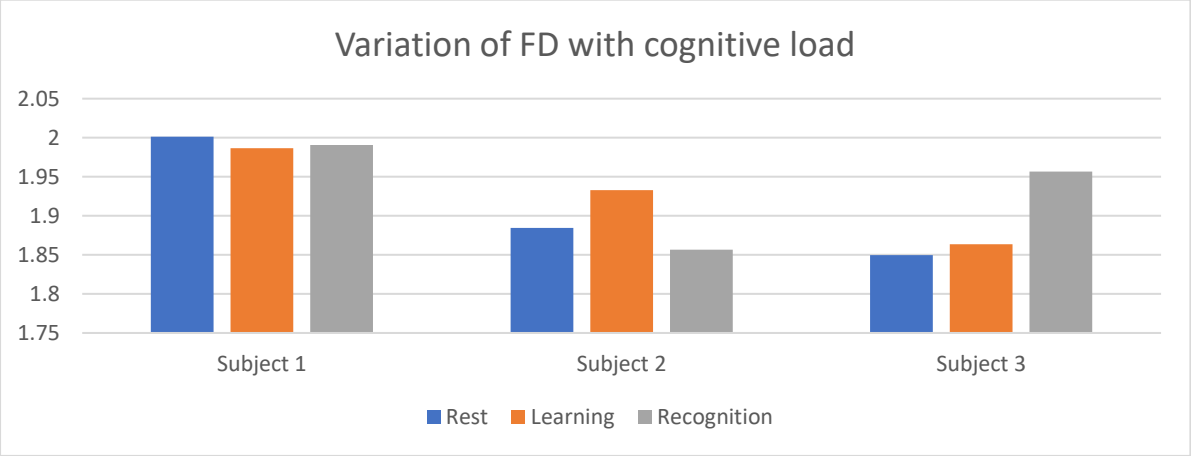

Figure 4.3-2 Variation of Fractal Dimension with cognitive load

- In all the three subjects, the variation of fractal dimension with cognitive load is subjective, which is coherence with results acquired from previous parameters. Thus fractal dimension is unable to successfully capture the effect of music during the processes of learning and recognition.

4.4 Dynamics of Brain with Music

Variation in Power Across Different Regions of Brain with Music

Subject 1 –

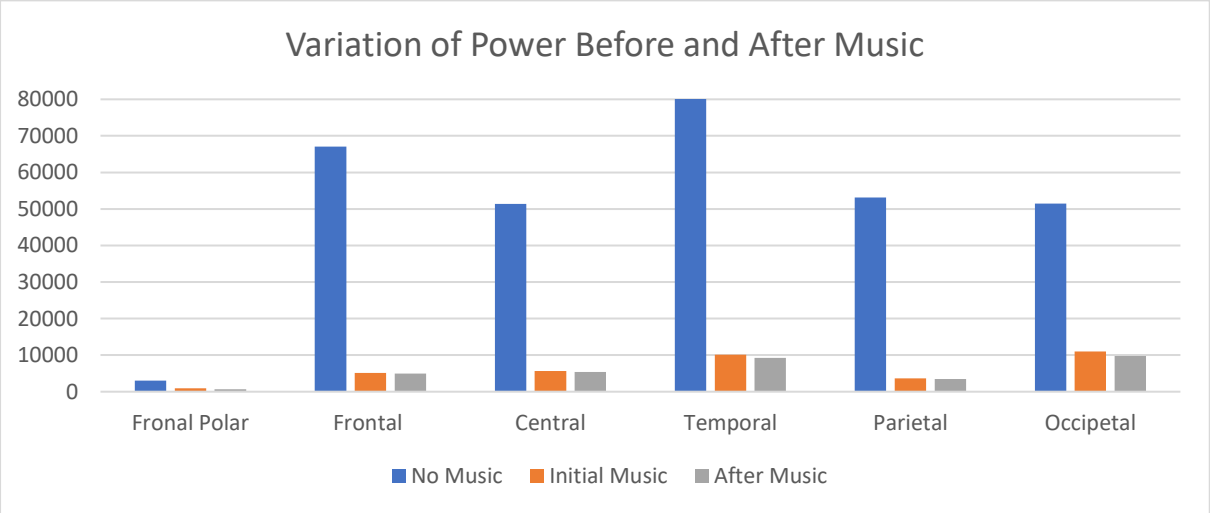

Figure 4.4-1 Variation in power across different regions of brain with music – Subject 1

Subject 2 –

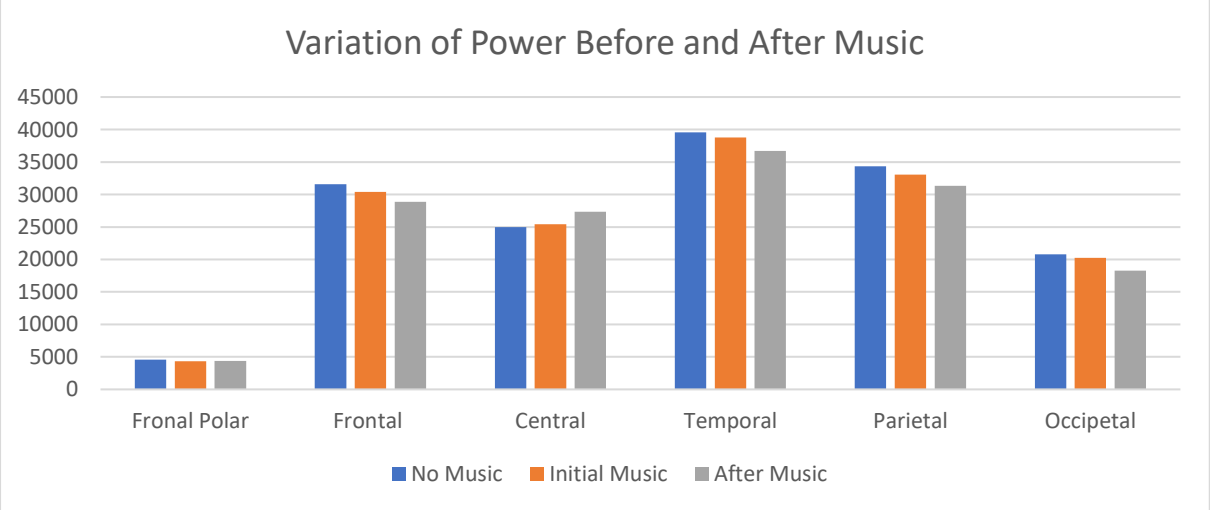

Figure 4.4-2 variation in power across different regions of brain with music - Subject 2

Subject 3 –

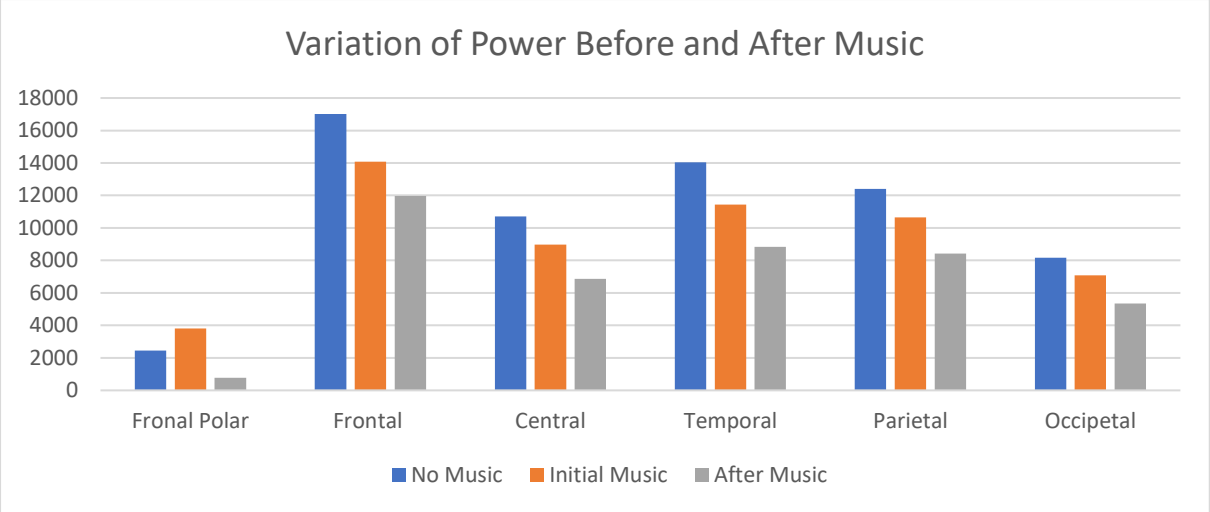

Figure 4.4-3 variation in power across different regions of brain with music - Subject 3

- There is a significant decrease in average power in all regions of the brain with music. This can be attributed to stress relaxing effect of music.
- The magnitude of this decrease in power is different for different subjects. Thus, the appreciation of music is highly subjective.
- After the music has stopped, average power of various regions of brain do not rise back to its original level, but decreases even further, suggesting the effect of music continues even after the music stimulus has been removed
- Total power and subsequent decrease of power in the frontal polar region is not significant.
- In one of the subjects, average power in central region increases slightly with music stimulus.

DISTRIBUTION OF POWER ACROSS REGIONS OF BRAIN WITH AND WITHOUT MUSIC

Subject 1 –

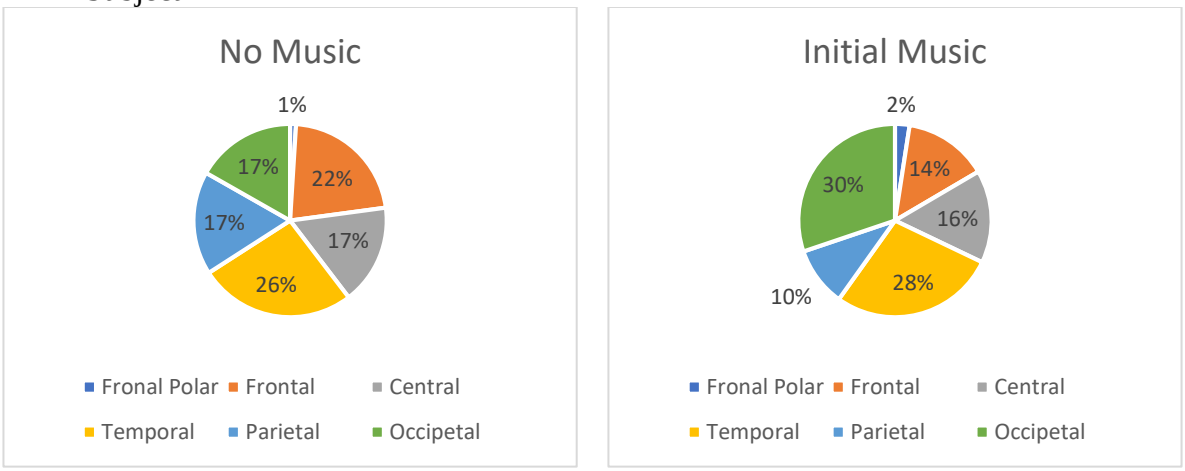

Figure 4.4-4 Distribution of power across regions of brain with music - Subject 1

Subject 2 –

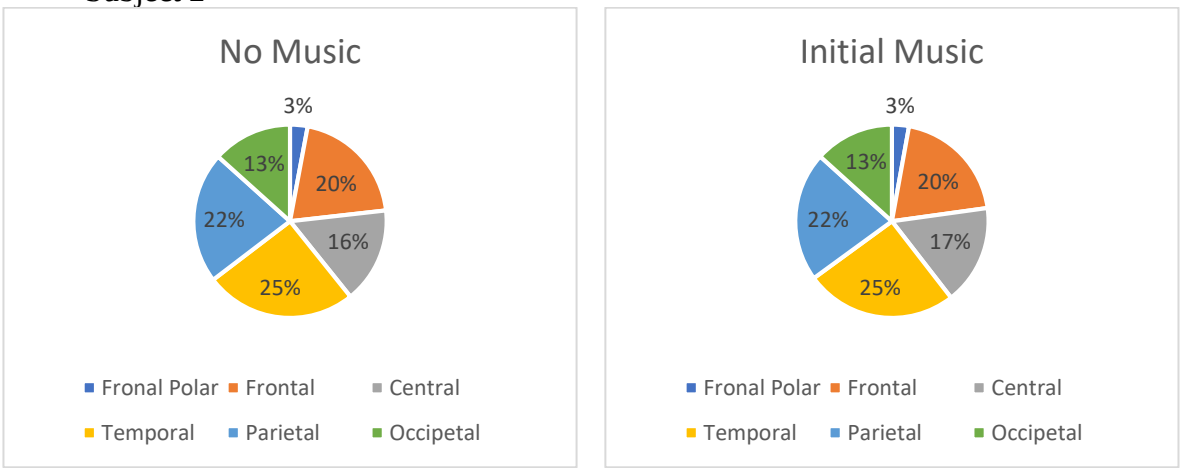

Figure 4.4-5 Distribution of power across regions of brain with music - Subject 2

Subject 3 –

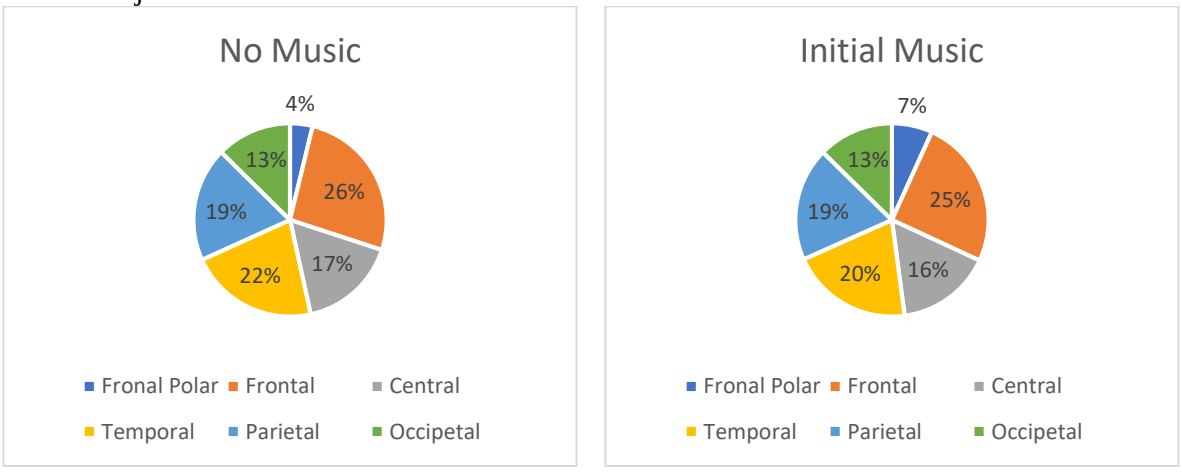

Figure 4.4-6 Distribution of power across regions of brain with music - Subject 3

- Distribution of power in various regions of the brain in resting condition is very similar in all the subjects.
- Change in the distribution of power with application of music is not very significant.

VARIATION OF POWER ACROSS DIFFERENT REGIONS WITH COGNITIVE LOAD

Subject 1 –

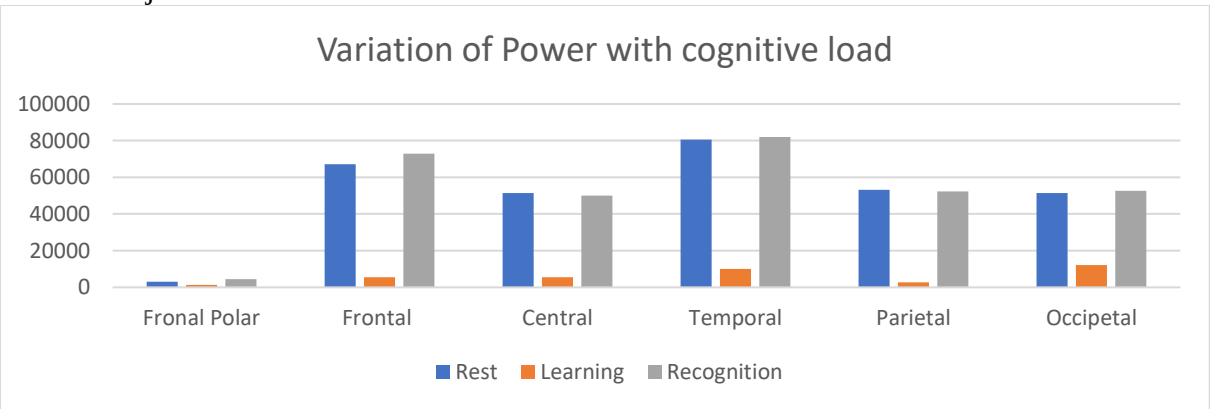

Figure 4.4-7 Variation of Power across different regions with cognitive load - Subject 1

Subject 2 –

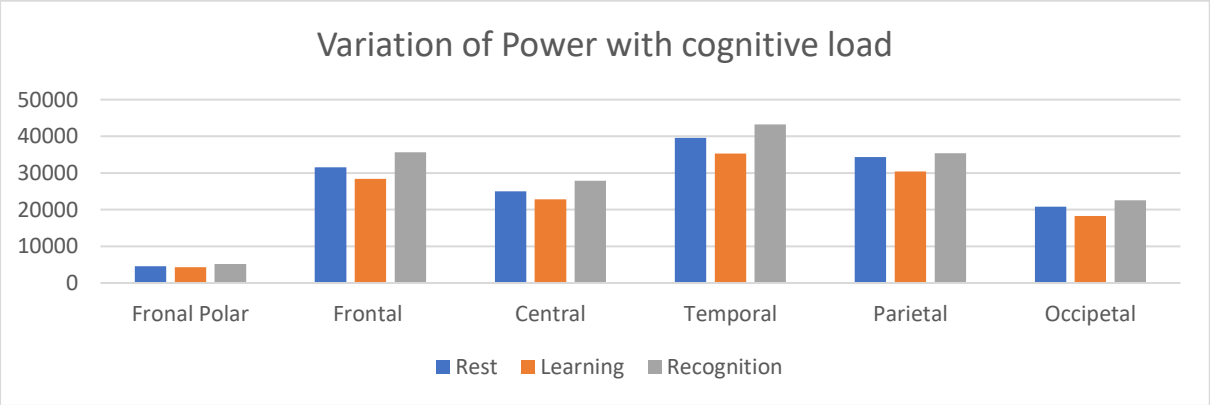

Figure 4.4-8 Variation of Power across different regions with cognitive load - Subject 2

Subject 3 –

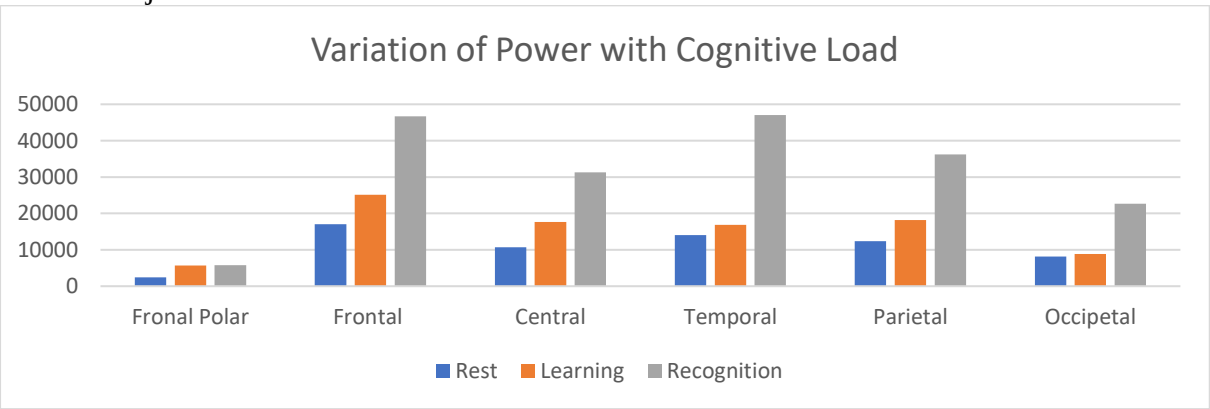

Figure 4.4-9 Variation of Power across different regions with cognitive load - Subject 3

- When subject is asked to listen to the music and try to understand and memorise it, the variation of power in the three phases, that is, rest, learning, and recognition is different for different subjects.
- Two subjects show a decrease in power during learning phase, with one subject showing very significant fall in average power across all regions of the brain during learning phase, while one subject shows continuous rise of average power in all regions.
- It can be considered that decrease in average power may be due to decrease in neural activity due to the effect of music, or may be due to uncoordinated neural activity, as brain tries to find musical patterns and extract features resulting in an overall decrease in power.
- Since, this is a cognitive task, and an example of unsupervised learning, it is expected that different subjects will show different results.

POWER OF ALPHA, BETA AND THETA WAVES BEFORE AND AFTER MUSIC

Subject 1 –

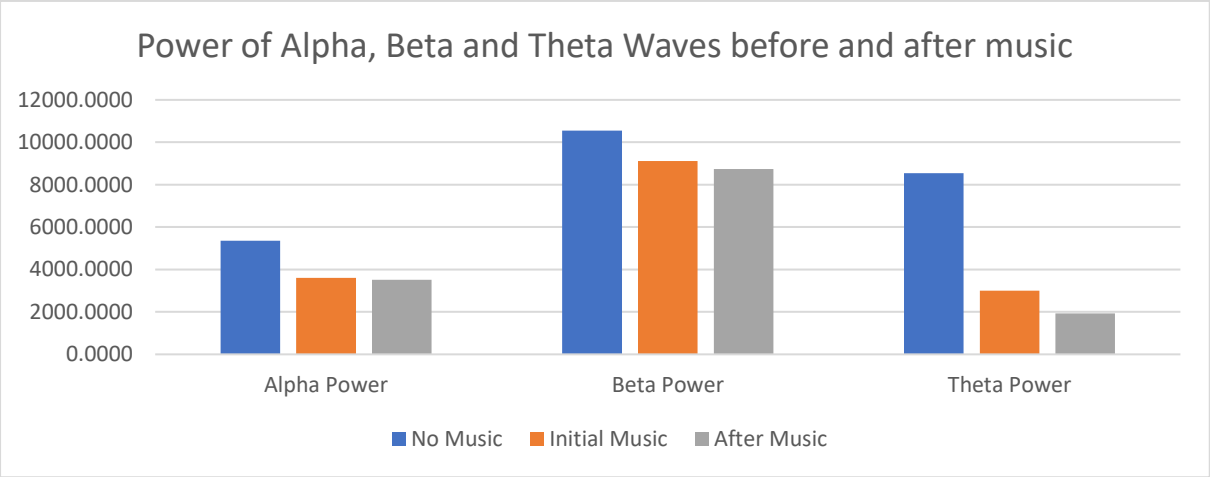

Figure 4.4-10 Power of alpha, beta and theta waves before and after music - Subject 1

Subject 2 –

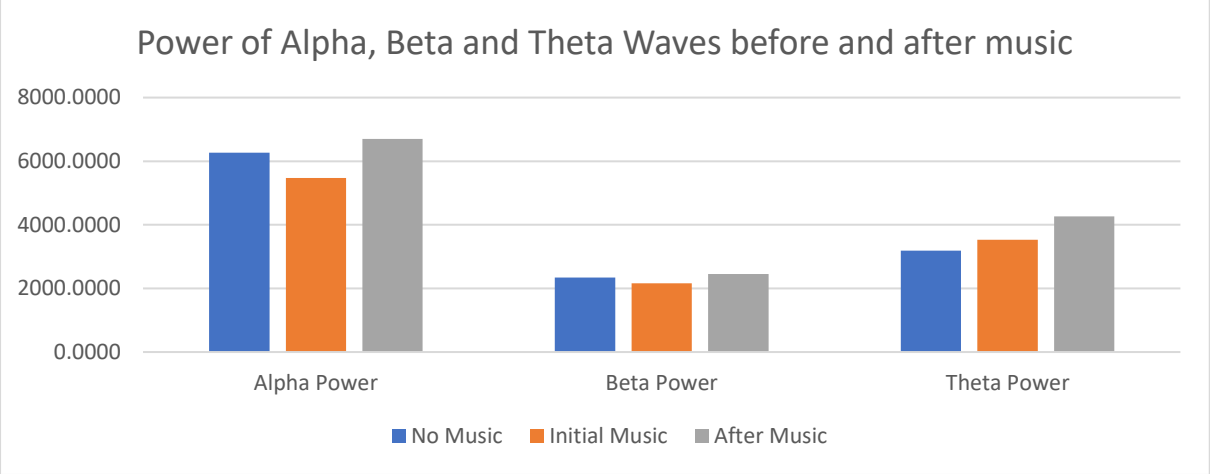

Figure 4.4-11 Power of alpha, beta and theta waves before and after music - Subject 2

Subject 3 –

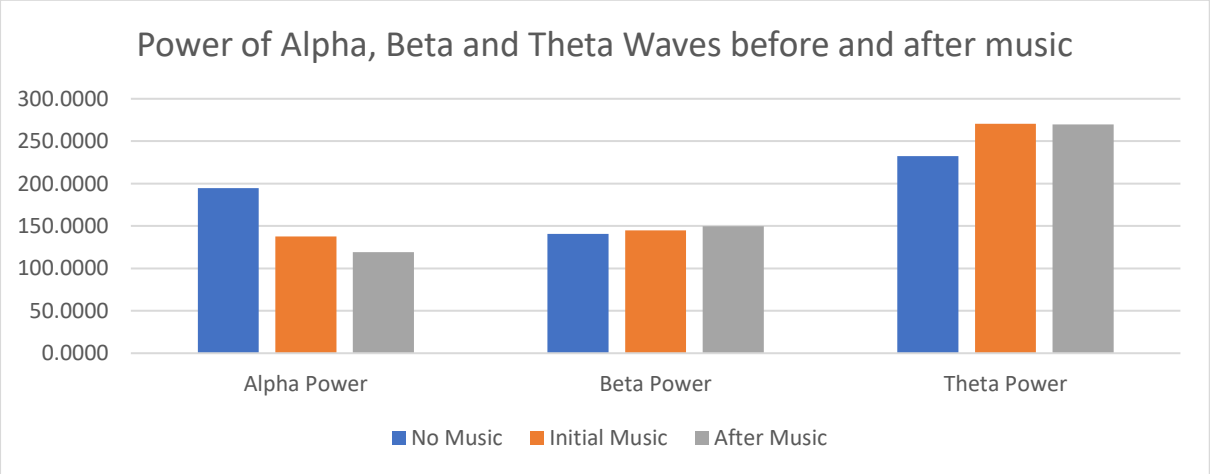

Figure 4.4-12 Power of alpha, beta and theta waves before and after music – Subject 3

- Average power of alpha wave decreases with musical stimulus. The preceding literature review accept that alpha wave is a marker of the resting condition of brain and decrease in alpha power means increase in cortical activity. Thus, from the above given results it is seen application of music cause the effect of arousal.
- Variation of beta wave is neither conspicuous nor consistent. Since beta activity is linked with cognitive response to task, it can be said that for an untrained music listener, the effect of appreciation music is more predominant over the cognitive understanding of the musical segment. Since this process is highly subjective, variation of beta power with music segment should be different for different users, which can be seen from the above given results.
- In the preceding literature review, it is seen that activity of theta wave is a marker of emotional and subconscious response. Thus, the variation of theta wave is highly subjective. In some subjects there is a consistent rise in theta activity while some users show consistent decrease in theta activity, which can be attributed to how strongly the subject concentrated on the task.

POWER OF ALPHA, BETA AND THETA WAVES WITH COGNITIVE LOAD

Subject 1 –

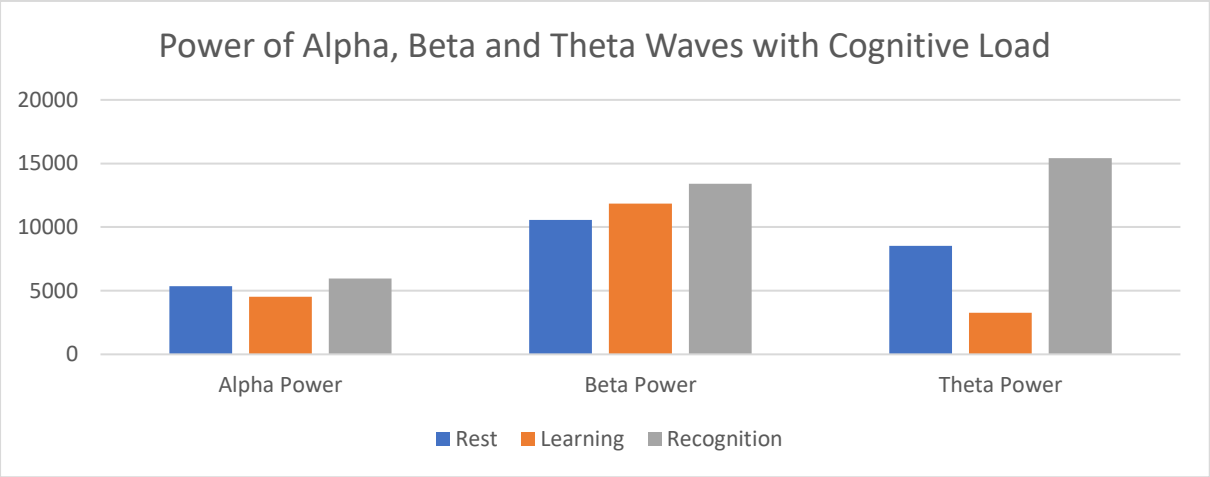

Figure 4.4-13 Power of alpha, beta and theta waves with cognitive load – Subject 1

Subject 2 –

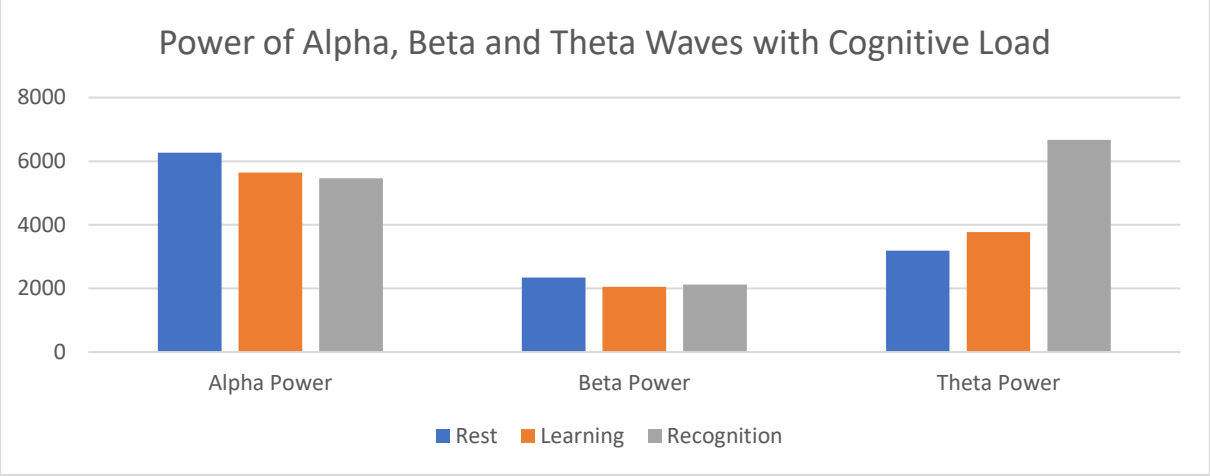

Figure 4.4-14 Power of alpha, beta and theta waves with cognitive load – Subject 2

Subject 3 –

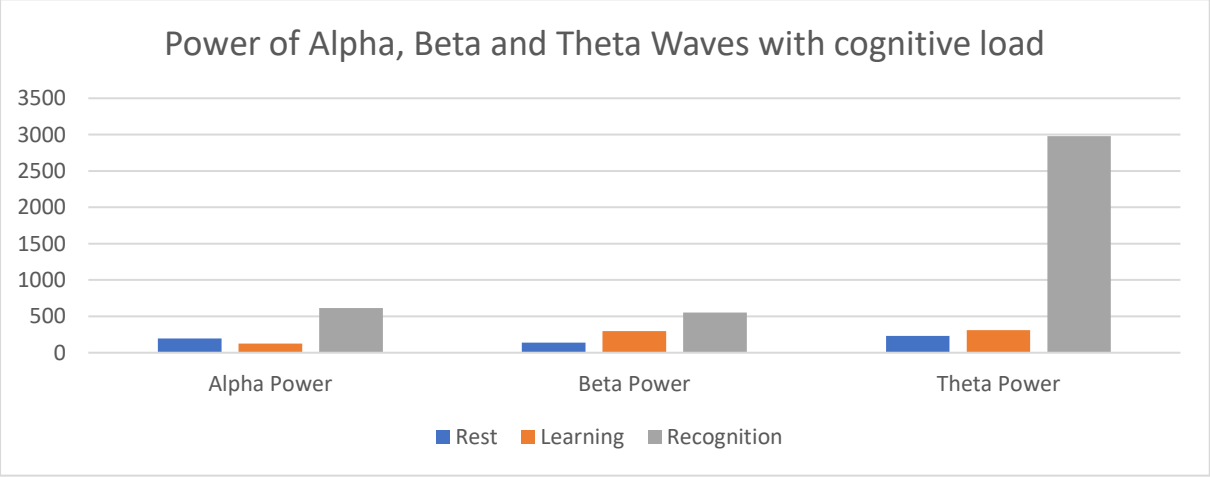

Figure 4.4-15 Power of alpha, beta and theta waves with cognitive load – Subject 3

- Average power of alpha wave decreases in all subjects during learning phase. Thus, during learning phase there is an increase in cortical activity. In recognition phase, different users show different results. This may be due to the fact that some subjects can easily recognise the music while others may face difficulty. Subject 2 shows a decrease in alpha power in recognition phase, suggesting further increase in cortical activity, which is supported by the fact that subject 2 had problems in recognising the music, while the other two subjects easily recognised the music, which is reflected in decrease in cortical activity during recognition phase.
- Since beta activity is linked to cognitive response to task, a rise in beta power was expected with cognitive load on all subjects, but in one subject there was a consistent decrease in beta power. This may be attributed to the effect of music and the approach of the subject towards the task. Since all the subjects could recognise the unknown music with equal proficiency, it can be concluded that recognition of musical segments does not always depend upon conscious reasoning. Even though the subject was unlearned in music and was unable to recognise specific musical characteristics, yet the subject was able to successfully recognise the music. Thus, the effect of music can be attributed to unconscious retention of musical patterns by brain.
- Even though variation of theta wave is not consistent due to learning phase, there is a significant rise in theta activity during recognition phase.

VARIATION OF DELTA POWER BEFORE AND AFTER MUSIC

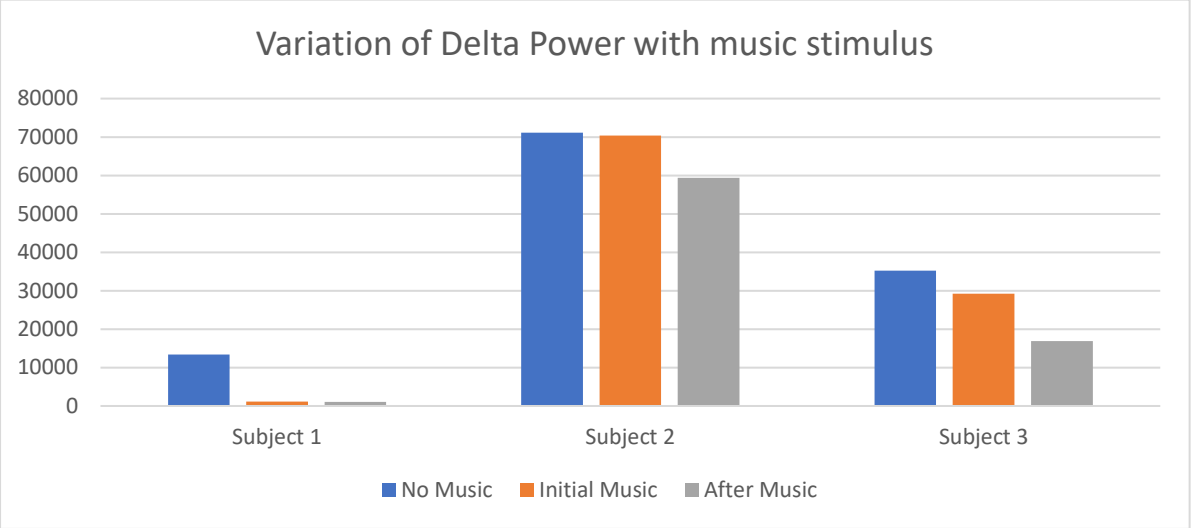

Figure 4.4-16 Variation of Delta Power with music stimulus

- In all subjects, average delta power decreases with application of music. Since, rise in delta activity is seen in sleep, the decrease in delta activity with music may indicate an effect of arousal with music.
- Average delta power remains low or decreases further even after music has stopped.

VARIATION OF DELTA POWER WITH COGNITIVE LOAD

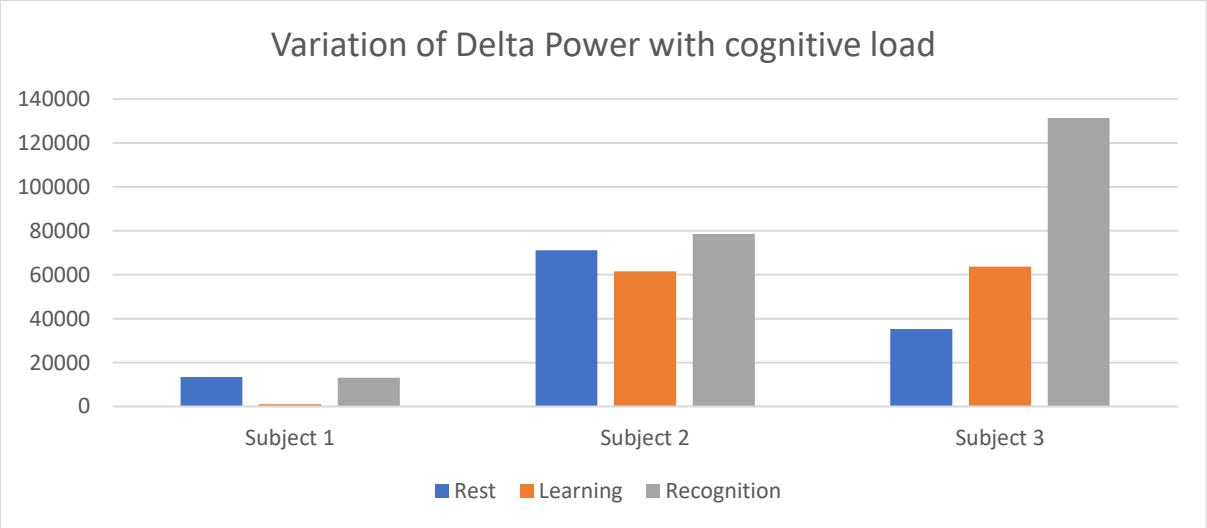

Figure 4.4-17 Variation of Delta Power with cognitive load

- Variation of delta power with cognitive load is different subjects.

4.5 Fractal Analysis of Brain Dimension

Variation of Fractal Dimension Before and After Music

Subject 1 –

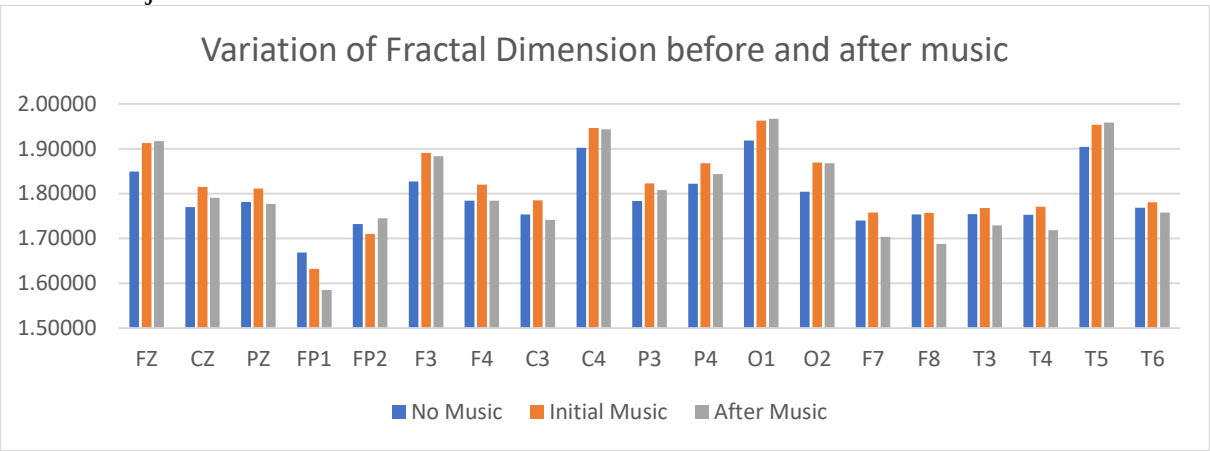

Figure 4.5-1 Variation of Fractal Dimension with music stimulus - Subject 1

Subject 2 –

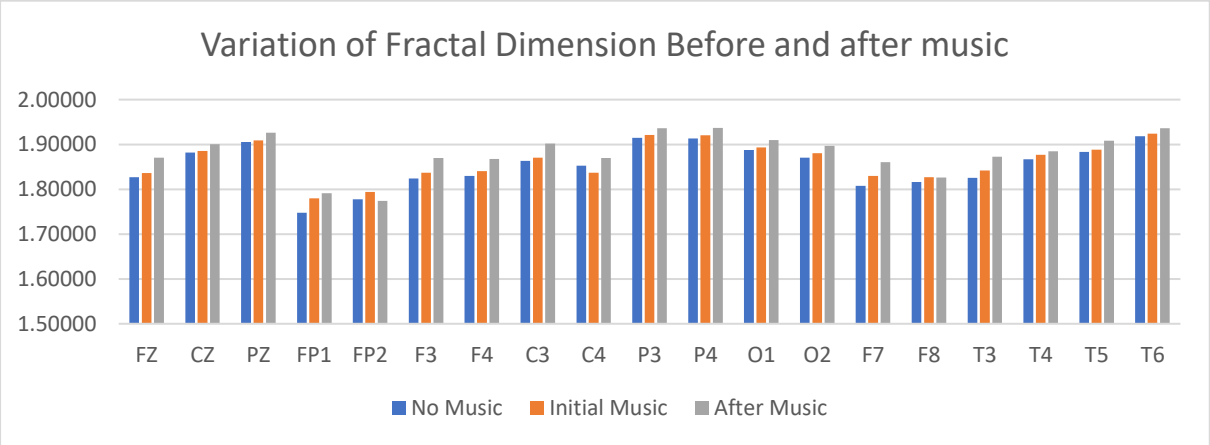

Figure 4.5-2 Variation of Fractal Dimension with music stimulus - Subject 2

Subject 3 –

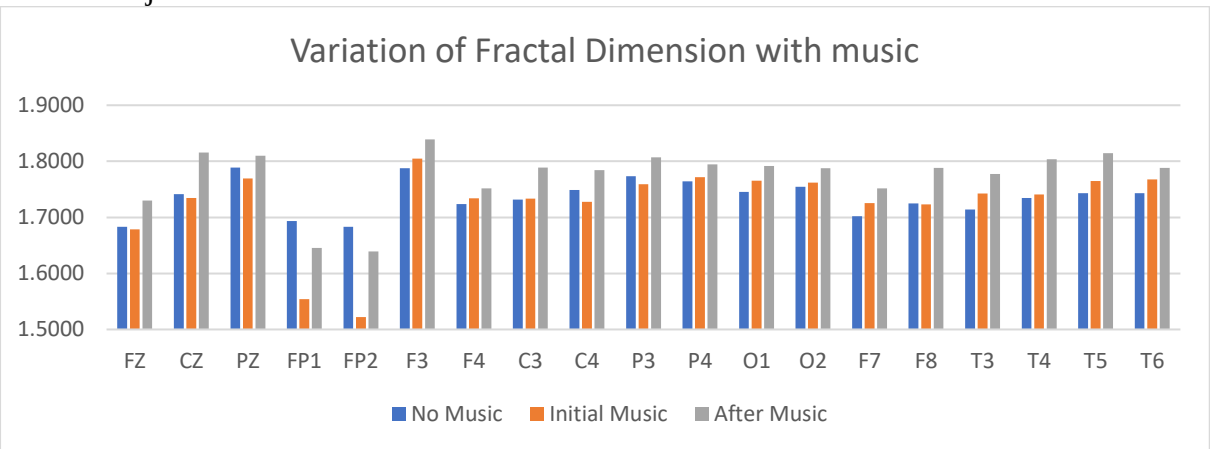

Figure 4.5-3 Variation of Fractal Dimension with music stimulus - Subject 3

- Fractal dimension, which is a measure of complexity of a signal, rises in most of the electrodes with music in all subjects.
- After the music has stopped, complexity of signal from most of the electrodes do not return back to the pre-music values, suggesting persistence of the effect of music in most regions of the brain.

VARIATION OF FRACTAL DIMENSION WITH COGNITIVE LOAD

Subject 1 –

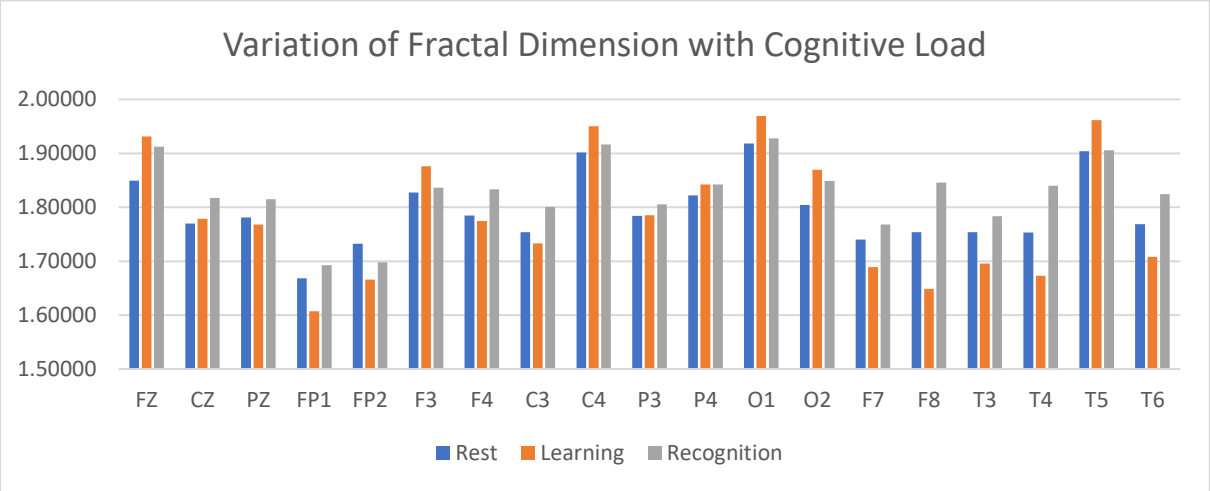

Figure 4.5-4 Variation of Fractal Dimension with Cognitive Load - Subject 1

Subject 2 –

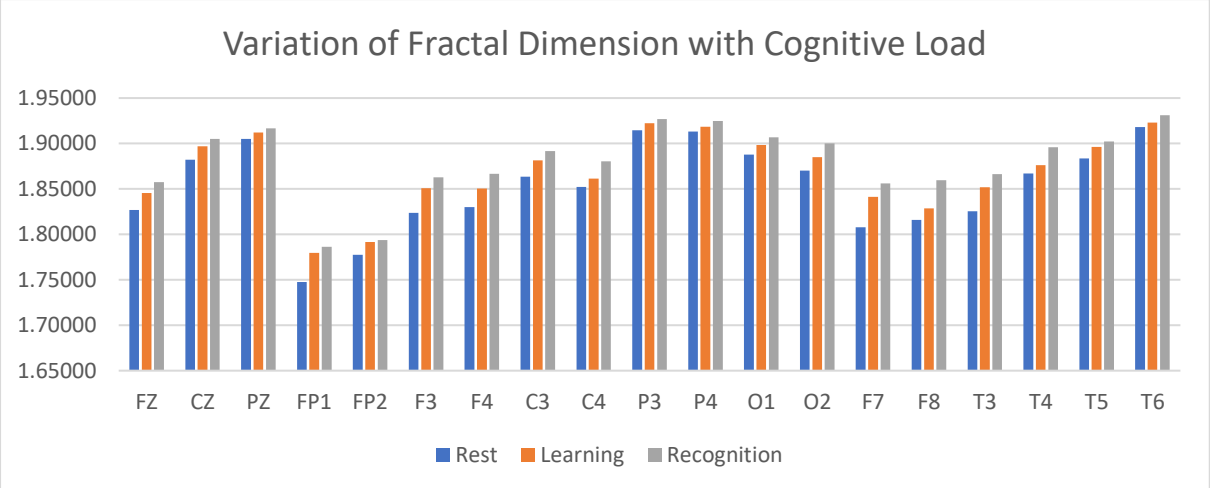

Figure 4.5-5 Variation of Fractal Dimension with Cognitive Load - Subject 1

Subject 3 –

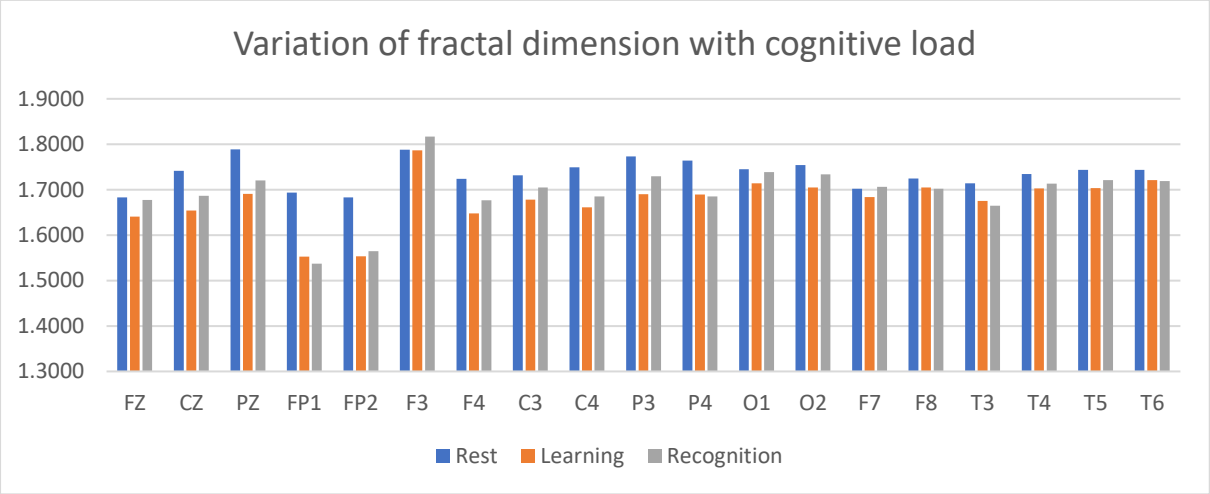

Figure 4.5-6 Variation of Fractal Dimension with Cognitive Load - Subject 1

- Variation of fractal dimension with cognitive load is different for different users.
- In Subject 1, in signals from some electrodes show decrease in complexity during learning phase, while some show increase in complexity. Fz, F3, C4, O1,O2 and T5 show significant rise in complexity during learning phase. Except T5, all signals from the temporal region show decrease in complexity during learning phase.
- In Subject 2, complexity rises in all the signals from all 19 electrodes. Complexity rises further during recognition phase.
- In Subject 3, there is a decrease in complexity during learning phase in all the signals.

4.6 CORRELATION ANALYSIS

CORRELATION OF EEG SIGNALS IN EACH SUBJECT (DURING REST)

Subject 1 –

Subject 1	FZ	CZ	PZ	FP1	FP2	F3	F4	C3	C4	P3	P4	O1	O2	F7	F8	T3	T4	T5	T6
FZ	1	0.96663	0.95465	0.48361	-0.357	0.98546	0.96769	0.94888	0.95891	0.9491	0.96795	0.9082	0.9492	0.94142	0.85963	0.9519	0.90142	0.94111	0.93003
CZ		1	0.99228	0.48343	-0.3765	0.97465	0.98773	0.98489	0.89949	0.98901	0.98217	0.8342	0.97642	0.96438	0.90059	0.97765	0.94403	0.88267	0.9695
PZ			1	0.4664	-0.3812	0.96401	0.98313	0.98351	0.88955	0.99412	0.98452	0.82833	0.98122	0.95693	0.90763	0.97446	0.95399	0.87575	0.97628
FP1				1	-0.3104	0.54155	0.43781	0.5086	0.40671	0.49482	0.42333	0.41057	0.46118	0.60982	0.23707	0.56655	0.3077	0.45947	0.39881
FP2					1	-0.3949	-0.3101	-0.4025	-0.2695	-0.3977	-0.3315	-0.289	-0.3605	-0.4543	-0.1466	-0.4453	-0.2623	-0.33	-0.3288
F3						1	0.96428	0.96584	0.93583	0.96603	0.96528	0.89394	0.95829	0.97231	0.83463	0.97708	0.88854	0.93584	0.93112
F4							1	0.96929	0.91182	0.97549	0.98684	0.83967	0.97244	0.93784	0.93139	0.95627	0.96111	0.88228	0.97299
C3								1	0.8739	0.98642	0.9647	0.81625	0.96643	0.96878	0.87131	0.97863	0.92292	0.8691	0.95405
C4									1	0.87663	0.93247	0.9635	0.89977	0.85071	0.83433	0.86923	0.86011	0.96601	0.87808
P3										1	0.97449	0.81944	0.97735	0.96727	0.88697	0.98116	0.93873	0.8725	0.968
P4											1	0.87649	0.98229	0.92997	0.92929	0.95348	0.9638	0.91118	0.97733
O1												1	0.85439	0.8088	0.74667	0.82529	0.78384	0.98276	0.81504
O2													1	0.94348	0.89725	0.96353	0.94528	0.89482	0.97042
F7														1	0.78615	0.99285	0.85587	0.86794	0.91341
F8															1	0.82706	0.97704	0.77427	0.93799
T3																1	0.89191	0.88146	0.93885
T4																	1	0.81773	0.97168
T5																		1	0.85589
T6																			1

Figure 4.6-1 Correlation of EEG signal of each pair of electrodes in Subject 1 during rest, with pairs of electrodes having high correlation marked with colour

Subject 2 –

Subject 2	FZ	CZ	PZ	FP1	FP2	F3	F4	C3	C4	P3	P4	O1	O2	F7	F8	T3	T4	T5	T6
FZ	1	0.92284	0.87548	0.74912	0.72936	0.96923	0.98317	0.92685	0.96474	0.82529	0.85941	0.88387	0.89968	0.91351	0.69105	0.91951	0.87218	0.88893	0.80414
CZ		1	0.91158	0.69586	0.66371	0.91452	0.91324	0.91503	0.93398	0.8565	0.8774	0.87198	0.87297	0.86636	0.64539	0.87925	0.83909	0.87743	0.8006
PZ			1	0.64764	0.63082	0.87771	0.87393	0.93375	0.9203	0.95094	0.96231	0.92291	0.90088	0.83467	0.62832	0.86862	0.85826	0.92445	0.8708
FP1				1	0.32885	0.83188	0.66392	0.78961	0.6609	0.64269	0.60377	0.66688	0.63669	0.88799	0.1797	0.83338	0.49786	0.72296	0.52308
FP2					1	0.60989	0.79585	0.59104	0.7613	0.57695	0.65909	0.65284	0.7098	0.4963	0.86357	0.54423	0.81219	0.60426	0.67866
F3						1	0.92841	0.96493	0.92612	0.84266	0.84382	0.88253	0.87863	0.97767	0.55579	0.9629	0.80642	0.91019	0.77233
F4							1	0.89519	0.97977	0.8147	0.87169	0.87967	0.90793	0.85339	0.78054	0.87461	0.91596	0.8692	0.82907
C3								1	0.91481	0.92437	0.88855	0.92797	0.90415	0.9547	0.55243	0.96417	0.82377	0.95843	0.82049
C4									1	0.85152	0.92347	0.89944	0.92274	0.85774	0.75782	0.88169	0.92606	0.88947	0.8642
P3										1	0.90729	0.93951	0.88839	0.81944	0.56896	0.8658	0.81705	0.94793	0.85749
P4											1	0.91299	0.91753	0.79438	0.66908	0.83702	0.89919	0.89613	0.92895
O1												1	0.97637	0.85544	0.64872	0.91324	0.89536	0.97708	0.90919
O2													1	0.83808	0.71664	0.89548	0.94188	0.941	0.93707
F7														1	0.42473	0.97545	0.72754	0.89796	0.72229
F8															1	0.51124	0.85875	0.58468	0.70906
T3																1	0.79445	0.94638	0.78727
T4																	1	0.85302	0.93789
T5																		1	0.86876
T6																			1

Figure 4.6-2 Correlation of EEG signal of each pair of electrodes in Subject 2 during rest, with pairs of electrodes having high correlation marked with colour

Subject 3 –

Subject 3	FZ	CZ	PZ	FP1	FP2	F3	F4	C3	C4	P3	P4	O1	O2	F7	F8	T3	T4	T5	T6
FZ	1	0.77417	0.65813	0.4436	0.53095	0.5666	0.73035	0.74998	0.71659	0.65055	0.67045	0.63804	0.64237	0.71866	0.72361	0.67786	0.66952	0.67591	0.67352
CZ		1	0.90866	0.35651	0.55691	0.70465	0.91868	0.92357	0.92624	0.88439	0.89492	0.90117	0.88908	0.87659	0.91462	0.89728	0.91564	0.9195	0.90777
PZ			1	0.24401	0.43292	0.64516	0.82619	0.8598	0.86523	0.89246	0.887	0.89882	0.8914	0.81387	0.84433	0.86494	0.87751	0.90953	0.88656
FP1				1	0.76167	0.38182	0.41007	0.31352	0.29181	0.24432	0.23794	0.20839	0.19223	0.41565	0.36103	0.35242	0.2718	0.22357	0.22009
FP2					1	0.50788	0.64774	0.49877	0.49704	0.42858	0.44336	0.40266	0.41157	0.55638	0.6107	0.51026	0.52167	0.42765	0.45498
F3						1	0.6964	0.68007	0.64536	0.61845	0.63953	0.64267	0.64197	0.71046	0.67634	0.68926	0.65858	0.65645	0.64993
F4							1	0.85808	0.8834	0.81512	0.83764	0.83808	0.83538	0.84518	0.90365	0.85823	0.8744	0.84157	0.85111
C3								1	0.89136	0.85148	0.85414	0.85868	0.85018	0.84525	0.85274	0.8663	0.8622	0.87708	0.86686
C4									1	0.84132	0.85851	0.85882	0.8454	0.82192	0.87023	0.83939	0.87169	0.87238	0.86441
P3										1	0.88337	0.89868	0.89452	0.84277	0.84303	0.88084	0.87773	0.90834	0.88771
P4											1	0.90158	0.89631	0.83468	0.85201	0.8679	0.88391	0.90347	0.89555
O1												1	0.93253	0.81849	0.86217	0.89651	0.90489	0.95528	0.92948
O2													1	0.8309	0.87086	0.8931	0.91068	0.93286	0.93248
F7														1	0.83369	0.86637	0.84803	0.85162	0.83817
F8															1	0.85638	0.90653	0.87945	0.89059
T3																1	0.88091	0.90988	0.88149
T4																	1	0.90551	0.91221
T5																		1	0.93674
T6																			1

Figure 4.6-3 Correlation of EEG signal of each pair of electrodes in Subject 3 during rest, with pairs of electrodes having high correlation marked with colour

CORRELATION OF EEG SIGNALS IN EACH SUBJECT (LEARNING PHASE)

Subject 1 –

Subject 1	FZ	CZ	PZ	FP1	FP2	F3	F4	C3	C4	P3	P4	O1	O2	F7	F8	T3	T4	T5	T6
FZ	1	0.60128	0.46456	0.18644	0.12896	0.84166	0.61477	0.47979	0.91606	0.42155	0.68376	0.83113	0.71332	0.47343	0.35075	0.46315	0.3704	0.83606	0.3643
CZ		1	0.86979	0.27886	0.18591	0.79966	0.87333	0.88306	0.52429	0.83513	0.83486	0.3568	0.74968	0.76336	0.64635	0.79243	0.71558	0.41058	0.68127
PZ			1	0.25959	0.17806	0.70339	0.80701	0.91565	0.41939	0.93423	0.83568	0.28295	0.75611	0.74392	0.6622	0.81069	0.76206	0.3385	0.73321
FP1				1	-0.0038	0.32821	0.24331	0.3479	0.10309	0.29538	0.17533	0.07516	0.18519	0.51315	-0.0257	0.4398	0.03851	0.11664	0.14305
FP2					1	0.09245	0.29755	0.1078	0.14268	0.11192	0.23586	0.06228	0.15361	-0.0345	0.48893	0.00093	0.36915	0.0594	0.20432
F3						1	0.77544	0.74907	0.78141	0.68506	0.83002	0.67476	0.82073	0.76274	0.43377	0.74955	0.51218	0.72544	0.53175
F4							1	0.79933	0.54488	0.75404	0.84181	0.36554	0.72942	0.68505	0.74947	0.71049	0.77347	0.40967	0.67865
C3								1	0.39783	0.92651	0.78511	0.27218	0.72534	0.8425	0.57711	0.8826	0.69571	0.33889	0.6934
C4									1	0.36186	0.68863	0.90463	0.71872	0.35665	0.34421	0.36774	0.35315	0.89617	0.33381
P3										1	0.77227	0.24968	0.72172	0.77676	0.58594	0.83714	0.70829	0.3161	0.70113
P4											1	0.56274	0.90977	0.65151	0.69441	0.71608	0.75166	0.6046	0.70081
O1												1	0.67371	0.27539	0.19784	0.29003	0.21532	0.97409	0.23564
O2													1	0.64823	0.57954	0.71874	0.66017	0.71115	0.66486
F7														1	0.33373	0.93465	0.47863	0.34855	0.55803
F8															1	0.4362	0.8941	0.21713	0.67523
T3																1	0.58734	0.36115	0.64473
T4																	1	0.245	0.75053
T5																		1	0.27529
T6																			1

Figure 4.6-4 Correlation of EEG signal of each pair of electrodes in Subject 1 during learning phase, with pairs of electrodes having high correlation marked with colour

Subject 2 –

Subject 2	FZ	CZ	PZ	FP1	FP2	F3	F4	C3	C4	P3	P4	O1	O2	F7	F8	T3	T4	T5	T6
FZ	1	0.90119	0.86935	0.76082	0.76778	0.96882	0.98195	0.92123	0.92131	0.82129	0.84863	0.87358	0.88787	0.91242	0.76808	0.9051	0.87302	0.86971	0.79294
CZ		1	0.89291	0.6859	0.6766	0.89355	0.88685	0.89177	0.87354	0.84225	0.84914	0.84813	0.84681	0.84895	0.69743	0.85549	0.82287	0.84762	0.77463
PZ			1	0.64462	0.65837	0.87405	0.87012	0.93057	0.88213	0.95451	0.96099	0.92134	0.90053	0.83508	0.70185	0.866	0.86838	0.91616	0.87193
FP1				1	0.52544	0.81238	0.68843	0.76262	0.65134	0.63445	0.60395	0.66123	0.64017	0.84784	0.35032	0.79533	0.5413	0.69635	0.53472
FP2					1	0.6658	0.81226	0.63437	0.74389	0.60072	0.6677	0.658	0.70216	0.56399	0.86493	0.58762	0.79217	0.62073	0.66579
F3						1	0.93132	0.96198	0.88969	0.84286	0.83926	0.88064	0.87696	0.97599	0.65624	0.95422	0.82057	0.89792	0.77056
F4							1	0.8939	0.93487	0.81215	0.8645	0.87021	0.8956	0.85923	0.8433	0.86657	0.91314	0.85428	0.81782
C3								1	0.88055	0.92642	0.88686	0.92761	0.90498	0.95514	0.64884	0.96526	0.84108	0.95152	0.82154
C4									1	0.82179	0.88184	0.86123	0.87998	0.8304	0.78633	0.84553	0.88891	0.846	0.82242
P3										1	0.91104	0.94112	0.89171	0.82472	0.6396	0.86873	0.83045	0.94364	0.86433
P4											1	0.91178	0.91646	0.79549	0.72685	0.83388	0.90355	0.88847	0.93097
O1												1	0.97627	0.86331	0.7137	0.9187	0.90109	0.96924	0.90884
O2													1	0.84733	0.77266	0.9021	0.94348	0.93313	0.9357
F7														1	0.53815	0.97485	0.75325	0.89437	0.72935
F8															1	0.59929	0.89484	0.65659	0.7492
T3																1	0.8139	0.94292	0.79052
T4																	1	0.85862	0.93529
T5																		1	0.86378
T6																			1

Figure 4.6-5 Correlation of EEG signal of each pair of electrodes in Subject 2 during learning phase, with pairs of electrodes having high correlation marked with colour

Subject 3 –

Subject 3	FZ	CZ	PZ	FP1	FP2	F3	F4	C3	C4	P3	P4	O1	O2	F7	F8	T3	T4	T5	T6
FZ	1	0.94864	0.89155	0.64845	0.3614	0.83001	0.93095	0.88103	0.92333	0.78918	0.52072	0.735	0.34541	0.64325	0.15372	-0.1106	0.61719	0.77872	0.33679
CZ		1	0.94834	0.61968	0.35784	0.83509	0.95972	0.92167	0.96482	0.85502	0.57666	0.82814	0.4425	0.70258	0.23959	-0.0336	0.68995	0.86238	0.44434
PZ			1	0.53374	0.30149	0.82678	0.92455	0.90546	0.9248	0.88839	0.66193	0.84823	0.55365	0.7359	0.28	0.0842	0.7482	0.85407	0.52746
FP1				1	0.7016	0.51009	0.58521	0.50176	0.57546	0.38353	0.13479	0.30435	-0.0576	0.31242	-0.0881	-0.4247	0.10011	0.40404	-0.1223
FP2					1	0.2453	0.35835	0.2463	0.35305	0.17697	0.07791	0.16828	0.03764	0.16637	0.3214	-0.2623	0.04393	0.27619	0.01479
F3						1	0.83593	0.81911	0.81103	0.79963	0.61799	0.71489	0.47047	0.69153	0.17086	0.09914	0.64892	0.71263	0.40886
F4							1	0.89673	0.94685	0.84782	0.62988	0.7815	0.45896	0.69428	0.24574	-0.0209	0.7176	0.80229	0.43732
C3								1	0.90339	0.87041	0.64533	0.82178	0.54422	0.76806	0.25271	0.12938	0.72807	0.83965	0.52916
C4									1	0.83165	0.58128	0.80567	0.45196	0.68728	0.26926	-0.0281	0.69976	0.8457	0.46963
P3										1	0.80147	0.84887	0.70659	0.81284	0.32578	0.33533	0.82974	0.80803	0.6417
P4											1	0.6583	0.79916	0.72173	0.41322	0.52995	0.80398	0.56843	0.68088
O1												1	0.69024	0.75679	0.45071	0.34197	0.79149	0.89673	0.71636
O2													1	0.71982	0.60024	0.70781	0.78055	0.60925	0.84354
F7														1	0.36005	0.45076	0.70706	0.77178	0.64265
F8															1	0.4836	0.51175	0.43693	0.6731
T3																1	0.5002	0.22883	0.67959
T4																	1	0.71205	0.785
T5																		1	0.66413
T6																			1

Figure 4.6-6 Correlation of EEG signal of each pair of electrodes in Subject 3 during learning phase, with pairs of electrodes having high correlation marked with colour

CORRELATION OF EEG SIGNALS IN EACH SUBJECT (RECOGNITION PHASE)

Subject 1 –

Subject 1	FZ	CZ	PZ	FP1	FP2	F3	F4	C3	C4	P3	P4	O1	O2	F7	F8	T3	T4	T5	T6
FZ	1	0.89903	0.87019	0.58315	-0.2309	0.93562	0.89222	0.87796	0.96393	0.85302	0.88648	0.93939	0.90784	0.84809	0.63096	0.85159	0.7231	0.95408	0.83037
CZ		1	0.98795	0.58627	-0.2775	0.9651	0.97725	0.98039	0.89602	0.96646	0.97871	0.81646	0.97469	0.91138	0.75459	0.92645	0.86673	0.86987	0.95317
PZ			1	0.58051	-0.2875	0.95275	0.97278	0.98449	0.8717	0.97365	0.97943	0.79506	0.9743	0.90725	0.7648	0.92906	0.88096	0.85069	0.95982
FP1				1	-0.6847	0.71902	0.50439	0.67761	0.44107	0.63216	0.49048	0.50784	0.5586	0.82564	-0.0004	0.78382	0.19488	0.59984	0.44713
FP2					1	-0.3785	-0.1781	-0.3715	-0.1379	-0.3599	-0.2028	-0.2281	-0.2722	-0.5028	0.20627	-0.4723	-0.0041	-0.3012	-0.1966
F3						1	0.93526	0.97678	0.88891	0.94978	0.93239	0.85474	0.95311	0.96718	0.60808	0.96857	0.74537	0.91442	0.88922
F4							1	0.95095	0.89881	0.93011	0.98011	0.79857	0.96367	0.8592	0.82238	0.88385	0.90259	0.84573	0.95293
C3								1	0.84837	0.98189	0.95308	0.79232	0.96015	0.95838	0.66835	0.97106	0.80745	0.86124	0.92823
C4									1	0.83669	0.91089	0.94149	0.91969	0.76557	0.74248	0.78621	0.81116	0.93973	0.86049
P3										1	0.94364	0.78069	0.94831	0.92616	0.67816	0.94228	0.81496	0.84261	0.92427
P4											1	0.82518	0.9852	0.85355	0.82663	0.88685	0.91961	0.86554	0.96943
O1												1	0.86743	0.75673	0.58284	0.76593	0.67964	0.97018	0.77106
O2													1	0.88641	0.76581	0.91254	0.87875	0.90885	0.95884
F7														1	0.46048	0.98604	0.62864	0.84083	0.81896
F8															1	0.51741	0.96044	0.58044	0.84059
T3																1	0.68195	0.84821	0.85229
T4																	1	0.69342	0.93443
T5																		1	0.81149
T6																			1

Figure 4.6-7 Correlation of EEG signal of each pair of electrodes in Subject 1 during recognition phase, with pairs of electrodes having high correlation marked with colour

Subject 2 –

Subject 2	FZ	CZ	PZ	FP1	FP2	F3	F4	C3	C4	P3	P4	O1	O2	F7	F8	T3	T4	T5	T6
FZ	1	0.91826	0.89958	0.78913	0.79174	0.97705	0.98554	0.93415	0.97142	0.851	0.88008	0.90301	0.91385	0.93155	0.80976	0.9267	0.89902	0.90813	0.82808
CZ		1	0.91249	0.72342	0.70487	0.90842	0.90191	0.90108	0.92363	0.86262	0.86854	0.87367	0.87177	0.87078	0.74012	0.87779	0.84561	0.87955	0.8037
PZ			1	0.70736	0.70856	0.90056	0.89864	0.93888	0.93847	0.96208	0.9659	0.9408	0.92446	0.86633	0.75763	0.89145	0.89436	0.94036	0.89478
FP1				1	0.62936	0.8289	0.72903	0.79245	0.72407	0.69391	0.67233	0.72469	0.70886	0.85797	0.454	0.81743	0.62024	0.75636	0.61307
FP2					1	0.71138	0.82499	0.67764	0.79662	0.64889	0.71658	0.7045	0.74204	0.62744	0.86361	0.63269	0.80554	0.68381	0.7049
F3						1	0.94867	0.96567	0.94643	0.8684	0.87314	0.91019	0.90671	0.98188	0.71972	0.96695	0.85883	0.9289	0.81217
F4							1	0.91284	0.98336	0.84161	0.8948	0.90093	0.92179	0.88972	0.87422	0.89621	0.93363	0.89668	0.85079
C3								1	0.93138	0.92858	0.90475	0.94087	0.92401	0.95921	0.70384	0.96555	0.86662	0.95996	0.84858
C4									1	0.87799	0.93756	0.92167	0.93761	0.89303	0.85718	0.90636	0.94406	0.9168	0.88204
P3										1	0.92061	0.94624	0.9055	0.85202	0.68974	0.88393	0.85056	0.95087	0.87786
P4											1	0.93261	0.93969	0.83514	0.78124	0.86474	0.92621	0.91856	0.94577
O1												1	0.97966	0.89232	0.7637	0.93372	0.92008	0.98237	0.92198
O2													1	0.87884	0.81438	0.92126	0.95756	0.95573	0.94827
F7														1	0.61651	0.98094	0.80032	0.92164	0.7758
F8															1	0.66282	0.91259	0.72792	0.78899
T3																1	0.84697	0.95918	0.82293
T4																	1	0.89523	0.94616
T5																		1	0.89282
T6																			1

Figure 4.6-8 Correlation of EEG signal of each pair of electrodes in Subject 2 during recognition phase, with pairs of electrodes having high correlation marked with colour

Subject 3 –

Subject 3	FZ	CZ	PZ	FP1	FP2	F3	F4	C3	C4	P3	P4	O1	O2	F7	F8	T3	T4	T5	T6
FZ	1	0.97131	0.93079	0.66195	0.6162	0.83734	0.96068	0.9206	0.96251	0.82087	0.64235	0.73458	0.64778	0.83279	0.51168	0.34557	0.71285	0.90023	0.52563
CZ		1	0.9632	0.57946	0.54896	0.83781	0.96979	0.946	0.98208	0.87716	0.69031	0.81301	0.72003	0.87492	0.57099	0.41658	0.7747	0.95396	0.607
PZ			1	0.47634	0.48638	0.86402	0.94792	0.94652	0.9614	0.90637	0.78608	0.83656	0.78991	0.89477	0.60287	0.49383	0.8141	0.94997	0.65946
FP1				1	0.74289	0.43259	0.57517	0.48051	0.56041	0.34498	0.13547	0.2109	0.10841	0.40276	0.05553	-0.0978	0.18525	0.4391	-0.0003
FP2					1	0.51374	0.63496	0.50859	0.55194	0.48119	0.38764	0.37263	0.36849	0.48843	0.48177	0.24552	0.48402	0.4701	0.34479
F3						1	0.8678	0.87658	0.84936	0.85788	0.80274	0.80383	0.79655	0.86585	0.65768	0.60927	0.82016	0.84839	0.69721
F4							1	0.94016	0.96773	0.88817	0.75505	0.81585	0.75842	0.8829	0.64776	0.48108	0.82955	0.92864	0.65428
C3								1	0.94401	0.92388	0.78884	0.85899	0.80993	0.9251	0.6361	0.56732	0.83919	0.94703	0.70075
C4									1	0.88119	0.7122	0.80846	0.73001	0.86901	0.57725	0.42505	0.78348	0.94285	0.61205
P3										1	0.86981	0.92758	0.91057	0.94048	0.76023	0.73648	0.91429	0.93904	0.83611
P4											1	0.84168	0.92785	0.8481	0.78595	0.82207	0.91502	0.77496	0.86118
O1												1	0.92192	0.90856	0.79531	0.77583	0.91885	0.90951	0.88728
O2													1	0.9007	0.84353	0.87192	0.95674	0.83855	0.94483
F7														1	0.73159	0.73337	0.89976	0.9311	0.82144
F8															1	0.81772	0.88814	0.66751	0.89722
T3																1	0.82967	0.58472	0.91472
T4																	1	0.85868	0.93836
T5																		1	0.74874
T6																			1

Figure 4.6-9 Correlation of EEG signal of each pair of electrodes in Subject 3 during recognition phase, with pairs of electrodes having high correlation marked with colour

PAIRS OF ELECTRODES WITH HIGH CORRELATION IN ALL SUBJECTS

FZ CZ	FZ PZ	FZ FP1	FZ FP2	FZ F3	FZ F4	FZ C3	FZ C4	FZ P3	FZ P4	FZ O1	FZ O2	FZ F7	FZ F8	FZ T3	FZ T4	FZ T5	FZ T6
	CZ PZ	CZ FP1	CZ FP2	CZ F3	CZ F4	CZ C3	CZ C4	CZ P3	CZ P4	CZ 01	CZ O2	CZ F7	CZ F8	CZ T3	CZ T4	CZ T5	CZ T6
		PZ FP1	PZ FP2	PZ F3	PZ F4	PZ C3	PZ C4	PZ P3	PZ P4	PZ O1	PZ O2	PZ F7	PZ F8	PZ T3	PZ T4	PZ T5	PZ T6
			FP1 FP2	FP1 F3	FP1 F4	FP1 C3	FP1 C4	FP1 P3	FP1 P4	FP1 O1	FP1 O2	FP1 F7	FP1 F8	FP1 T3	FP1 T4	FP1 T5	FP1 T6
				FP2 F3	FP2 F4	FP2 C3	FP2 C4	FP2 P3	FP2 P4	FP2 O1	FP2 O2	FP2 F7	FP2 F8	FP2 T3	FP2 T4	FP2 T5	FP2 T6
					F3 F4	F3 C3	F3 C4	F3 P3	F3 P4	F3 O1	F3 O2	F3 F7	F3 F8	F3 T3	F3 T4	F3 T5	F3 T6
						F4 C3	F4 C4	F4 P3	F4 P4	F4 O1	F4 O2	F4 F7	F4 F8	F4 T3	F4 T4	F4 T5	F4 T6
							C3 C4	C3 P3	C3 P4	C3 O1	C3 O2	C3 F7	C3 F8	C3 T3	C3 T4	C3 T5	C3 T6
								C4 P3	C4 P4	C4 O1	C4 O2	C4 F7	C4 F8	C4 T3	C4 T4	C4 T5	C4 T6
									P3 P4	P3 O1	P3 O2	P3 F7	P3 F8	P3 T3	P3 T4	P3 T5	P3 T6
										P4 O1	P4 O2	P4 F7	P4 F8	P4 T3	P4 T4	P4 T5	P4 T6
											O1 O2	O1 F7	O1 F8	O1 T3	O1 T4	O1 T5	O1 T6
												O2 F7	O2 F8	O2 T3	O2 T4	O2 T5	O2 T6
													F7 F8	F7 T3	F7 T4	F7 T5	F7 T6
														F8 T3	F8 T4	F8 T5	F8 T6
															T3 T4	T3 T5	T3 T6
																T4 T5	T4 T6
																	T5 T6

High Correlation During Rest
High Correlation During Learning Phase
High Correlation During Recognition Phase
High Correlation During Rest and Learning
High Correlation During Learning and Recognition
High Correlation During All Phases

Figure 4.6-10 Pairs of Electrodes with High Correlation in All Subjects

5. Discussion

The day science begins to study non-physical phenomena, it will make more progress in one decade than in all the previous centuries of its existence.

- Nikola Tesla

In the first part of our study, we found out the variation of SNR of various FIR and IIR filters with change in filter order. It was seen that in all filters, both FIR and IIR, with increasing filter order, SNR increased but was saturated after a specific filter order or started decreasing. Thus, for ECG denoising, continual increase in filter order will not achieve better filtering but may lead to loss of essential information. The optimal filter order for each filter in both diagnostic and monitoring mode has been stated in the result section.

For a more comprehensive approach towards ECG denoising, we then compared FIR and IIR filters with wavelet based denoising techniques and Savitzky Golay Filters. Additional Gaussian noise was added to test the performance of the filters with different levels of noise. In this comparative study, RMSE was also calculated along with SNR. It was seen that the performance of FIR and IIR filters decreased with increasing amount of Gaussian Noise. Wavelet based denoising techniques on the other hand was excellent in removal of Gaussian Noise, giving clean ECG signal at all levels of noise. Savitzky Golay Filters performed better than FIR and IIR filters. The optimum parameters for Savitzky Golay Filters at various levels of noise was identified. Another interesting conclusion from this experiment was the importance of RMSE along with SNR to describe performance of denoising techniques. For bio-signals, a filter with high SNR is not enough if it removes essential physiological features of the signal. Thus RMSE, which quantifies the accuracy of the filtering process by comparing the filtered signal with the original noise-free signal has been identified as an essential criterion to describe performance of denoising techniques.

In the next phase, we studied dynamics of cardiovascular system with music. It was seen that heart rate rises with music stimulus, and then decreases when the stimulus is removed.

Thus, the application of music causes an effect of arousal. It was also seen that with cognitive load (in this case music) causes a rise in heart rate. Thus, cardiac output is increased with music, and also with learning phase. These results were consistent among the subjects. But during recognition phase variation of heart rate was different in different subjects. This is due to the fact that the process of recognition is subjective. Some subject may recognise the music segment easily whereas some subjects might have a lot of difficulty in recognising.

Study of spectral components of HRV revealed that music caused both arousal and stress relaxing effects in subjects. The variation of LF/HF ratio and HF component with music stimulus was consistent among subjects. But the variation of these parameters with cognitive task was not consistent, a possible explanation of which has been provided in the preceding paragraph. The results clearly signify the stress relaxing effect of music, which is reflected in the conspicuous fall in LF/HF ratio and subsequent rise in HF component with music stimulus and the opposite occurring after the stimulus has been removed.

Fractal analysis of HRV show that complexity of HRV signal rises with music stimulus. Whereas variation of fractal dimension is not consistent in learning and recognition phase, which again brings us to the conclusion that learning, and recognition are highly subjective processes. Proper physiological implication of the complexity of HRV signal requires further research work with much more data.

While analysing the dynamics of brain with music stimulus it was seen that average power across various regions of the brain decreased significantly. The magnitude of the decrease was highly subjective and is based on the perception of the music segment by the subject. The decrease in average power can be attributed to the stress relaxing effect of music. Also, a hysteresis like effect was observed as average power across all regions of the brain do not rise back to their original values after the musical stimulus has been removed.

A consistent decrease of alpha power with music stimulus in all subjects reveal that music causes the effect of arousal in subjects. Low variation of beta wave suggest that cognitive reasoning of music is not present in untrained listeners, and the fact this process will be highly subjective is reflected in the results. A decrease in alpha component was seen with cognitive load, which is understandable as cognitive processes are accompanied by a decrease in alpha power. But there was no significant rise in beta power. Thus, it can be concluded that even

though learning and recognition is supposed to require high cognitive processing and a rise in beta component, musical recognition might not require cognitive processing. Some subjects recognise music based on emotion recognition whereas some subjects may recognise the music by relating to certain events or occurrences.

Variation of fractal dimension show that there is a rise in the complex nature of EEG signals with music stimulus. Also, a hysteresis like effect is observed here, with the complexity of EEG signals not returning to their original values after the music has stopped. Thus, the effect of music persists in the mind of the listener even after the music has stopped.

From the correlation analysis, the pairs of electrodes having high correlation in all subjects during different phases of the experiment were recognized. There were significant differences among the different phases. Some pairs of electrodes were consistently correlated in all phases suggesting that they were not affected by music and might relate to other physiological processes. Some pair of electrodes showed high correlation only during specific phases like learning and recognition. Through this analysis, we can identify and link specific electrodes to specific processes, but such an analysis would require further statistical analysis with much larger sets of data.

6. Conclusion

In our study, the effects of music on brain and cardiovascular system were analysed. The methodology for testing the learning and recognition of instrumental Indian Classical Music was successful as all the subjects successfully recognized the music segment with utmost proficiency. Thus, even under the abstract nature of music there are distinctive differences which can be recognised even by an untrained subject.

Some significant effects of music were recognized, like the results consistently showed the stress relaxing effects of music, while on the other hand music also causes arousal. Learning and recognition processes are on the other hand are highly subjective, as reflected by the results, yet in each case the subject could successfully learn and recognise the unknown music.

In order to concretely establish the effects of music further studies with much larger sets of data and statistical analysis is required.

7. Future Scope

Human body is a still a mystery yet to be unravelled. New discoveries are constantly being made which are giving us new insights into the working of our mind and body. There is huge scope of research in this field. Music on the other hand has influenced human mind and body since ages and yet how music affects us so deeply is not yet well understood. With newer computation methods and better analysis methodologies huge progress can be made in research in this field which will reveal to us deeper insight into the working of our mind and body.

8. References

[1] Rao, C. R., & Guha, S. K. (2001). *Principles of medical electronics and biomedical instrumentation*. Universities Press.

[2] Vyas, N. (2011). *Biomedical Signal Processing*. Laxmi Publications.

[3] Khandpur, R. S. (1992). *Handbook of biomedical instrumentation*. Tata McGraw-Hill Education.

[4] Rangayyan, R. M. (2015). *Biomedical signal analysis* (Vol. 33). John Wiley & Sons.

[5] Kaniusas, E. (2012). Fundamentals of biosignals. In *Biomedical Signals and Sensors I* (pp. 1-26). Springer, Berlin, Heidelberg.

[6] Pesic, P. (2015). Music, mechanism, and the "Sonic Turn" in physical diagnosis. *Journal of the history of medicine and allied sciences*, *71*(2), 144-172.

[7] Rivera-Ruiz, M., Cajavilca, C., & Varon, J. (2008). Einthoven's string galvanometer: the first electrocardiograph. *Texas Heart Institute Journal*, *35*(2), 174.

[8] Haas, L. F. (2003). Hans berger (1873–1941), richard caton (1842–1926), and electroencephalography. *Journal of Neurology, Neurosurgery & Psychiatry*, *74*(1), 9-9.

[9] Towle, V. L., Bolaños, J., Suarez, D., Tan, K., Grzeszczuk, R., Levin, D. N., ... & Spire, J. P. (1993). The spatial location of EEG electrodes: locating the best-fitting sphere relative to cortical anatomy. *Electroencephalography and clinical neurophysiology*, *86*(1), 1-6.

[10] Luo, S., & Johnston, P. (2010). A review of electrocardiogram filtering. *Journal of electrocardiology*, *43*(6), 486-496.

[11] Hao, W., Chen, Y., & Xin, Y. (2011, August). ECG baseline wander correction by mean-median filter and discrete wavelet transform. In *Engineering in Medicine and Biology Society, EMBC, 2011 Annual International Conference of the IEEE* (pp. 2712-2715). IEEE.

[12] Fasano, A., & Villani, V. (2013, September). ECG baseline wander removal and impact on beat morphology: A comparative analysis. In *Computing in Cardiology Conference (CinC), 2013* (pp. 1167-1170). IEEE.

[13] Das, A. K., & Halder, S. (2017). Baseline Wander Correction and Impulse Noise Suppression Using Cascaded Empirical Mode Decomposition and Improved Morphological Algorithm. *International Journal of Applied Engineering Research*, *12*(10), 2329-2337.

[14] Han, G., Lin, B., & Xu, Z. (2017). Electrocardiogram signal denoising based on empirical mode decomposition technique: An overview. *Journal of Instrumentation*, *12*(03), P03010.

[15] Pan, N., Mang, V., & Un, M. P. (2007, October). Accurate removal of baseline wander in ECG using empirical mode decomposition. In *Noninvasive Functional Source Imaging of the Brain and Heart and the International Conference on Functional Biomedical Imaging, 2007. NFSI-ICFBI 2007. Joint Meeting of the 6th International Symposium on* (pp. 177-180). IEEE.

[16] Blanco-Velasco, M., Weng, B., & Barner, K. E. (2008). ECG signal denoising and baseline wander correction based on the empirical mode decomposition. *Computers in biology and medicine*, *38*(1), 1-13.

[17] Stojanovic, V. S., & Stankovic, M. S. (2000). Optimal FIR filter for suppression of power line frequency component. *International journal of electronics*, *87*(5), 569-574.

[18] Rani, S., Kaur, A., & Ubhi, J. S. (2011). Comparative study of FIR and IIR filters for the removal of Baseline noises from ECG signal.

[19] Ferdjallah, M., & Barr, R. E. (1994). Adaptive digital notch filter design on the unit circle for the removal of powerline noise from biomedical signals. *IEEE Transactions on Biomedical Engineering*, *41*(6), 529-536.

[20] Jiruska, P., Cmejla, R., Powell, A. D., Chang, W. C., Vreugdenhil, M., & Jefferys, J. G. (2009). Reference noise method of removing powerline noise from recorded signals. *Journal of neuroscience methods*, *184*(1), 110-114.

[21] Savitzky, A., & Golay, M. J. (1964). Smoothing and differentiation of data by simplified least squares procedures. *Analytical chemistry*, *36*(8), 1627-1639.

[22] Schafer, R. W. (2011). What is a Savitzky-Golay filter?[lecture notes]. *IEEE Signal processing magazine*, *28*(4), 111-117.

[23] Chakraborty, M., & Das, S. (2012). Determination of signal to noise ratio of electrocardiograms filtered by band pass and Savitzky-Golay filters. *Procedia Technology*, *4*, 830-833.

[24] Orfanidis, S. (2010). *Introduction to signal processing*. Pearson Education.

[25] Agarwal, S., Rani, A., Singh, V., & Mittal, A. P. (2017). EEG signal enhancement using cascaded S-Golay filter. *Biomedical Signal Processing and Control*, *36*, 194-204.

[26] Acharya, D., Rani, A., Agarwal, S., & Singh, V. (2016). Application of adaptive Savitzky–Golay filter for EEG signal processing. *Perspectives in Science*, *8*, 677-679.

[27] Taouli, S. A., & Bereksi-Reguig, F. (2010). Noise and baseline wandering suppression of ECG signals by morphological filter. *Journal of medical engineering & technology*, *34*(2), 87-96.

[28] Sørensen, J. S., Johannesen, L., Grove, U. S. L., Lundhus, K., Couderc, J. P., & Graff, C. (2010, September). A Comparison of IIR and Wavelet Filtering for Noise Reduction of the ECG. In *Computing in Cardiology, 2010* (pp. 489-492). IEEE.

[29] Singh, B. N., & Tiwari, A. K. (2006). Optimal selection of wavelet basis function applied to ECG signal denoising. *Digital signal processing*, *16*(3), 275-287.

[30] Awal, M. A., Mostafa, S. S., & Ahmad, M. (2011). Performance analysis of Savitzky-Golay smoothing filter using ECG signal. *International Journal of Computer and Information Technology*, *1*(02).

[31] Mamun, M., Al-Kadi, M., & Marufuzzaman, M. (2013). Effectiveness of wavelet denoising on electroencephalogram signals. *Journal of applied research and technology*, *11*(1), 156-160.

[32] Daud, S. S., & Sudirman, R. (2015, February). Butterworth bandpass and stationary wavelet transform filter comparison for electroencephalography signal. In *Intelligent Systems, Modelling and Simulation (ISMS), 2015 6th International Conference on* (pp. 123-126). IEEE.

[33] Albera, L., Kachenoura, A., Comon, P., Karfoul, A., Wendling, F., Senhadji, L., & Merlet, I. (2012). ICA-based EEG denoising: a comparative analysis of fifteen methods. *Bulletin of the Polish Academy of Sciences: Technical Sciences*, *60*(3), 407-418.

[34] Chen, Y., Akutagawa, M., Katayama, M., Zhang, Q., & Kinouchi, Y. (2008, August). Neural network based EEG denoising. In *Engineering in Medicine and Biology Society, 2008. EMBS 2008. 30th Annual International Conference of the IEEE* (pp. 262-265). IEEE.

[35] Banerjee, A., Sanyal, S., Sengupta, R., & Ghosh, D. (2015). Music and its Effect on Body, Brain/Mind: A Study on Indian Perspective by Neurophysical Approach. *Insights in Blood Pressure*, *1*(1).

[36] Chowdhury, P. (2001). Essays on Indian Classical Music - Sitar Maestro Prabal Chowdhury. Retrieved from http://sitarmaestro-prabalchowdhury.com/

[37] Chowdhury, P. (2001). The history of the origin of Indian Classical Music – Sitar Maestro Prabal Chowdhury. Retrieved from http://sitarmaestro-prabalchowdhury.com/history-of-the-origin-of-indian-classical-music/

[38] Chowdhury, P. (2001). Ragas and Raginis of Different Seasons – Sitar Maestro Prabal Chowdhury. Retrieved from http://sitarmaestro-prabalchowdhury.com/ragas-and-raginis-of-different-seasons/

[39] Raman,ChandrasekharaVenkata (1921) "On some Indian stringed instruments."*Proceedings of the Indian Association for the Cultivation of Science*7: 29-33.

[40] Raman CV (1935) "The Indian musical drums", *Proc Indian AcadSci*A1: 179-188.

[41] Banerjee, A., Sanyal, S., Patranabis, A., Banerjee, K., Guhathakurta, T., Sengupta, R., ... & Ghose, P. (2016). Study on brain dynamics by non linear analysis of music induced EEG signals. *Physica A: Statistical Mechanics and its Applications*, *444*, 110-120.

[42] Möckel, M., Röcker, L., Störk, T., Vollert, J., Danne, O., Eichstädt, H., ... & Hochrein, H. (1994). Immediate physiological responses of healthy volunteers to different types of music: cardiovascular, hormonal and mental changes. *European journal of applied physiology and occupational physiology*, *68*(6), 451-459.

[43] Möckel, M., Störk, T., Vollert, J. E. A., Röcker, L., Danne, O., Hochrein, H., ... & Frei, U. (1995). Stress reduction through listening to music: effects on stress hormones, hemodynamics and mental state in patients with arterial hypertension and in healthy persons. *Deutsche medizinische Wochenschrift (1946)*, *120*(21), 745-752.

[44] Vollert, J. O., Stork, T., Rose, M. E. A., Rocker, L., Klapp, B. F., Heller, G., ... & Mockel, M. (2002). Reception of music in patients with systemic arterial hypertension and coronary artery disease: endocrine changes, hemodynamics and actual mood. *PERFUSION-MUNICH THEN NURNBERG-*, *15*(4), 142-152.

[45] Henry, Linda L (1995) "Music therapy: a nursing intervention for the control of pain and anxiety in the ICU: a review of the research literature."*Dimensions of critical care nursing*14: 295-304.

[46] Ciccone Marco Matteo (2010) "Feasibility and effectiveness of a disease and care management model in the primary health care system for patients with heart failure and diabetes (Project Leonardo)." *Vascular health and risk management* 6: 297.

[47] Ezzone Susan (1998) "Music as an adjunct to antiemetic therapy." *Oncology nursing forum* 25: 9.

[48] Migneault Brigitte (2004) "The effect of music on the neurohormonal stress response to surgery under general anesthesia." *Anesthesia & Analgesia*98: 527-532.

[49] Montinaro, A. (2010). The musical brain: myth and science. *World neurosurgery*, *73*(5), 442-453.

[50] Klimesch, W. (1999). EEG alpha and theta oscillations reflect cognitive and memory performance: a review and analysis. *Brain research reviews*, *29*(2-3), 169-195.

[51] Lappe, C., Herholz, S. C., Trainor, L. J., & Pantev, C. (2008). Cortical plasticity induced by short-term unimodal and multimodal musical training. *Journal of Neuroscience*, *28*(39), 9632-9639.

[52] Watanabe, T., Yagishita, S., & Kikyo, H. (2008). Memory of music: roles of right hippocampus and left inferior frontal gyrus. *Neuroimage*, *39*(1), 483-491.

[53] Tsang, C. D., Trainor, L. J., Santesso, D. L., Tasker, S. L., & Schmidt, L. A. (2001). Frontal EEG responses as a function of affective musical features. *Annals of the New York Academy of Sciences*, *930*(1), 439-442.

[54] Schmidt, L. A., & Trainor, L. J. (2001). Frontal brain electrical activity (EEG) distinguishes valence and intensity of musical emotions. *Cognition & Emotion*, *15*(4), 487-500.

[55] Sammler, D., Grigutsch, M., Fritz, T., & Koelsch, S. (2007). Music and emotion: electrophysiological correlates of the processing of pleasant and unpleasant music. *Psychophysiology*, *44*(2), 293-304.

[56] Davidson, R. J. (1988). EEG measures of cerebral asymmetry: Conceptual and methodological issues. *International journal of neuroscience*, *39*(1-2), 71-89.

[57] Mizuki, Y., Kajimura, N., Kai, S., Suetsugi, M., Ushijima, I., & Yamada, M. (1992). Differential responses to mental stress in high and low anxious normal humans assessed by frontal midline theta activity. *International Journal of Psychophysiology*, *12*(2), 169-178.

[58] Suetsugi, M., Mizuki, Y., Ushijima, I., Kobayashi, T., Tsuchiya, K., Aoki, T., & Watanabe, Y. (2000). Appearance of frontal midline theta activity in patients with generalized anxiety disorder. *Neuropsychobiology*, *41*(2), 108-112.

[59] Sakharov, D. S., Davydov, V. I., & Pavlygina, R. A. (2005). Intercentral relations of the human EEG during listening to music. *Human Physiology*, *31*(4), 392-397.

[60] Müller, M. M., Keil, A., Gruber, T., & Elbert, T. (1999). Processing of affective pictures modulates right-hemispheric gamma band EEG activity. *Clinical Neurophysiology*, *110*(11), 1913-1920.

[61] Balconi, M., & Lucchiari, C. (2008). Consciousness and arousal effects on emotional face processing as revealed by brain oscillations. A gamma band analysis. *International Journal of Psychophysiology*, *67*(1), 41-46.

[62] Bhattacharya, J., Petsche, H., & Pereda, E. (2001). Long-range synchrony in the γ band: role in music perception. *Journal of Neuroscience*, *21*(16), 6329-6337.

[63] Bhattacharya, J., & Petsche, H. (2001). Enhanced phase synchrony in the electroencephalograph γ band for musicians while listening to music. *Physical Review E*, *64*(1), 012902.

[64] Ghosh, D. (2013). MEASUREMENT OF EMOTION INDUCED BY HINDUSTANI MUSIC—A HUMAN RESPONSE AND EEG STUDY. *ninad*, *26*, 49.

[65] Heller, W. (1993). Neuropsychological mechanisms of individual differences in emotion, personality, and arousal. *Neuropsychology*, *7*(4), 476.

[66] Lindsley, D. B., & Wicke, J. D. (1974). The electroencephalogram: Autonomous electrical activity in man and animals. In *Bioelectric recording techniques* (pp. 3-83).

[67] Iwanaga, M., Kobayashi, A., & Kawasaki, C. (2005). Heart rate variability with repetitive exposure to music. *Biological psychology*, *70*(1), 61-66.

[68] Iwanaga, M., & Tsukamoto, M. (1997). Effects of excitative and sedative music on subjective and physiological relaxation. *Perceptual and motor skills*, *85*(1), 287-296.

[69] Camm, A. J., Malik, M., Bigger, J. T., Breithardt, G., Cerutti, S., Cohen, R. J., ... & Lombardi, F. (1996). Heart rate variability. Standards of measurement, physiological interpretation, and clinical use. *European heart journal*, *17*(3), 354-381.

[70] Yanagihashi, R., Ohira, M., Kimura, T., & Fujiwara, T. (1997). Physiological and psychological assessment of sound. *International journal of biometeorology*, *40*(3), 157-161.

[71] Goldberger, A. L. (2000). AL Goldberger, LAN Amaral, L. Glass, JM Hausdorff, PC Ivanov, RG Mark, JE Mietus, GB Moody, C.-K. Peng, and HE Stanley, Circulation 101, e215 (2000). *Circulation*, *101*, e215.

[72] Lugovaya, T. S. (2005). Biometric human identification based on ECG. *PhysioNet*.

[73] Bruce, E. N. (2001). *Biomedical signal processing and signal modeling* (pp. 335-336). New York:: Wiley.

[74] Polikar, R. (1996). The wavelet tutorial.

[75] Graps, A. (1995). An introduction to wavelets. *IEEE computational science and engineering*, *2*(2), 50-61.

[76] Savitzky, A., & Golay, M. J. (1964). Smoothing and differentiation of data by simplified least squares procedures. *Analytical chemistry*, *36*(8), 1627-1639.

[77] Schafer, R. W. (2011). What is a Savitzky-Golay filter?[lecture notes]. *IEEE Signal processing magazine*, *28*(4), 111-117.

[78] Dash, P. K. (2002). Electrocardiogram monitoring. *Indian J. Anaesth*, *46*(4), 251-260.

[79] Pan, J., & Tompkins, W. J. (1985). A real-time QRS detection algorithm. *IEEE transactions on biomedical engineering*, (3), 230-236.

[80] Tompkins, W. J. (1993). Biomedical digital signal processing. *Editorial Prentice Hall*.

[81] Ebden, M. (2002). A Comparison of HRV Techniques: The Lomb Periodogram versus The Smoothed Pseudo Wigner-Ville Distribution. *A report submitted to Prof. Lionel Tarassenko*, *23*(1), 325-364.

[82] Lomb, N. R. (1976). Least-squares frequency analysis of unequally spaced data. *Astrophysics and space science*, *39*(2), 447-462.

[83] Scargle, J. D. (1982). Studies in astronomical time series analysis. II-Statistical aspects of spectral analysis of unevenly spaced data. *The Astrophysical Journal*, *263*, 835-853.

[84] Welch, P. (1967). The use of fast Fourier transform for the estimation of power spectra: a method based on time averaging over short, modified periodograms. *IEEE Transactions on audio and electroacoustics*, *15*(2), 70-73.

[85] Rödel, E. (1971). Fisher RA Statistical Methods for Research Workers. *Oliver & Boyd, Edinburgh, London. XIII*, *12*, 429-30.

[86] Albers, D., & Alexanderson, G. L. (2008). *Mathematical people: Profiles and interviews*. CRC Press.

[87] Lopes, R., & Betrouni, N. (2009). Fractal and multifractal analysis: a review. *Medical image analysis*, *13*(4), 634-649.

[88] Mandelbrot, B. (1967). How long is the coast of Britain? Statistical self-similarity and fractional dimension. *science*, *156*(3775), 636-638.

[89] Higuchi, T. (1988). Approach to an irregular time series on the basis of the fractal theory. *Physica D: Nonlinear Phenomena*, *31*(2), 277-283.

[90] Accardo, A., Affinito, M., Carrozzi, M., & Bouquet, F. (1997). Use of the fractal dimension for the analysis of electroencephalographic time series. *Biological cybernetics*, *77*(5), 339-350.

[91] Liu, Y., Sourina, O., & Nguyen, M. K. (2010, October). Real-time EEG-based human emotion recognition and visualization. In *Cyberworlds (CW), 2010 International Conference on* (pp. 262-269). IEEE.

[92] Klonowski, W., Olejarczyk, E., & Stepien, R. (2004). 'Epileptic seizures' in economic organism. *Physica A: Statistical Mechanics and its Applications*, *342*(3-4), 701-707.

9. Publications

[1] Das, N., & Chakraborty, M. (2017, November). Performance analysis of FIR and IIR filters for ECG signal denoising based on SNR. In *Research in Computational Intelligence and Communication Networks (ICRCICN), 2017 Third International Conference on* (pp. 90-97). IEEE.

[2] (Under Review) Optimization of ECG denoising techniques – DSP Approach; submitted to International Journal of Electronics, Taylor and Francis Publications.